

JOURNAL OF BIOMEDICINE AND TRANSLATIONAL RESEARCH

Available online at JBTR website: <https://jbtr.fk.undip.ac.id>

Copyright©2023 by Faculty of Medicine Universitas Diponegoro, Indonesian Society of Human Genetics and Indonesian Society of Internal Medicine

Original Research Article

The Effect of Liprotide-Encapsulated Vitamin D₃ on MDA and SOD in Rats Deficient Vitamin D and Calcium

Untari¹, Faizah Fulyani², Adriyan Pramono¹, Endang Mahati³, Sylvia Rahmi Putri¹, Reza Achmad Maulana⁴, Gemala Anjani^{1*}

¹Department of Nutrition Science, Faculty of Medicine, Universitas Diponegoro, Indonesia

²Department of Medical Biology and Biochemistry, Faculty of Medicine, Universitas Diponegoro, Indonesia

³Departement of Pharmacology and Therapy, Faculty of Medicine, Universitas Diponegoro, Semarang, Indonesia

⁴Department of Nutrition Science, Faculty of Public Health, Universitas Ahmad Dahlan, Yogyakarta, Indonesia

Article Info

History

Received: 27 Oct 2022

Accepted: 07 Feb 2023

Available: 30 Apr 2023

Abstract

Background: Vitamin D deficiency is frequently correlated with elevated malondialdehyde (MDA) levels and decreased superoxide dismutase (SOD) activity. Several studies have demonstrated that vitamin D₃ can reverse intracellular oxidative stress. However, vitamin D is prone to deterioration and instability. Liprotides contain lipids and proteins that can prevent vitamin D from oxidizing.

Objective: This study aims to investigate the effects of liprotide-encapsulated vitamin D₃ on MDA concentrations and SOD activity in calcium and vitamin D-deficient rat models.

Methods: The experimental post-test-only control group study used 24 Wistar rats randomly in 4 groups. Groups K(-), K(+), and P were fed a vitamin D and calcium-depleted AIN-93M diet for 14 days. Standard feed AIN-93M was received by normal groups (KN). Groups K- were deficient rats in vitamin D and calcium without intervention. The groups of K+ and P were given vitamin D₃ (180 IU) which was non-encapsulated and liprotide-encapsulated for 28 days. The SOD activity was quantified with Superoxide Dismutase (SOD) Activity Assay Kit, while MDA levels were determined using Thiobarbituric Acid Reactive Substance (TBARS) method. The statistical analysis used One-way ANOVA test with Least Significant Difference follow-up test.

Results: The MDA levels and SOD activity in the K+ and P groups had significant differences ($p < 0.05$) against the control group. Liprotides-encapsulated vitamin D₃ significantly reduced MDA levels and enhanced SOD activity compared to non-encapsulated in rats with a deficiency in vitamin D and calcium.

Conclusion: Liprotide-encapsulated vitamin D₃ has the potential to increase SOD activity and decrease MDA levels.

Keywords: Vitamin D₃; nanoencapsulation; liprotide; MDA; SOD

Permalink/ DOI: <https://doi.org/10.14710/jbtr.v9i1.16289>

INTRODUCTION

More than half of people of all ages are affected by vitamin D deficiency in the world.¹ Vitamin D deficiency can occur not only in Western countries but also in tropical countries.² Vitamin D deficiency is prevalent in both children and adults. In the United States, 50% of children ages 1–5 and 70% of children ages 6–11 had vitamin D levels < 30 ng/mL.³ In Jakarta and Kuala Lumpur, 60% of 504 women between the ages

of 18 and 40 were vitamin D deficient.⁴ The cross-sectional study in North Sumatra, Indonesia, found that 95% of the 156 subject women were vitamin D deficient or inadequate.⁵

* Corresponding author:

E-mail: gemaanjani@gmail.com
(Gemala Anjani)

Vitamin D deficiency is linked to several clinical disorders and mortality rates.⁶ A lot of chronic conditions, including diabetes mellitus, cardiovascular disease, kidney disease, and autoimmune disease, are associated with the rising incidence of vitamin D deficiency.^{7,8} According to several studies, deficiency of vitamin D contributes to oxidative stress and inflammation.^{9,10,11} Several factors have been associated with vitamin D deficiency such as inadequate sun exposure, medications, skin pigmentation and low vitamin D consumption.³

Vitamin D plays a key role in absorption and homeostasis calcium.¹² Optimal vitamin D levels are necessary to increase the efficiency of calcium absorption.¹³ Without adequate vitamin D, the body absorbs no more than 10% to 15% of dietary calcium.¹³ Calcium deficiency can cause metabolic or potential pathological changes.¹⁴ There are close connections between oxidative stress and calcium homeostasis.¹⁵ In mitochondria, calcium plays an important role in the formation of ATP and reactive oxygen species (ROS).¹⁶ At the cellular level, a deficiency of vitamin D increases oxidative stress, inflammation indicators, and mitochondrial damage.¹⁷ An imbalance between the production of ROS and antioxidant activities results in oxidative stress.¹⁸ Numerous signaling pathways are activated by oxidative stress, which ultimately increased lipid and protein peroxidation-induced tissue damage.^{19,20} High levels of malondialdehyde (MDA) and low levels of superoxide dismutase (SOD) activity are indicators of oxidative stress. The high level of MDA is an indicator of lipid peroxidation initiated by reactive oxygen species (ROS).²¹ Natural defense mechanisms in the body include glutathione enzymes and superoxide dismutase (SOD).²² The SOD enzyme effectively converts superoxide anions into dioxygen and hydrogen peroxide in physiological conditions.²³ According to biochemical studies, the highest SOD activity was presented in liver and kidney tissue.²²

Vitamin D supplementation in food is an appealing alternative to elevate the serum level of vitamin D in the population.^{24,25} Oxidation, high temperatures, and an acidic environment can easily harm vitamin D.^{26,27} Nanoencapsulation is a method for preserving a coated substance by enclosing it in a matrix in its liquid, solid, or gaseous states.²⁸ Cores are the materials that have been encased, while shells are the materials that have been coated. The substance should be biocompatible and edible for food purposes.²⁹ Previous research indicates that nanostructured lipid carriers (NLCs) can be controlled to release vitamin D₃ safely and to prevent degradation of vitamin D₃ in simulated stomach fluids, while also releasing more than 90% in simulated intestinal fluids.³⁰

Liprotide is a form complex made up of partially denatured protein and lipids that can protect bioactive compounds like vitamin D. To protect the bioactive compound, the protein forms a shell around a fatty acid core.³¹ One of the materials used to encapsulate vitamin D₃ is protein-lactoglobulin.³² Oleic acid and β -lactoglobulin were used to make liprotide in this study, which can increase the bioavailability and protection against acid, heat, and UV light.^{31,32} This study was aimed to evaluate vitamin D₃-encapsulated by liprotides

on MDA level and SOD activity in the liver of rat models with vitamin D and calcium deficient diets.

MATERIALS AND METHODS

Ethical Statement

This study was approved with ethical approval from the Ethical Commission of Health Research, Medical Faculty, Sultan Agung Islamic University (Ethical clearance number: 29/I/2022/Bioethics Commission).

Chemical and Reagent

Cholecalciferol Vitamin D ($\geq 98\%$), β -lactoglobulin ($\geq 90\%$ pure), and oleic acid ($\geq 99\%$ pure) were purchased from Sigma Aldrich (Germany). Support materials other such as potassium hydroxide (KOH, 1310-58-3), absolute ethanol (1.00983.2500), concentrate liquid PBS OmniPur® (6506-1LCN), ultra centrifugal filter unit Amicon® (UFC901008), and MiliQ water.

Preparation of Liprotides

The oleic acid (38 mg/mL) was dissolved in 99% ethanol. Six (6) mg/ml β -lactoglobulin, mixed with 1.5 mg/ml oleic acid in 10 mM KOH (pH 10.5) and incubated at 45° C for 30 minutes.³¹ Then, the sample mixture was cooled and the pH was adjusted to 7.4 using a PBS solution. Samples were vortexed and centrifuged at 4,000 rpm for 8 minutes.³¹ In this study, the liprotides form a clear solution.

Vitamin D Encapsulation

Vitamin D₃ was dissolved in 96% ethanol to a concentration of 115 mM. Then vitamin D₃ was mixed with liprotides that have been formed with a final concentration of 4 mg/ml. The sample was homogenized with a vortex then centrifuged using an ultra centrifugal filter unit for 8 minutes, 30° C, and 4000 rpm.³¹ Vitamin D concentration, efficiency, and successful encapsulation were seen using HPLC (Shimadzu corp LC20AD® Serial Number : L20105130725, Kyoto Japan) and SEM (Jeol JSM-6510LA, Japan®). The research was conducted at the Diponegoro University Integrated Laboratory.

Experimental Animals

This was a true experimental study with a post-test-only control group design. Twenty-four male Wistar rats (8-12 weeks) weighing between 150 and 200 grams were acclimatized for 7 days to room temperatures 20-25° C, humidity between 60-70%, and 12 hours of the normal cycle with food and water ad libitum. The study was conducted in the Experimental Animal Laboratory of the Center for Food and Nutrition at Gajah Mada University between January and March of 2022. All of the rats were separated into 4 groups: normal group (KN), deficient vitamin D and calcium group with no intervention (K-), non-encapsulated vitamin D₃ (K+), and liprotide-encapsulated vitamin D₃ (P). The normal/healthy groups (KN) only received standard food AIN-93M.³³ For 14 days, rats in groups (K-), (K+), and P were fed modified AIN-93M (vitamin D and calcium depleted) to produce vitamin D and calcium deficient rats. Rats received a normal AIN-93M diet after the vitamin D and calcium depletion phase. Group (K-) was presented as deficient rats without any treatment. The intervention groups were

given lipotide-encapsulated vitamin D₃ (P) and non-encapsulated vitamin D₃ (K+) for 28 days. The doses of vitamin D₃ that were used in previous studies were 180 IU/200g for rats.³⁴

Biomarkers Analysis

The rats received 100 mg/kg intramuscular ketamine after 28 days intervention period. The MDA concentration in liver tissue was tested using the TBARS method. Liver tissue with a weight of 1 gram was put into a cold mortar. Then 500 µl 0.9% NaCl was added and homogenized. The homogenate was taken and transferred to an Eppendorf tube. The homogenate was centrifuged at 8000 rpm for 20 minutes and retrieved the supernatant. Then 100 µL supernatants were put into a test tube, add 550 µl NaCl, 100 µl TCA, 100 µL HCL 1 N, 100 µL Na-Thio 1 % and homogenized again. After that, the supernatants were centrifuged at 1500 rpm for 10 minutes and heated in a 100°C water bath for 30 minutes. The sample absorbance was measured with a spectrophotometer at a length maximum wavelength of 532 nm.

The Superoxide Dismutase (SOD) Activity Assay Kit from Biovision Inc. was used to quantitatively measure SOD activity in the supernatant of liver tissue samples. A Microplate reader was used to determine the absorbance of the supernatant at a wavelength of 450 nm.

Statistical Analysis

Statistical analysis was performed with SPSS 20 (IBM/SPSS Inc). The Shapiro-Wilk normality test was used to analyze the data research. The data post-test intervention was normally distributed and has the same data variance thus One-way ANOVA test was used to determine the difference between MDA levels and SOD activity. The post hoc LSD test was used to find out in which group there is a significant difference. The result was displayed as a mean \pm SD and $p < 0.05$ was considered to be significant.

RESULTS

Effect of Vitamin D₃ Encapsulated by Liprotides on MDA Levels

Table 1 shows lower levels of MDA in the K+ and P groups than K- group after the interventions. There was a significant difference in the mean MDA levels in rat livers after the intervention between all groups using the one-way ANOVA test ($p < 0.001$). MDA levels in K+ (3.19 ± 0.55 nmol/g) and P (2.57 ± 0.46 nmol/g) groups are lower than group K- (9.79 ± 0.28 nmol/g). MDA levels in group P were lower than K+ group. While both MDA levels were still higher than the normal control group KN (1.19 ± 0.22 nmol/g). The LSD test results showed that all

groups had significantly different MDA levels in liver tissue ($p < 0.05$).

Effect of Vitamin D₃ Encapsulated by Liprotides on SOD Activity

The result of the mean in SOD activity is shown in **Table 1** which shows higher SOD activity in the K+ and P groups than K- group after 28 days of intervention. The one-way ANOVA test showed significant differences in SOD activity after intervention in all groups ($p < 0.001$). SOD activity in the P group (68.03 ± 4.72 %) is higher than in the K+ group (61.47 ± 4.48 %). While, both SOD activities were still lower than the normal control group KN (79.51 ± 3.06 %). The LSD test showed that all groups had significantly different SOD activity in liver tissue ($p < 0.05$).

DISCUSSION

The results of this study showed that lipotide-encapsulated vitamin D₃ could lower MDA levels and increase SOD activity in vitamin D and calcium-deficient rats' livers. In addition, the use of liprotides encapsulation affects the MDA levels and SOD activity. Liprotide-encapsulated vitamin D₃ improved MDA and SOD in rat liver tissue better than non-encapsulated. Liprotides-encapsulated vitamin D₃ has previously been shown to increase stability, bioavailability, and resistance to pH, temperature, and UV light.^{31,32}

Deficiency of vitamin D and calcium in rat models by given feeding modified AIN-93M for 14 days (vitamin D and calcium depleted). In this study, there was an increase in MDA levels and decreased SOD activity in deficient vitamin D and calcium diet groups. Nutritional deficiencies such as vitamins and minerals can reduce metabolic status which can increase reactive oxygen species (ROS).³⁵ Dysregulation of vitamin D and calcium causes decreased mitochondrial respiration which induces reactive oxygen species and contributes to the accumulation of cellular oxidative damage.^{16,36,37}

Vitamin D is known to play an essential role in maintaining calcium.³⁸ Calcium is essential for controlling mitochondrial respiration because it is the main production of cellular ATP and ROS.¹⁶ The deficiency of calcium can cause lower superoxide dismutase (SOD).³⁹ In this study, adequate vitamin D intake can increase calcium absorption in the intestine.⁴⁰ Adequate calcium uptake can maintain the antioxidative capacity (superoxide dismutase, glutathione peroxidase, glutathione) to avoid excessive ROS production.¹⁶

Oxidative stress due to increased ROS can cause the peroxidation of proteins, nucleic acids, and lipids.^{37,41} Lipid peroxidation products discovered in the liver, brain, kidney, lung, and skeletal muscle such as MDA, 4-HNE, and F-2 isoprostanes.³⁷ Malondialdehyde is a

Table 1. The mean data MDA levels and SOD activity in all groups

Variables	Treatment Groups (n=6)				p
	KN	K-	K+	P	
MDA (nmol/g)	1.19 \pm 0.22 ^a	9.79 \pm 0.28 ^b	3.19 \pm 0.55 ^c	2.57 \pm 0.46 ^d	<0.000*
SOD (%)	79.51 \pm 3.06 ^a	32.24 \pm 3.53 ^b	61.47 \pm 4.48 ^c	68.03 \pm 4.72 ^d	<0.000*

*OneWay ANOVA test * $p < 0.001$

^{a,b,c,d} Post Hoc LSD Test, significantly different $p < 0.05$

peroxidation product of polyunsaturated fatty acids, such as phospholipids and triglycerides.^{42,43,44} In animal studies showed that deficiency of vitamin D and calcium caused increased MDA levels in liver tissue.^{39,45} Increased ROS leads decrease endogenous antioxidants such as glutathione, superoxide dismutase, catalase, and peroxiredoxin.^{42,46} Previous studies demonstrated that deficiency of vitamin D decreased the activity of glutathione peroxidase, catalase, and superoxide dismutase in the liver.⁴⁵

The administration of non-encapsulated and lipotides-encapsulated vitamin D₃ increased SOD activity and decreased MDA levels in liver rats. Vitamin D can enhance natural antioxidant defenses. Numerous studies have shown that vitamin D₃ increases SOD activity in the serum and liver tissue of experimental animals.^{45,47,48} The administration of vitamin D will maintain calcium homeostasis in the body.⁴⁹ Calcium controlled redox regulation and oxidative stress in mitochondrial.¹⁶ Vitamin D was activated enzyme glucose-6-phosphate-dehydrogenase produces glutathione which reduces nitrogen oxides and SOD that is responsible for transforming O₂⁻ into H₂O₂.^{44,50,51} The other research shows that supplementing with vitamin D₃ can lower MDA concentrations in liver tissue.^{45,48,52} However, several studies have shown that vitamin D supplementation does not significantly lower MDA levels.^{53,39}

Active vitamin D bound to VDR (vitamin D receptors) can alter the activity of multiple signaling pathways both non-genomically and genomically.⁵⁴ Vitamin D₃ administration has been shown in some studies to increase the production of the transcription factor Nrf2 which can increase antioxidant capacity through binding to the antioxidant response elements (ARE).^{50,55} Vitamin D₃ markedly increased protein expression of Nrf2. It means that Vitamin D₃ can activate the expression of Nrf2 and in turn promote the synthesis of antioxidant-associated proteins. Consequently, the damage caused by oxidative stress to the liver can be attenuated.⁴⁷ This is supported by the results of other studies which state that crosstalk occurs between the NF-κB- and Nrf2 pathways.⁵⁶ NF-κB (p65) can interact with Keap1 to inhibit activation of the Nrf2-ARE pathway. Meanwhile, the activation level of NF-κB phosphorylation (p65) is positively associated with the secretion of proinflammatory cytokines such as IL-1β, IL-6, and TNF-α and negatively correlated with the secretion of the anti-inflammatory cytokine IL-10.^{47,56}

In this study, groups of lipotides-encapsulated vitamin D₃ improved MDA levels and SOD activity better than non-encapsulated groups. In line with other studies, the administered vitamin D encapsulated had significantly higher levels of vitamin D in their blood than non-encapsulated recipients.^{29,32,57} This is associated with the provision of encapsulation can increase the bioavailability of vitamin D in the blood.³¹ Vitamin D₃ may be bound in a hydrophobic region that shields it from oxidative damage, high temperatures, and UV rays, which improves its stability and bioavailability.³¹

Lipotides have good interaction with the membranes. In the vitamin D₃ transfer assay to the phospholipid membrane, it was shown that >80% of the

hydrophobic lipotide components (vitamin D₃ and oleic acid) transferred well to the vesicles.³¹ The β-lactoglobulin protein is an effective carrier encapsulant for vitamin D because of the van der Waals and hydrogen bond involved in the binding of fatty acid to these proteins.⁵⁸ Other studies have shown that vitamin D₃ cross seed mucilage-β-lactoglobulin nanocomplexes can affect the speed of content delivery which in vitro tests using SGF (simulated gastric fluid) and SIF (simulated intestinal fluid) showed that the release in the stomach was small and would increase in the intestine.⁵⁹ The limitations of this study show that the results have been able to reduce MDA levels and increase SOD activity, but it has not been able to reach normal conditions.

CONCLUSION

The administration of both non-encapsulated and lipotide-encapsulated vitamin D₃ can improve MDA levels and SOD activity. In this study, it can be concluded that the administration of lipotide-encapsulated vitamin D₃ can reduce MDA levels and increase SOD activity in the liver better than non-encapsulated. Studies of longer duration may be needed to determine how long the MDA levels and SOD activity to return to normal.

ACKNOWLEDGMENTS

This research was part of "The Study Bioavailability of Vitamin D₃ Encapsulated Lipotides in Rats on a Vitamin D and Calcium Deficiency Diet." It was supported by Indonesian Ministry of Education, Culture, Research, and Technology with Grant Number: No.187-13/UN7.6.1/PP/2022.

REFERENCES

1. Palacios C, Gonzalez L. Is vitamin D deficiency a major global public health problem? *J Steroid Biochem Mol Biol.* 2014;144(PART A):138-145.
2. Chin KY, Ima-Nirwana S, Ibrahim S, Mohamed IN, Ngah WZW. Vitamin D status in Malaysian men and its associated factors. *Nutrients.* 2014;6(12):5419-5433. doi:10.3390/nu6125419
3. Holick MF. The vitamin D deficiency pandemic: Approaches for diagnosis, treatment and prevention. *Rev Endocr Metab Disord.* 2017;18(2):153-165. doi:10.1007/s11154-017-9424-1
4. Green TJ, Skeaff CM, Rockell JEP, et al. Vitamin D status and its association with parathyroid hormone concentrations in women of child-bearing age living in Jakarta and Kuala Lumpur. *Eur J Clin Nutr.* 2008;62(3):373-378. doi:10.1038/sj.ejcn.1602696
5. Keumala S D, Alrasyid D H, L N, L Z. Occurrence of Vitamin D Deficiency among Women in North Sumatera, Indonesia. *Malays J Nutr.* 2014;20(1):63-70.
6. Stavenuiter AWD, Arcidiacono MV, Ferrantelli E, et al. A novel rat model of vitamin D deficiency: Safe and rapid induction of vitamin D and calcitriol deficiency without hyperparathyroidism. *Biomed Res Int.* 2015;2015. doi:10.1155/2015/604275

7. Hyppönen E, Läärä E, Reunanen A, Järvelin MR, Virtanen SM. Intake of vitamin D and risk of type 1 diabetes: A birth-cohort study. *Lancet*. 2001;358(9292):1500-1503. doi:10.1016/S0140-6736(01)06580-1
8. Mokhtari Z, Hekmatdoost Z, Nourian M. Antioxidant efficacy of vitamin D. *J Parathyroid Dis*. 2017;5:11-16.
9. Asghari S, Hamed-Shahraki S, Amirkhizi F. Vitamin D status and systemic redox biomarkers in adults with obesity. *Clin Nutr ESPEN*. 2021;45:292-298. doi:10.1016/j.clnesp.2021.07.032
10. Colombo M, Sangiovanni A. Vitamin D deficiency and liver cancer: More than just an epidemiological association? *Hepatology*. 2014;60(4):1130-1132. doi:10.1002/hep.27178
11. Judd SE, Tangpricha V. Vitamin D deficiency and risk for cardiovascular disease. *Am J Med Sci*. 2009;338(1):40-44. doi:10.1097/MAJ.0b013e3181a9ee91
12. Murdaca G, Tonacci A, Negrini S, et al. Emerging role of vitamin D in autoimmune diseases: An update on evidence and therapeutic implications. *Autoimmun Rev*. 2019;18(9):102350. doi:10.1016/j.autrev.2019.102350
13. Natasha Khazai, MD, Suzanne E. Judd, MPH, and Vin Tangpricha, MD P. Calcitriol.pdf. *Curr Rheumatol Rep*. 2009;10(2):110-117.
14. Wang M, Yang X, Wang F, et al. Calcium-deficiency assessment and biomarker identification by an integrated urinary metabolomics analysis. *BMC Med*. 2013;11(1):86. doi:10.1186/1741-7015-11-86
15. Ly LD, Xu S, Choi S-K, et al. Oxidative stress and calcium dysregulation by palmitate in type 2 diabetes. *Exp Mol Med*. 2017;49(2):1-12. doi:10.1038/emm.2016.157
16. Bertero E, Maack C. Calcium signaling and reactive oxygen species in Mitochondria. *Circ Res*. 2018;122(10):1460-1478. doi:10.1161/CIRCRESAHA.118.310082
17. Sanz R, Mazzei L, Santino N, Ingrassia M, Manucha W. Vitamin D-mitochondria cross-talk could modulate the signalling pathway involved in hypertension development: a translational integrative overview. *Clínica e Investig en Arterioscler (English Ed)*. 2020;32(4):144-155. doi:10.1016/j.artere.2020.02.003
18. Liu Z, Ren Z, Zhang J, et al. Role of ROS and nutritional antioxidants in human diseases. *Front Physiol*. 2018;9(MAY):1-14. doi:10.3389/fphys.2018.00477
19. Chatterjee S. *Oxidative Stress, Inflammation, and Disease*. Elsevier Inc.; 2016. doi:10.1016/B978-0-12-803269-5.00002-4
20. Dzik KP, Kaczor JJ. Mechanisms of vitamin D on skeletal muscle function: oxidative stress, energy metabolism and anabolic state. *Eur J Appl Physiol*. 2019;119(4):825-839. doi:10.1007/s00421-019-04104-x
21. Avelar TMT, Storch AS, Castro LA, Azevedo GVMM, Ferraz L, Lopes PF. Oxidative stress in the pathophysiology of metabolic syndrome: Which mechanisms are involved? *J Bras Patol e Med Lab*. 2015;51(4):231-239. doi:10.5935/1676-2444.20150039
22. Frederiks WM, Bosch KS. Localization of superoxide dismutase activity in rat tissues. *Free Radic Biol Med*. 1997;22(1-2):241-248. doi:10.1016/S0891-5849(96)00328-0
23. Fridovich I. The superoxide radical is an agent of oxygen toxicity; superoxide dismutase provide an important defense. *Biol Oxyg Radicals*. 1978;201:875-880.
24. Kiely M, Black LJ. Dietary strategies to maintain adequacy of circulating 25-hydroxyvitamin D concentrations. *Scand J Clin Lab Invest*. 2012;72(SUPPL. 243):14-23. doi:10.3109/00365513.2012.681893
25. Högl W, Munns CF. Rickets and osteomalacia: A call for action to protect immigrants and ethnic risk groups. *Lancet Glob Heal*. 2016;4(4):e229-e230. doi:10.1016/S2214-109X(16)00061-9
26. Combs GF, James P. McClung. *The Vitamins Fundamental Aspects in Nutrition and Health*. Fifth. Elsevier Inc.; 2017.
27. Verkaik-Kloosterman J, Seves SM, Ocké MC. Vitamin D concentrations in fortified foods and dietary supplements intended for infants: Implications for vitamin D intake. *Food Chem*. 2017;221:629-635. doi:10.1016/j.foodchem.2016.11.128
28. Pateiro M, Gómez B, Munekata PES, et al. Nanoencapsulation of promising bioactive compounds to improve their absorption, stability, functionality and the appearance of the final food products. *Molecules*. 2021;26(6). doi:10.3390/molecules26061547
29. Jannasari N, Fathi M, Moshtaghian SJ, Abbaspourrad A. Microencapsulation of vitamin D using gelatin and cress seed mucilage: Production, characterization and in vivo study. *Int J Biol Macromol*. 2019;129:972-979. doi:10.1016/j.ijbiomac.2019.02.096
30. Park SJ, Garcia C V, Shin GH, Kim JT. Development of nanostructured lipid carriers for the encapsulation and controlled release of vitamin D3. *Food Chem*. 2017;225:213-219. doi:10.1016/j.foodchem.2017.01.015
31. Pedersen JN, Frislev HS, Pedersen JS, Otzen DE. Using protein-fatty acid complexes to improve vitamin D stability. *J Dairy Sci*. 2016;99(10):7755-7767. doi:10.3168/jds.2016-11343
32. Diarrassouba F, Garrait G, Remondetto G, Alvarez P, Beyssac E, Subirade M. Improved bioavailability of vitamin D3 using a β -lactoglobulin-based coagulum. *Food Chem*. 2015;172:361-367. doi:10.1016/j.foodchem.2014.09.054
33. Reeves PG, Suppl M. Symposium : Animal Diets for Nutritional and Toxicological Research Components of the AIN-93 Diets as Improvements in the AIN-76A Diet 1 , 2. *Exp Biol*. 1997;127(March):838-841.

34. Heaney RP, Davies KM, Chen TC, Holick MF, Janet Barger-Lux M. Human serum 25-hydroxycholecalciferol response to extended oral dosing with cholecalciferol. *Am J Clin Nutr.* 2003;77(1):204-210. doi:10.1093/ajcn/77.1.204
35. Gemcioglu E, Baser S, Yilmaz Cakmak N, et al. Assessing Oxidative Stress by Thiol/Disulfide Homeostasis Among Vitamin D-Deficient Patients. *Cureus.* 2021;13(12):1-7. doi:10.7759/cureus.20400
36. Berridge MJ. Vitamin D deficiency accelerates ageing and age-related diseases: a novel hypothesis. *J Physiol.* 2017;595(22):6825-6836. doi:10.1113/JP274887
37. Kregel KC, Zhang HJ. An integrated view of oxidative stress in aging: Basic mechanisms, functional effects, and pathological considerations. *Am J Physiol - Regul Integr Comp Physiol.* 2007;292(1):18-36. doi:10.1152/ajpregu.00327.2006
38. Pan K, Tu R, Yao X, Zhu Z. Associations between serum calcium, 25(OH)D level and bone mineral density in adolescents. *Adv Rheumatol.* 2021;61(1):1-9. doi:10.1186/s42358-021-00174-8
39. Choi MJ, Jung YJ. Effects of taurine and vitamin D on antioxidant enzyme activity and lipids profiles in rats fed diet deficient calcium. *Adv Exp Med Biol.* 2017;975:1081-1092. doi:10.1007/978-94-024-1079-2_86
40. Civitelli R, Ziambaras K, Ward WE. *Calcium, Magnesium, and Vitamin D Absorption; Metabolism and Deficiency.* 2nd ed. Elsevier Inc.; 2020. doi:10.1016/b978-0-12-801238-3.66113-5
41. Blumberg J. Use of biomarkers of oxidative stress in research studies. *J Nutr.* 2004;134(11):3188-3189.
42. Halliwell B. Free Radicals and Other Reactive Species in Disease. *eLS.* 2015;(11):1-9. doi:10.1002/9780470015902.a0002269.pub3
43. Halliwell B, Chirico S. Lipid peroxidation: significance and its mechanism. *Am J Clin Nutr.* 1993;57(February):715-725.
44. Hauck AK, Bernlohr DA. Thematic review series: Lipotoxicity: Many roads to cell dysfunction and cell death: Oxidative stress and lipotoxicity. *J Lipid Res.* 2016;57(11):1976-1986. doi:10.1194/jlr.R066597
45. Wu C, Lu B, Wang Y, Jin C, Zhang Y, Ye J. Effects of dietary vitamin D3 on growth performance, antioxidant capacities and innate immune responses in juvenile black carp *Mylopharyngodon piceus*. *Fish Physiol Biochem.* 2020;46(6):2243-2256. doi:10.1007/s10695-020-00876-8
46. Pervaiz S, Bellot GL, Lemoine A, Brenner C. *Redox Signaling in the Pathogenesis of Human Disease and the Regulatory Role of Autophagy.* Vol 352. 1st ed. Elsevier Inc.; 2020. doi:10.1016/bs.ircmb.2020.03.002
47. Zhang H, Liu Y, Fang X, et al. Vitamin D3 Protects Mice from Diquat-Induced Oxidative Stress through the NF- κ B/Nrf2/HO-1 Signaling Pathway. *Oxid Med Cell Longev.* 2021;2021. doi:10.1155/2021/6776956
48. Adelani IB, Ogadi EO, Onuzulu C, Rotimi OA, Maduagwu EN, Rotimi SO. Dietary vitamin D ameliorates hepatic oxidative stress and inflammatory effects of diethylnitrosamine in rats. *Heliyon.* 2020;6(9):e04842. doi:10.1016/j.heliyon.2020.e04842
49. Dogan M, Cesur Y, Dogan SZ, Kaba S, Bulan K, Cemek M. Oxidant/antioxidant system markers and trace element levels in children with nutritional rickets. *J Pediatr Endocrinol Metab.* 2012;25(11-12):1129-1139.
50. Wimalawansa SJ. Vitamin D Deficiency : Effects on Oxidative Stress , Epigenetics, Gene Regulation, and Aging. *Biology (Basel).* 2019;8(2):1-15.
51. Liu Y, Hyde AS, Simpson MA, Barycki JJ. Emerging regulatory paradigms in glutathione metabolism. *Adv Cancer Res.* 2014;122(402):69-101. doi:10.1016/B978-0-12-420117-0.00002-5
52. Zhu CG, Liu YX, Wang H, et al. Active form of vitamin D ameliorates non-alcoholic fatty liver disease by alleviating oxidative stress in a high-fat diet rat model. *Endocr J.* 2017;64(7):663-673. doi:10.1507/endocrj.EJ16-0542
53. Wee CL, Mokhtar SS, Banga Singh KK, Rasool AHG. Vitamin D deficiency attenuates endothelial function by reducing antioxidant activity and vascular eNOS expression in the rat microcirculation. *Microvasc Res.* 2021;138(July):104227. doi:10.1016/j.mvr.2021.104227
54. Berridge MJ. Vitamin D, reactive oxygen species and calcium signalling in ageing and disease. *Philos Trans R Soc B Biol Sci.* 2016;371(1700):20150434. doi:10.1098/rstb.2015.0434
55. Nakai K, Fujii H, Kono K, et al. Vitamin D activates the Nrf2-keap1 antioxidant pathway and ameliorates nephropathy in diabetic rats. *Am J Hypertens.* 2014;27(4):586-595. doi:10.1093/ajh/hpt160
56. Hu B, Wei H, Song Y, et al. NF- κ B and Keap1 Interaction Represses Nrf2-Mediated Antioxidant Response in Rabbit Hemorrhagic Disease Virus Infection. *J Virol.* 2020;94(10):1-14.
57. Diarrassouba F, Garrait G, Remondetto G, Alvarez P, Beyssac E, Subirade M. Food protein-based microspheres for increased uptake of Vitamin D3. *Food Chem.* 2015;173:1066-1072. doi:10.1016/j.foodchem.2014.10.112
58. Fang B, Zhang M, Tian M, Ren FZ. Self-assembled β -lactoglobulin-oleic acid and β -lactoglobulin-linoleic acid complexes with antitumor activities. *J Dairy Sci.* 2015;98(5):2898-2907. doi:10.3168/jds.2014-8993
59. Taheri A, Kashaninejad M, Tamaddon AM, Jafari SM. Vitamin D3 cross seed mucilage - β -lactoglobulin nanocomplexes: Synthesis, characterization, encapsulation and simulated intestinal fluid in vitro release. *Carbohydr Polym.* 2021;256(September 2020):117420. doi:10.1016/j.carbpol.2020.117420

JOURNAL OF BIOMEDICINE AND TRANSLATIONAL RESEARCH

Available online at JBTR website: <https://jbtr.fk.undip.ac.id>

Copyright©2023 by Faculty of Medicine Universitas Diponegoro, Indonesian Society of Human Genetics and Indonesian Society of Internal Medicine

Original Research Article

Potential of B-Cell Epitopes Protein Ag85 Complex *Mycobacterium tuberculosis* as Serodiagnostic Antigen of Tuberculosis by In Silico Study

Diana Chusna Mufida^{1*}, Ayu Munawaroh Aziz², Nurrul Izza Misturiansyah³

¹Department of Microbiology, Faculty of Medicine, University of Jember, Indonesia

²Department of Histology, Faculty of Medicine, University of Jember, Indonesia

³Faculty of Medicine, University of Jember, Indonesia

Article Info

History

Received: 05 Nov 2022

Accepted: 26 Apr 2023

Available: 30 Apr 2023

Abstract

Background: The high case of tuberculosis which isn't followed by good detection becomes an urgency for the diagnostic developments. One of them with immunodiagnostic principle uses B-cell Ag85 complex epitope. The design of the diagnostic epitope was performed by mapping the B cell epitope used in silico studies.

Objective: The purpose of this research is to analyze antigenicity, physicochemical which affect immunogenicity, and homology of B-cell Ag85 complex epitope with the strain which circulates in Indonesia.

Methods: The samples used were taken from the NCBI protein bank with access numbers P9WQP3 for Ag85A, P9WQP1 for Ag85B, and P9WQN9 for Ag85C. The sequences were analyzed using IEDB (Bepipred) software as the epitope prediction, VaxiJen as antigenicity prediction, ProtParam as physicochemical properties prediction, and BLASTP NCBI as sequence alignment.

Results: Twenty seven epitopes were antigenic with 0.4297 to 2.6007 scores and the molecular weight was from 619.59 Da to 3145.36 Da. This research also obtained eleven stable and hydrophilic epitopes. The alignment of 11 candidate epitopes with the strain which circulates in Indonesia, had a similarity percentage of 85.71% -100% and 3 epitopes had a more significant score.

Conclusion: Three epitopes of Ag85 complex; Ag85A (212-235), Ag85B (209-237), and Ag85C (283-310), were universal antigens and can be developed into diagnostic antigens in Indonesia.

Keywords: B-cell epitope; Ag85 complex; diagnostic antigen; in silico.

Permalink/ DOI: <https://doi.org/10.14710/jbtr.v9i1.16379>

INTRODUCTION

Tuberculosis (TB), caused by *Mycobacterium tuberculosis*, is a disease that mainly affects the lungs (pulmonary TB) and various organs (extrapulmonary TB). It is a world health problem and an infectious disease ranking among the top ten causes of death.¹ Indonesia is the 3rd country with the highest incidence of TB globally, contributing 8.4% of the cases. Furthermore, in 2020, only 351,936 (41.7%) incidences of TB were reported to the Ministry of Health, and 58.3% of other issues were undetected.² The use of *M. tuberculosis* antigen B cell epitope is one of the diagnostic developments performed with the immunodiagnostic principle.

The antigen 85 complex is the most commonly secreted protein from *M. tuberculosis* in liquid culture. It plays an essential role in the virulence of TB.³ This immunodominant protein triggers the body's humoral immune response, which is characterized by the formation of protective antibodies and induce TCD8⁺ Th1 CD4⁺ for the production of cytokines such as IFN- γ and IL-2.⁴ Based on antibody detection; commercial serodiagnosis has inconsistent sensitivity and specificity, namely 0-100% and 31-100%.⁵

* Corresponding author:
E-mail: chusna.fk@unej.ac.id
(Diana Chusna Mufida)

Table 1. Prediction and antigenicity test of B-cell linear epitope of Ag85 Complex

Name	Start	End	Peptide	Length	Antigenicity (T=0.4)	
					Score	Interpretation
Ag85A	35	49	VGGTATAGAFSRPGL	15	0.6074	Antigen
	54	63	LQVPSPSMGR	10	1.0688	Antigen
	70	76	QSGGANS	7	2.6007	Antigen
	86	99	RAQDDFSGWDINTP	14	0.958	Antigen
	101	104	FEWY	4	-	Non-Antigen
	106	106	Q	1	-	Non-Antigen
	115	123	VGGQSSFYS	9	0.5325	Antigen
	126	135	YQPACGKAGC	10	1.9389	Antigen
	137	137	T	1	-	Non-Antigen
	157	163	HVKPTGS	7	0.8572	Antigen
	196	203	LDPSQAMG	8	0.269	Non-Antigen
	212	235	GDAGGYKASDMWGPKEPAWQRND	24	0.7449	Antigen
	256	267	NGKPSDLGGNNL	12	1.6823	Antigen
	286	308	AYNAGGGHNGVDFPDGTHSWE	23	0.8642	Antigen
	316	316	A	1	-	Non-Antigen
	319	320	PD	2	-	Non-Antigen
	322	322	Q	1	-	Non-Antigen
Ag85B	33	46	GGAATAGAFSRPGL	14	0.5111	Antigen
	51	60	LQVPSPSMGR	10	1.0688	Antigen
	67	74	QSGGNNSP	8	1.6042	Antigen
	83	96	RAQDDYNGWDINTP	14	1.2099	Antigen
	113	132	GGQSSFYSDWYSPACGKAGC	20	1.0201	Antigen
	134	134	T	1	-	Non-Antigen
	153	162	RAVKPTGSAA	10	0.4297	Antigen
	194	201	DPSQGMGP	8	0.7686	Antigen
	209	237	GDAGGYKAADMWGPSSDPAWERNPTQQI	29	0.6896	Antigen
	253	264	NGTPNELGGANI	12	0.4363	Antigen
	283	289	AYNAAGG	7	1.5285	Antigen
	295	305	NFPNGTHSWE	11	0.3702	Non-Antigen
Ag85C	316	317	GD	2	-	Non-Antigen
	15	16	TT	2	-	Non-Antigen
	37	52	TFGGPATAGAFSRPGL	16	- 0.0863	Non-Antigen
	59	59	V	1	-	Non-Antigen
	61	65	SASMG	5	-	Non-Antigen
	72	78	FQGGGPH	7	1.4682	Antigen
	87	105	RAQDDYNGWDINTPAFEEY	19	0.9835	Antigen
	107	107	Q	1	-	Non-Antigen
	117	139	GGQSSFYTDWYQPSQSNQNYTY	23	0.5401	Antigen
	156	166	NKGVSTGNAA	11	0.5434	Antigen
	172	172	S	1	-	Non-Antigen
	184	190	PQQFPYA	7	0.2671	Non-Antigen
	197	204	LNPSEWW	8	- 0.7119	Non-Antigen
	213	239	NDSGGYNANSMWGPSSDPAWKRNDPMV	27	0.7312	Antigen
	257	269	NGTPSDLGGDNIP	13	1.1086	Antigen
	283	310	TFRDTYAADGGRNGVFNPNGTHSWPY	28	0.663	Antigen

Furthermore, the low sensitivity and specificity in using protein antigens in serological assays allow cross-reactions. The replacement of antigenic proteins with more specific epitopes recognized by the immune system can be used to develop more effective serological assays.⁶ A study evaluated serodiagnosis ELISA to detect antibodies in *M. tuberculosis* using a combination of epitopes RD1 and RD2 antigens resulted in a sensitivity of 83.3% for acid fast bacilli (+), 62.5 % for acid fast bacilli (-), and a specificity of 100%.⁷ In its application, Epitope Diagnostics, Inc., San Diego, USA has developed an epitope diagnostic kit product using the ELISA technique for the detection of *Novel coronavirus*

antibodies with a sensitivity up to 94% for IgM and 100% for IgG detection.⁸

The initial concept of the diagnostic design was performed by mapping the B cell epitope within silico studies using computational and bioinformatics. Furthermore, antigenic and immunogenic B cell epitopes are used as diagnostic antigens.⁹ There is currently little information about the B cell epitope of antigen 85 complexes that can be used to develop a tuberculosis diagnosis. Therefore, this study predicts the epitope of the Ag85 complex, which is a potential diagnostic antigen.

Table 2. Physicochemical properties of B-cell linear epitope of Ag85A

Name	Start	End	molecular weight (Da)	Instability Index		GRAVY score	
				Score	Interpretation	Score	Interpretation
Ag85A	35	49	1361.52	26.26	stable	0.42	hydrophobic
	54	63	1071.26	135.78	unstable	- 0.33	hydrophilic
	70	76	619.59	76.84	unstable	- 1.086	hydrophilic
	86	99	1621.68	20.41	stable	- 1.236	hydrophilic
	115	123	930.97	119.61	unstable	- 0.111	hydrophilic
	126	135	997.15	82.97	unstable	- 0.25	hydrophilic
	157	163	724.81	-18.44	stable	- 0.914	hydrophilic
	212	235	2651.81	28.06	stable	- 1.592	hydrophilic
	256	267	1185.26	2.54	stable	- 1.158	hydrophilic
	286	308	2422.47	35.92	stable	- 0.809	hydrophilic

Table 3. Physicochemical properties of B-cell linear epitope of Ag85B

Name	Start	End	molecular weight (Da)	Instability Index		GRAVY score	
				Score	Interpretation	Score	Interpretation
Ag85B	33	46	1232.36	33.49	stable	0.329	hydrophobic
	51	60	1071.26	135.78	unstable	- 0.33	hydrophilic
	67	74	759.73	123.41	unstable	- 1.812	hydrophilic
	83	96	1664.71	15.06	stable	-1.721	hydrophilic
	113	132	2071.22	112.9	unstable	- 0.47	hydrophilic
	153	162	957.1	-9.91	stable	- 0.23	hydrophilic
	194	201	787.84	56.9	unstable	- 1.238	hydrophilic
	209	237	3121.3	32.7	stable	- 1.193	hydrophilic
	253	264	1156.22	29.39	stable	- 0.617	hydrophilic
	283	289	622.64	26.2	stable	- 0.029	hydrophilic

Table 4. Physicochemical properties of B-cell linear epitope of Ag85C

Name	Start	End	molecular weight (Da)	Instability Index		GRAVY score	
				Score	Interpretation	Score	Interpretation
Ag85C	72	78	698.74	43.83	unstable	- 0.957	hydrophilic
	87	105	2304.37	41.02	unstable	- 1.463	hydrophilic
	117	139	2678.72	86.89	unstable	- 1.53	hydrophilic
	156	166	1015.09	47.41	unstable	- 0.636	hydrophilic
	213	239	2954.15	49.6	unstable	- 1.244	hydrophilic
	257	269	1256.29	47.03	unstable	- 0.892	hydrophilic
	283	310	3145.36	17.54	stable	- 0.939	hydrophilic

MATERIALS AND METHODS

Sequence Preparation

This research was going on November 2021-January 2022 online-virtually from the Faculty of Medicine, University of Jember, Jember, East Java. This study is an experimental research and the samples used were taken from the NCBI protein bank with access numbers P9WQP3 for Ag85A, P9WQP1 for Ag85B, and P9WQN9 for Ag85C. VaxiJen v2.0 was used to test the antigenicity of Ag85 complex sequence samples (Ag85A, Ag85B, Ag85C). VaxiJen v2.0 server (<https://www.ddg-pharmfac.net/vaxijen>) predicts protective antigens of bacteria, viruses, and tumors with an accuracy of 70-97%.¹⁰ This works with an auto cross-covariance (ACC) transformation approach of protein sequences based on the primary physicochemical properties of amino acids. Protein sequences are entered in fasta form, and bacteria were selected as target organisms, while the threshold value was set at 0.4.

B-cell Epitope Prediction and Antigenicity Test

B-cell epitopes were predicted from protein sequence using the IEDB (<http://tools.iedb.org/bcell/>). The method used is linear BepiPred 1.0 with a threshold of 0.35. Furthermore, BepiPred by default is provided by the IEDB server for predicting B cell linear epitope locations of proteins with 75% specificity and 49% sensitivity at a threshold of 0.35. It predicts the location of the epitope using a combination approach of the HMM algorithm (Hidden Markov Model), Parker hydrophilicity, and Levitt secondary structure.¹¹ Then, the predicted epitopes were tested for antigenicity using the VaxiJen v2.0 server (<https://www.ddg-pharmfac.net/vaxijen>). The inputted sequence is a residual type with a threshold of 0.4.

Physicochemical Test

The physicochemical characteristics were determined by testing the linear epitopes of B cells classified as antigenic using ExPASy ProtParam (<http://www.expasy.org/tools/protparam.html>), which is

a reliable tool for computing various physicochemical properties that can be deduced from a protein sequence. Furthermore, ProtParam sums up the contributions of the different amino acids, not taking into account secondary or tertiary structure. A physicochemical test was used to determine the immunogenicity characteristics of the predicted epitope. Its sought were molecular weight, instability index, and GRAVY score.

Alignment of B-cell Epitope with Indonesian Strain

The linear epitopes of B cells Ag85 complex had a similarity percentage of 85.71%-100% with the strains in Indonesia. Also, the e-values obtained vary from the highest 85×10^{-3} to the smallest 3×10^{-26} . Table 5 shows details of alignment results with Indonesian strains.

Table 5. Alignment of epitope with *M. tuberculosis* Indonesian strain

Name	Start	End	Str. Beijing/NITR203		Str. CAS/NITR204		Str. Haarlem/NITR202		Str. EAI5/NITR206	
			e-value	Percent identity	e-value	Percent identity	e-value	Percent identity	e-value	Percent identity
Ag85A	86	99	2×10^{-10}	100%	2×10^{-10}	100%	1×10^{-7}	85.71%	1×10^{-8}	92.86%
	157	163	85×10^{-3}	100%	85×10^{-3}	100%	85×10^{-3}	100%	85×10^{-3}	100%
	212	235	3×10^{-21}	100%	3×10^{-21}	100%	3×10^{-21}	100%	3×10^{-21}	100%
	256	267	1×10^{-6}	100%	1×10^{-6}	100%	1×10^{-6}	100%	1×10^{-6}	100%
	286	308	3×10^{-19}	100%	3×10^{-19}	100%	3×10^{-19}	100%	3×10^{-19}	100%
Ag85B	83	96	8×10^{-11}	100%	8×10^{-11}	100%	2×10^{-9}	92.86%	8×10^{-11}	100%
	153	162	4×10^{-4}	100%	4×10^{-4}	100%	4×10^{-4}	100%	4×10^{-4}	100%
	209	237	3×10^{-26}	100%	3×10^{-26}	100%	3×10^{-26}	100%	3×10^{-26}	100%
	253	264	9×10^{-7}	100%	9×10^{-7}	100%	9×10^{-7}	100%	9×10^{-7}	100%
	283	289	1×10^{-2}	100%	1×10^{-2}	100%	1×10^{-2}	100%	1×10^{-2}	100%
Ag85C	283	310	2×10^{-25}	100%	2×10^{-25}	100%	2×10^{-25}	100%	2×10^{-25}	100%

Sequence Alignment

The candidate epitope were aligned from the strain of Ag85 complex in Indonesia (str. Beijing, str. Haarlem, str. CAS, str. EAI) using BLASTP NCBI (<https://blast.ncbi.nlm.nih.gov/Blast.cgi>).

RESULTS

Antigenicity of Ag85 Complex Sequence

The results showed that the total value exceeded the threshold of 0.4 with details of 0.5259, 0.5842, 0.4402 on Ag85A, A85B, and Ag85C, respectively.

Prediction and Antigenicity Test of Ag85 Complex B-cell Epitope

The prediction results using IEDB showed only 10 of 17 Ag85A epitopes, 10 of 13 Ag85B epitopes, and 7 of 15 Ag85C epitopes are antigenic and can respond to B cells. Table 1 show the detailed score of predicted B cell epitope antigenicity.

Physicochemical Test of Ag85 Complex B-cell Epitope

The antigenic epitopes were subjected to a physicochemical test with ExPASy ProtParam. The results showed that each linear epitope of B cells had varying molecular weights from 619.59 to 3145.36 Da. The stability index and GRAVY score obtained 13 stable and 14 unstable epitopes, as well as 25 hydrophilic and 2 hydrophobic epitopes. Also, there are 11 stable and hydrophilic B cell epitopes, namely Ag85A and Ag85B with 5 epitopes for each and Ag85C with an epitope. Tables 2-4 show the results.

DISCUSSION

Antigenicity of Ag85 Complex Sequence

The three antigenicity values showed that the Ag85 complex protein sequence was antigenic, implying that it could bind to an antibody. TB antibodies formed due to the interaction of costimulatory signals of B and Th1 cells previously activated by antigens.¹² Furthermore, the serum immunoglobulin titers in TB patients are elevated by 90% against mycobacterial antigens at the time of clinical presentation. This correlation between the antibody response and active TB disease has led to the development of antibodies as diagnostic markers.¹³ The results of this study are also in line with the development of the Ag85 complex as a diagnostic antigen for antibody detection. Meanwhile, the previous study by Kumar et al. (2008) successfully evaluated the accuracy of Ag85 complex for antibody detection in ELISA serodiagnosis in children aged 0-18 years.¹⁴ Another study by Mani et al. (2016), using a microchip-based TB ELISA (MTBE) technique that can detect antibodies in less than 15 minutes, showed that the sensitivity and specificity of Ag85A are 52% and 76%, respectively.¹⁵ The result showed that Ag85B has the highest antigenicity score, and it is a potential biomarker for the diagnosis of TB in its complexity because this protein is the most secreted (40%) of *M. tuberculosis*.¹⁶

Prediction and Antigenicity Test of Ag85 Complex B-cell Epitope

Fortyfive epitope regions of Ag85A, Ag85B, and Ag85C were identified through the prediction of B cell epitopes from Ag85 complex samples. As a candidate for

a diagnostic antigen epitope, antigenicity is essential. The epitope prediction on the Ag85 complex was continued with an antigenicity test using Vaxijen v2.0. The results of the B cell epitope showed that the antigens Ag85A, Ag85B, and Ag85C contain 10, 10, and 7 antigenic epitopes, respectively. This study's linear epitope antigenicity value of Ag85 complex B cells has a wide range of score variations from 0.4297 to 2.6007. It shows that antigenicity is not the only factor in planning the antigen epitope as diagnosis, but there is another factor that affects, like immunogenicity.⁹ Because epitopes are immunogenic, they can activate specific antibodies in the body. By following multi-epitope design studies for diagnosis, antigens exhibiting high antigenicity and immunogenicity were utilized.¹⁷⁻²⁰

Physicochemical Test of Ag85 Complex B-cell Epitope

A total of 27 antigenic epitopes were subjected to physicochemical tests to determine immunogenicity characteristics, such as molecular weight, instability index, and GRAVY score. These results obtained various molecular weights from 619.59 Da to 3145.36 Da. Furthermore, the immunological approach states that molecules less than 10 kDa are weakly immunogenic. Molecules with a molecular weight of more than 100 kDa (macromolecules) are highly potent immunogens.²¹ It was discovered that the highest epitope molecular weight was 3145.36 Da. Meanwhile, several studies showed that using multiple linker-associated epitopes produces molecular weights above 10 kDa and results in higher ELISA sensitivity.^{17,18,22} The diagnostic design uses multiple epitopes connected by a flexible linker (Gly-Ser-Gly-Ser-Gly).¹⁸ Different epitopes can be used as diagnostic markers to achieve high performance, as the use of multi-epitope peptides can express high density resulting in increased sensitivity and specificity.¹⁷

The order physicochemical properties obtained from this study were 13 stable and 14 unstable epitopes. Meanwhile, the stable epitopes will retain their structure when binding to antibodies or in response to physical and chemical environment changes.²³ Several studies concluded that hyper-stable proteins lose their capacity to induce antibodies due to inefficient processing and presentation.²⁴ Similarly, low stability makes proteins less immunogenic in antibody production due to the formation of tertiary structures leading to loss of B cell epitope.²⁵

Most of the epitopes in the GRAVY score were interpreted as hydrophilic residues. Several studies stated that the epitopes used as diagnostic antigens are hydrophilic.^{18,20} The predicted hydrophilicity parameters show the position of the residue across the antigen protein sequence. Protein antigens have a globular (spherical) tertiary structure. The residue in this nonpolar (hydrophobic) and polar (hydrophilic) structure tends to be on the inside and outer surface of the protein. Hydrophilic residues are discovered on the surface of the antigen, which is more easily exposed (surface-exposed domain).²⁴ According to Abbas et al. (2014) and Ahmad et al. (2019), the linear epitope is on the outer surface of the antigen; hence, it is easily recognized by part of the antibody structure (antigen-binding site).^{12,27}

Alignment of B-cell Epitope with Indonesian Strain

Eleven stable and hydrophilic epitopes were aligned using BLASTP on NCBI with complex Ag85 sequences from strains circulating in Indonesia. Therefore, the potential for developing serodiagnosis in Indonesia can be determined based on the percentage of similarity between each epitope derived from this alignment. The strains circulating in Indonesia and the NCBI database are the Beijing NITR203, the Central Asian NITR204, the Haarlem NITR202, and the East African Indian strain/NITR206. They were isolated from South India because the complex Ag85 protein sequences from Indonesian isolates were not yet available in the database.²⁸ The results indicated that the similarity was relatively high, ranging from 85.71% to 100%. Furthermore, a similarity percentage higher than 70% has a possibility of 90% similarity in the biological process, molecular function, and cellular component.²⁹

Three epitopes are more significant because they have a low e-value, namely 212GDAGGYKASDMWGPKEPAWQRND₂₃₅ from the Ag85A epitope with a value of 3×10^{-21} , 209GDAGGYKAADMWGPSSDPAW-ERNPTQQI₂₃₇ from the Ag85B with a value of 3×10^{-26} , and 283TFRDTYAADGGRNGVFNFPPNGTHSWPY₃₁₀ from the Ag85C with a value 2×10^{-25} . The e-value is an estimate that provides a statistical measure of the two sequences. It was discovered that the lower the e-value, the more significant the score and its alignment.³⁰ Additionally, the three epitopes have 100% similarity with all strains; hence, they were universal antigens and can be developed into serodiagnostic antigens in Indonesia. However, the results of research using the in-silico method are only predictions of amino acid sequence results that need to be revalidated with other research methods such as in vivo and in vitro with Indonesian isolates to prove the accuracy of the predictions.

The limitation of the result of this study using the in-silico method is only predicting the result of antigenic and immunogenic amino acid sequence. As an immunoassay development, it is necessary to stimulate the interaction between the ligand protein and the receptor protein to assess the binding score in 3D between the epitope and BCR immunoglobulin. Further studies need to be carried out in vivo with the construction, expression, purification of recombinant protein, followed by ELISA antigen-antibody immunoassay test and western blot analysis to prove the accuracy of these prediction.

CONCLUSION

There are three B cell epitopes of the Ag85 complex, namely Ag85A (212-235), Ag85B (209-237), and Ag85C (283-310), which are universal antigens and can be developed into diagnostic antigens in Indonesia. However, the results of research using the in silico method are only predictions of amino acid sequence results that need to be revalidated with other research methods such as in vivo and in vitro with Indonesian isolates to prove the accuracy of the predictions.

ACKNOWLEDGMENTS

The authors express our gratitude to all those involved in writing this article especially to Dr. dr. Yunita Armiyanti, M.Kes Sp.Par.K and dr. Rosita Dewi, M.Biotek who guided and provided the research idea. This research received no specific grant.

REFERENCES

- WHO. TB burden report 2018. Vol. 63, World Health Organization. 2018. 476 p. Available from: <https://apps.who.int/iris/handle/10665/274453>
- KEMENKES RI. Profil Kesehatan Indonesia 2020. Kementrian Kesehatan Republik Indonesia. 2021. 139 p. Available from: <https://pusdatin.kemkes.go.id/resources/download/pusdatin/profil-kesehatan-indonesia/Profil-Kesehatan-Indonesia-Tahun-2020.pdf>
- Karbalaei M, Soleimanpour S, Rezaee SA. Antigen 85 complex as a powerful *Mycobacterium tuberculosis* immunogene: Biology, immune-pathogenicity, applications in diagnosis, and vaccine design. *Microb Pathog*. 2017;112:20–9. doi: 10.1016/j.micpath.2017.08.040
- Huygen K. The immunodominant T-cell epitopes of the mycolyl-transferases of the antigen 85 complex of *M. tuberculosis*. *Front Immunol*. 2014;5(JUL):1–11. doi: 10.3389/fimmu.2014.00321
- Steingart KR, Flores LL, Dendukuri N, Schiller I, Laal S, Ramsay A, et al. Commercial Serological tests for the diagnosis of active pulmonary and extrapulmonary tuberculosis: An updated systematic review and Meta-Analysis. *PLoS Med*. 2011;8(8). doi: 10.1371/journal.pmed.1001062
- Carmona SJ, Sartor PA, Leguizamón MS, Campetella OE, Agüero F. Diagnostic Peptide Discovery: Prioritization of Pathogen Diagnostic Markers Using Multiple Features. *PLoS One*. 2012;7(12). doi: 10.1371/journal.pone.0050748
- Goyal B, Kumar K, Gupta D, Agarwal R, Latawa R, Sheikh JA, et al. Utility of B-cell epitopes based peptides of RD1 and RD2 antigens for immunodiagnosis of pulmonary tuberculosis. *Diagn Microbiol Infect Dis*. 2014;78(4):391–7. doi: 10.1016/j.diagmicrobio.2013.12.018
- Bundschuh C, Egger M, Wiesinger K, Gabriel C, Clodi M, Mueller T, et al. Evaluation of the EDI enzyme linked immunosorbent assays for the detection of SARS-CoV-2 IgM and IgG antibodies in human plasma. *Clin Chim Acta*. 2020;509(May):79–82. doi: 10.1016/j.cca.2020.05.047
- Hong SC, Chen H, Lee J, Park HK, Kim YS, Shin HC, et al. Ultrasensitive immunosensing of tuberculosis CFP-10 based on SPR spectroscopy. *Sensors Actuators, B Chem*. 2011;156(1):271–5. doi: 10.1016/j.snb.2011.04.032
- Dimitrov I, Atanasova M, Patronov A, Flower DR, Doytchinova I. A cohesive and integrated platform for immunogenicity prediction. *Methods Mol Biol*. 2016;1404:761–70. doi: 10.1007/978-1-4939-3389-1_50
- Larsen JEP, Lund O, Nielsen M. Improved method for predicting linear B-cell epitopes. *Immunome Res*. 2006;2(1):2. doi: 10.1186/1745-7580-2-2
- Abbas AK, Lichtman AH, Pillai S. Cellular and Molecular Immunology E-Book. 8th ed. California: Elsevier Health Sciences; 2014. Available from: <https://books.google.co.id/books?id=RWYWBAABQBAJ>
- Jacobs AJ, Mongkolsapaya J, Screaton GR, McShane H, Wilkinson RJ. Antibodies and tuberculosis. *Tuberculosis*. 2016;101:102–13. doi: 10.1016/j.tube.2016.08.001
- Kumar G, Dagur PK, Singh M, Yadav VS, Dayal R, Singh HB, et al. Diagnostic potential of Ag85C in comparison to various secretory antigens for childhood tuberculosis. *Scand J Immunol*. 2008;68(2):177–83. doi: 10.1111/j.1365-3083.2008.02133.x
- Mani V, Paleja B, Larbi K, Kumar P, Tay JA, Siew JY, et al. Microchip-based ultrafast serodiagnostic assay for tuberculosis. *Sci Rep*. 2016;6(September):1–11. doi: 10.1038/srep35845
- Lily Therese K, Gayathri R, Dhanurekha L, Sridhar R, Meenakshi N, Madhavan HN, et al. Detection of *Mycobacterium tuberculosis* directly from sputum specimens & phenotypic drug resistance pattern of *M. tuberculosis* isolates from suspected tuberculosis patients in Chennai. *Indian J Med Res*. 2012;135(5):778–82.
- Hajissa K, Zakaria R, Suppian R, Mohamed Z. Design and evaluation of a recombinant multi-epitope antigen for serodiagnosis of *Toxoplasma gondii* infection in humans. *Parasites and Vectors*. 2015;8(1):1–5. doi: 10.1186/s13071-015-0932-0
- Ebrahimi M, Seyyedtabaei SJ, Ranjbar MM, Tahvildar-biderouni F, Javadi Mamaghani A. Designing and Modeling of Multi-epitope Proteins for Diagnosis of *Toxocara canis* Infection. *Int J Pept Res Ther*. 2020;26(3):1371–80. doi: 10.1007/s10989-019-09940-1
- Ebrahimipour M, Afgar A, Barati M, Mohammadi MA, Harandi MF. Evaluation of the antigenic epitopes of EgAgB/1 and EgAgB/4 subunit antigens in G1 and G6 genotypes of *Echinococcus granulosus* using bioinformatics. *Gene Reports*. 2019;15(December 2018):100361. doi: 10.1016/j.genrep.2019.01.002
- Mahboobi M, Sedighian H, Malekara E, Khalili S, Rahbar MR, Ahmadi Zanoos K, et al. Harnessing an Integrative In Silico Approach to Engage Highly Immunogenic Peptides in an Antigen Design Against Epsilon Toxin (ETX) of *Clostridium perfringens*. *Int J Pept Res Ther*. 2021;27(2):1019–26. doi: 10.1007/s10989-020-10147-y
- Suardana IBK. Diktat Immunologi Dasar Sistem Imun. 2017;1–36. Available from: https://simdos.unud.ac.id/uploads/file_pendidikan_1_dir/284a0e69155751dc6c459b07f14bc03c.pdf
- Shen G, Behera D, Bhalla M, Nadas A, Laal S. Peptide-based antibody detection for tuberculosis diagnosis. *Clin Vaccine Immunol*. 2009;16(1):49–54. doi: 10.1128/CVI.00334-08
- Scheibhofer S, Laimer J, Machado Y, Weiss R, Thalhamer J. Influence of protein fold stability on immunogenicity and its implications for vaccine design. *Expert Rev Vaccines*. 2017;16(5):479–89. doi: 10.1080/14760584.2017.1306441

24. MacHado Y, Freier R, Scheiblhofer S, Thalhamer T, Mayr M, Briza P, et al. Fold stability during endolysosomal acidification is a key factor for allergenicity and immunogenicity of the major birch pollen allergen. *J Allergy Clin Immunol.* 2016;137(5):1525–34.
doi: 10.1016/j.jaci.2015.09.026
25. Thalhamer T, Dobias H, Stepanoska T, Pröll M, Stutz H, Dissertori O, et al. Designing hypoallergenic derivatives for allergy treatment by means of in silico mutation and screening. *J Allergy Clin Immunol.* 2010;125(4).
doi: 10.1016/j.jaci.2010.01.031
26. Subekti D, Artama W, Poerwanto S, Sulistyaningsih E, Sari Y. Analisis Imunogenitas Protein GRA1 dari Hasil Kloning Gen GRA 1 Takizoit *Toxoplasma gondi*. 2012;11(April).
27. Ahmad B, Ashfaq UA, Rahman M ur, Masoud MS, Yousaf MZ. Conserved B and T cell epitopes prediction of ebola virus glycoprotein for vaccine development: An immuno-informatics approach. *Microb Pathog.* 2019;132(April 2018):243–53.
doi: 10.1016/j.micpath.2019.05.010
28. Narayanan S, Deshpande U. Whole-genome sequences of four clinical isolates of *Mycobacterium tuberculosis* from Tamil Nadu, south India. *Genome Announc.* 2013;1(3):4430.
doi: 10.1128/genomeA.00186-13
29. Joshi T, Xu D. Quantitative assessment of relationship between sequence similarity and function similarity. *BMC Genomics.* 2007;8:1–10.
doi: 10.1186/1471-2164-8-222
30. Fassler J, Cooper P. BLAST Glossary. 2011;(Md):1–8.

JOURNAL OF BIOMEDICINE AND TRANSLATIONAL RESEARCH

Available online at JBTR website: <https://jbtr.fk.undip.ac.id>

Copyright©2023 by Faculty of Medicine Universitas Diponegoro, Indonesian Society of Human Genetics and Indonesian Society of Internal Medicine

Original Research Article

Detection of *Blastocystis hominis* by Method of Cultivation in The Feces of Orphanage Children in Pekanbaru, Riau Province, Indonesia

Esy Maryanti^{1*}, Suri Dwi Lesmana¹, Wira Firja², Muhammad Devlin², Mislindawati¹, Forman Erwin Siagian³

¹Department of Parasitology, Faculty of Medicine, Universitas Riau, Pekanbaru, Riau, Indonesia

²Faculty of Medicine, Universitas Riau, Pekanbaru, Riau, Indonesia

³Department of Parasitology Faculty of Medicine, Universitas Kristen Indonesia, Jakarta, Indonesia

Article Info

History

Received: 16 Dec 2022

Accepted: 20 Mar 2023

Available: 30 Apr 2023

Abstract

Background: *Blastocystis hominis* is an intestinal protozoan that can infect humans and animals. The distribution coverage is very wide and is transmitted through the fecal-oral route. The incidence of blastocystosis due to *Blastocystis hominis* is higher in developing countries because it is associated with poor hygiene practice, inadequate sanitation, close contact with pets domesticated animals and or contaminated food. *Blastocystis hominis* infection can cause clinical manifestations, from asymptomatic to chronic diarrhea, depending on the *Blastocystis* subtype and the patient's immune system.

Objective: The aim of this study was to detect and determine the incidence of *Blastocystis hominis* infection in the feces of children at the Pekanbaru Orphanage using the culture method.

Methods: This research was a descriptive study with a cross-sectional design, that aims to detection of *Blastocystis* by the modified Jone's Medium culture method but using sheep's serum. The sample is the feces of children from nine orphanages in Pekanbaru. The data is shown in the form of figures and distribution frequency tables.

Results: A total of 95 children's stool samples were examined from 9 orphanages in Pekanbaru, it was found that 63 children (66.3%) were positive for *Blastocystis hominis* using the culture method, positive *Blastocystis hominis* was found more in female than male, and based on age group, 6-12 years is almost the same as in the age group 13-17 years. Generally, the source of drinking water in orphanages is refilled drinking water and all orphanages have cats as pets, and a few have chickens, birds, and goats as pets

Conclusion: High incidence of *Blastocystis hominis* (66.3%) can be detected in the feces of Pekanbaru orphanage children using the culture method.

Keywords: *Blastocystis*; children; culture; orphanage.

Permalink/ DOI: <https://doi.org/10.14710/jbtr.v9i1.16470>

INTRODUCTION

Blastocystis hominis is an intestinal protozoan that is commonly found in humans and animals. Its distribution coverage is very wide and this parasite is transmitted by the fecal-oral route. The prevalence of *Blastocystis hominis* is more in developing countries than in developed countries, in developing countries the prevalence of *Blastocystis hominis* is more than 60% while in developed countries it is 5% - 20%.¹ The high incidence of *Blastocystis hominis* in developing

countries is closely related to poor personal hygiene and inappropriate sanitation, frequent exposure to or contact with pets domesticated animals, transmission occurs through food and beverage contaminated with *Blastocystis hominis*.^{1,2}

* Corresponding author:

E-mail: esy.maryanti@lecturer.unri.ac.id

(Esy Maryanti)

Blastocystosis or *Blastocystis hominis* infection can cause clinical manifestations from asymptomatic to symptoms of gastrointestinal disorders such as nausea, vomiting, bloating, abdominal pain, flatulence, acute and chronic diarrhea and sometimes constipation. This parasitic infection is sometimes associated with irritable bowel syndrome and inflammatory bowel disease.^{3,4} Besides gastrointestinal symptoms, it has also been reported to cause dermatological symptoms such as itching and rashes of the skin along with gastrointestinal symptoms.⁵ *Blastocystis hominis* is a protozoan that lives in the intestines, is a single-celled eukaryote, anaerobic. This parasite is a polymorphic protozoan because it has many forms, based on the literature in general there are four forms, namely vacuolar, granular, ameboid and cystic forms.^{2,6} Vacuolar and ameboid forms are forms that are often found in feces and cultured products.² Based on the literature, it has been reported that there are 32 subtypes of *Blastocystis hominis*.⁷ and the clinical manifestations in infected individuals depend on the subtype that infects and *Blastocystis* infection has been reported to occur in immunosuppressed patients such patients who received kidney transplants. It was also reported that *Blastocystis* was more commonly found in healthy people than people with inflammatory bowel disease and based on the literature it was also stated that people who contain *Blastocystis* in their intestines have a high bacterial diversity in their intestines, which means that the existence of *Blastocystis* will have a beneficial effect on the gut microbiota.⁸ However, the effect of *Blastocystis* also varies depending on the infecting subtype, therefore *Blastocystis hominis* is still a controversy whether it is pathogenic or commensal because of the very wide genetic variation.⁴

Diagnostic examination for *Blastocystis hominis* can be carried out by direct microscopic examination but this microscopic examination is very subjective depending on the skills and experience of the examiner in identifying *Blastocystis hominis*. The size and morphology of *Blastocystis hominis* varies greatly during its life cycle because these protozoa have a variety of shapes that are sometimes very similar to other intestinal protozoa or similar to contaminants or fecal debris, this leads to misdiagnosis. Several studies have reported methods for diagnostic *Blastocystis*; direct microscopic, culture, serology (ELISA) and molecular methods by using PCR. However, the culture method is the recommended method for the diagnosis of *Blastocystis*.^{2,9,10} Children who live in urban dense area with poor sanitation and inadequate hygiene behavior, eg., orphanages are children who are at risk for infection with *Blastocystis hominis*. Based on this, the researchers were interested in conducting research to detect *Blastocystis* in children's feces using the culture method.

MATERIALS AND METHODS

This research is a descriptive study with a cross-sectional design. The samples of this study were collected from the feces of children from nine orphanages in Pekanbaru City and examination of stool samples was carried out at the Parasitology Laboratory of the Faculty of Medicine, Riau University from August – October 2022. The stool that has been collected in a sterile tube is immediately taken to the Parasitology

Laboratory and examined within 12 hours after the stool is excreted. Data containing the identity of the subject and the environment of the orphanage were obtained from the administrators of the orphanage. Stool examination was carried out directly microscopically and cultured. *Blastocystis* culture used modified Jone's medium,¹¹ but in this study horse serum was replaced with sheep serum. After being planted in the media, it was incubated at 37°C for 48 – 72 hours. The culture results were then read after 48 hours with iodine's stain and then examined with a light microscope with a magnification of 400x. This study passed the ethical review by the ethical review board for medicine and health research Faculty of Medicine, Universitas Riau (No: B/115/UN19.5.1.18/UEPKK/2022).

RESULTS

In this study, 95 samples of orphanage children's feces were collected from 9 orphanages in Pekanbaru City. The characteristics of the orphanage children who are the subjects of this study are as shown in table 1 below.

Table 1. Characteristics of the subjects

Characteristics	N (95)	Percentage
Sex		
- Male	58	61.1%
- Female	37	38.9%
Age groups		
- ≤ 5 years	5	5.3%
- 6 – 12 years	77	81 %
- 13 – 17 years	13	13.7%

Table 1 shows that most of the subjects were male (61.1%) with the largest age group being the 6-12-year-old group (81%). A total of 95 children's stools examined from 9 orphanages obtained *Blastocystis* culture results as shown in table 2 below.

Table 2. Distributions of positive *Blastocystis* based on orphanage

Orphanage	N	<i>Blastocystis</i> (+)	
		Frequency	%
1	19	12	63.2%
2	8	5	62.5%
3	6	5	83.3%
4	10	6	60.0%
5	4	4	100%
6	12	4	33.3%
7	9	7	77.8%
8	9	5	55.6%
9	18	15	83.3%
Total	95	63	66.3%

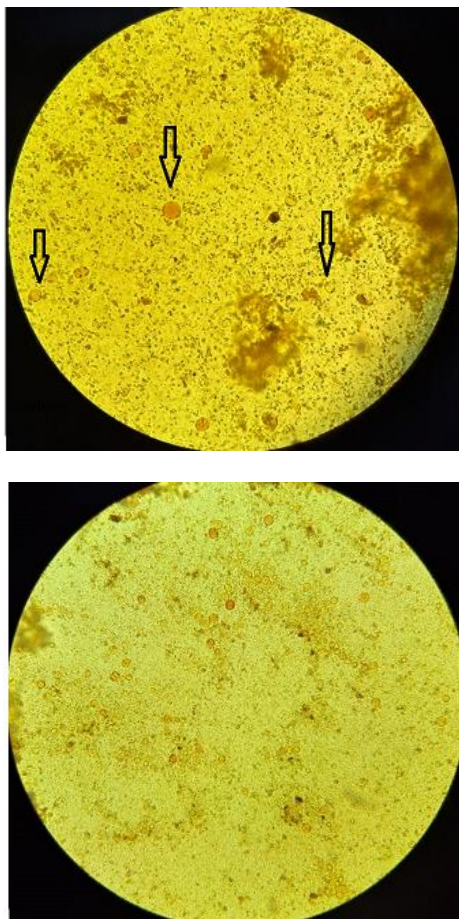
In table 2. it can be seen that from 95 stool samples examined, 63 children or 66.3% were positive for *Blastocystis hominis* by culture method.

Table 3. Distributions of positive *Blastocystis* based on sex and age groups

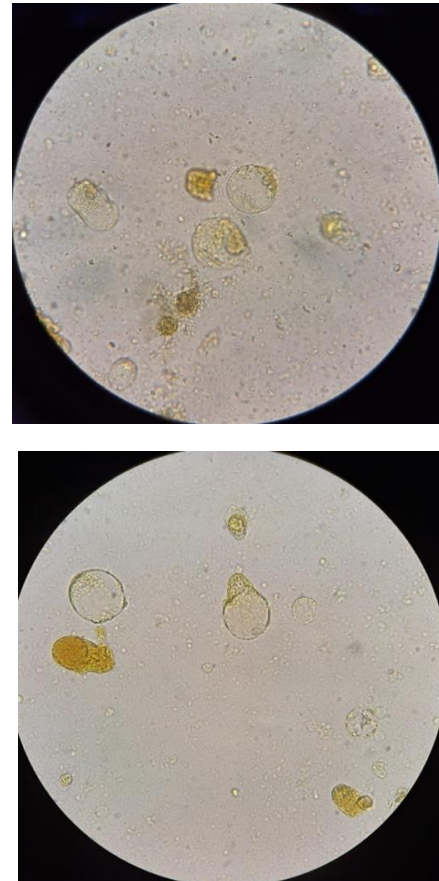
Variable	Culture of <i>Blastocystis</i>	
	Positive	Negative
Sex		
- Male	37	21
- Female	26	11
Age groups		
- ≤ 5	1	4
- 6 - 12	53	24
- 13 - 17	9	4

Based on table 3, it can be seen that there are many positive results in male or boys, but if it is based on the proportion of boys and girls, it is found that more girls are infected than boys. Based on age, the 6-12-year-old group detected more *Blastocystis hominis*, but based on the proportion of incidence of *Blastocystis hominis* infection in the age group 6-12 years it was not much different from the age group 13-17 years, namely 68.8% and 69.2%.

Figure 1 shows the results of the culture of *Blastocystis hominis* using Iodine's staining, from the image it appears that there are various sizes and shapes of *Blastocystis hominis* that grow in various shapes and most of them are vacuoles. Microscopic examination was carried out after 48 hours in culture and viewed with a light microscope with a magnification of 400x.

**Figure 1.** *Blastocystis hominis* with Iodine's stain from culture (400x magnification)

In this study, subcultures were also carried out, the results of the first culture were cultured again and after 48 hours viewed under a light microscope with a magnification of 400x. (figure 2). The picture shows that *Blastocystis hominis* has an amoeboid shape and is larger than the first culture results. Microscopic examination from culture using a light microscope with a magnification of 400x.

**Figure 2.** *Blastocystis* subculture showed amoeboid and vacuole forms using iodine's stain with a magnification of 400x

DISCUSSION

In this study, it was found that 66.3% or 63 samples from 95 children of orphanage were positive for *Blastocystis hominis* using the culture method; the high incidence of *Blastocystis hominis* infection was confirmed. In a study in Iran, 21.09% data were positive for *Blastocystis* in patients who did not have diarrhea.¹² In a study in Mugla, Turkey, the incidence of *Blastocystis* in school-age children was 35 out of 468 (7.4%),¹³ and a 2021 study in six countries (Azerbaijan, Czechia, Jordan, Nigeria, Sudan and Tanzania) found an incidence of *Blastocystis* in children was 36%¹⁴ and another study in Jakarta Indonesia found that the incidence of *Blastocystis* in primary school-aged children was 52.5%,⁹ This is caused by many factors, possibly because orphanage children have inappropriate hygiene behavior, life in an orphanage with many children and a crowded environment and lack of attention to personal hygiene can increase the risk of being infected with *Blastocystis*. In addition, all children in the nine orphanages in this study had cats as pets. Based on the literature, cats can act as reservoir host for this protozoa, the close contact between humans and cats makes it easy for disease transmission and it can caused zoonoses.^{2,15}

Blastocystis can infect male or female, in a study by Sankur et al, it was found that *Blastocystis* infection in males and females was almost the same.¹³ Data from some literatures show that boys are more infected than girls.^{3,16-19} The reason for this perhaps because boys prefer to play outside the house and have inappropriate personal hygiene,¹⁷ but in this study it was found that girls were more infected. These results are also the same as studies in China and Myanmar where there were more *Blastocystis* infections in girls (7.9%) than boys (4.8%).²⁰ Even though based on observations most boys prefer to play with animals such as cats, chickens and goats, compared to girls who are usually afraid or feel anxious or disgusted when holding pets. Based on these results, the possibility of *Blastocystis hominis* infection in girls can be obtained from factors such as food and drink contamination by *Blastocystis* cysts and poor personal hygiene behavior.^{21,22}

In this study, there was no difference in the age group infected with *Blastocystis* between the age group 6-12 years and 13-17 years, this is the same as the study in Argentina by Candela found there was no difference in intestinal parasite infection between the age group 6-12 years and the group aged 13 – 19 years.²³ Infection of *Blastocystis* is associated with several factors such as consumption of contaminated food, poor quality of drinking water, and close contact with animals, poor personal hygiene habits, and inappropriate sanitation.^{3,4,14-16} The results of this study are different from studies in China and Myanmar, where the age group of 7-12 years is the age group with the most positive *Blastocystis*.²⁰ Based on the literature, primary school age group is the group of children who are in their peak period of playing outside the home, these primary school age children also still have less knowledge about maintaining personal hygiene so they are easily infected with parasitic infections but in this study there was no difference between age groups 6 – 12 years with 13 – 17 years.²⁴ All the orphanages studied had children who were positive for *Blastocystis* with different proportions ranging from 33.3% to 100%. All children examined had no symptoms or asymptomatic. *Blastocystis* is still not certain whether commensal or pathogenic and this is still controversial, based on the literature the clinical symptoms of *Blastocystis* infection are very wide ranging from asymptomatic to acute and chronic diarrhea. These symptoms depend on the infecting *Blastocystis* subtype and the human immune system.²

In this study, data was also collected through questionnaires about sources of drinking water and pets in the orphanage. Based on the questionnaire data provided, it was found that the source of drinking water generally came from refilled water or bottled water and only one orphanage whose drinking water came from boiled well water. Drinking water sources can be a source of *Blastocystis* infection because it is contaminated with *Blastocystis* cysts from animals or humans. From the questionnaire data on pets, it was found that all orphanages had cats as pets and most of them also kept chickens, birds and goats. Based on the literature, pets such as cats, dogs, chickens and goats are reservoir animals for this parasite and this is a source of transmission for humans.^{15,25-27} In this study, *Blastocystis* examination used the culture method using

modified Jones medium¹¹ but in this study horse serum was replaced with sheep serum because it was difficult to obtain horse serum in our region. All stages of the procedure are in accordance with what is in the literature, only the serum are different. The culture results were examined after incubation at 37°C for 48 hours and 72 hours. Examination is carried out by taking 20 ul of feces, placed on an object glass that has been given a drop of iodine, the feces are mixed evenly and covered with a deck glass and examined by microscope with 400x magnification.¹¹ The results are shown in figure 1. in positive stools *Blastocystis* can be seen growing in various sizes and shapes, the most of which are vacuolar and granular forms. After 3 days, the positive results were partially subcultured and read under a microscope after 2 days and the results are shown in Figure 2. The microscopic examination results showed *Blastocystis* amoeboid and vacuolar forms with larger sizes. Examination by the culture method is superior and recommended for detecting *Blastocystis* compared to direct microscopic examination, because we can immediately see the parasites growing and the number is definitely more so there is no doubt, based on the literature the sensitivity of this culture method is 90% and the specificity is 100%,¹⁰ but the culture method takes 3-4 days compared to direct microscopic examination which can be directly examined when get a sample but need an expert because it is difficult to distinguish *Blastocystis* from yeast cells or fecal debris.^{2,9}

CONCLUSION

In the feces of the children at the Pekanbaru orphanage, *Blastocystis hominis* can be detected using the culture method and this study confirmed the high incidence of blastocystosis among orphanage children. Transmission occurred through fecal oral route by way of contaminated food and beverage and maintain and care for domesticated animals.

ACKNOWLEDGMENTS

This work was financially supported by Faculty of Medicine, Universitas Riau. Therefore, we are grateful for this funding and support of this research.

REFERENCES

1. Salehi Sangani G, Mirjalali H, Farnia S, Rezaeian M. Prevalence of intestinal coccidial infections among different groups of immunocompromised patients. Iran J Parasitol. 2016;11(3):332–8.
2. Tan KSW. New insights on classification, identification, and clinical relevance of *Blastocystis* spp. Clin Microbiol Rev. 2008;21(4):639–65.
3. Abdulsalam AM, Ithoi I, Al-Mekhlafi HM, Khan AH, Ahmed A, Surin J, et al. Prevalence, predictors and clinical significance of *Blastocystis* sp. in Sebha, Libya. Parasites and Vectors. 2013;6(1):4–11.
4. Deng L, Lee JWJ, Tan KSW. Infection with pathogenic *Blastocystis* ST7 is associated with decreased bacterial diversity and altered gut microbiome profiles in diarrheal patients. Parasites and Vectors. 2022;15(1):1–10.

5. Güreşer AS, Comba A, Karasartova D, Koşar N, Keskin A, Stensvold CR, et al. Detection of Blastocystis subtypes in children with functional abdominal pain and celiac disease in Çorum, Turkey. *Iran J Parasitol.* 2022;17(3):296–305.
6. Sanggari A, Komala T, Rauff-Adedotun AA, Awosolu OB, Attah OA, Farah Haziqah MT. Blastocystis in captivated and free-ranging wild animals worldwide: a review. *Trop Biomed.* 2022;39(3):338–72.
7. Liu X, Ni F, Wang R, Li J, Ge Y, Yang X, et al. Occurrence and subtyping of Blastocystis in coypus (*Myocastor coypus*) in China. *Parasites and Vectors.* 2022;15(1):1–8.
8. Siagian FE. Intestinal microflora vs protozoan parasites: from interaction to competition. *South Asian J Res Microbiol.* 2022;13(1):36–46.
9. Sari IP, Benung MR, Wahdini S, Kurniawan A. Diagnosis and identification of Blastocystis subtypes in primary school children in Jakarta. *J Trop Pediatr.* 2018;64(3):208–14.
10. Bodnia I, Pokhil S, Bodnia K, Pavliy V, Skoryk L. Distribution and frequency of Blastocystis sp. by methods of microscopy and cultivation in faeces of residents of Kahrkov Region. *Georgian Med News.* 2022;7(328):85–90.
11. Giezen M Van der. Modified Jones' Medium for in-vitro culture of Blastocystis. Internet [Internet]. 2016; Available from: <http://www.blastocystis.net/p/lab-stuff.html>
12. Jalallou N, Iravani S, Rezaeian M, Alinaghizade A, Mirjalali H. Subtypes distribution and frequency of Blastocystis sp. Isolated from diarrheic and non-diarrheic patients. *Iran J Parasitol.* 2017;12(1):63–8.
13. Sankur F, Ayturan S, Malatyali E, Ertabaklar H, Ertug S. The distribution of Blastocystis subtypes among school-aged children in mugla, turkey. *Iran J Parasitol.* 2017;12(4):580–6.
14. Cinek O, Polackova K, Odeh R, Alassaf A, Kramná L, Ibekwe MAU, et al. Blastocystis in the faeces of children from six distant countries: prevalence, quantity, subtypes and the relation to the gut bacteriome. *Parasites and Vectors.* 2021;14(1):1–17.
15. Shams M, Shamsi L, Yousefi A, Sadrebazzaz A, Asghari A, Mohammadi-Ghalehbin B, et al. Current global status, subtype distribution and zoonotic significance of Blastocystis in dogs and cats: a systematic review and meta-analysis. *Parasites and Vectors.* 2022;15(1):1–17.
16. Nimri L, Batchoun R. Intestinal colonization of symptomatic and asymptomatic schoolchildren with Blastocystis hominis. *J Clin Microbiol.* 1994;32(11):2865–6.
17. Maryanti E, Hamidy MRA, Haslinda L. Identifikasi protozoa usus oportunistik dan faktor risikonya pada anak Panti Asuhan Kota Pekanbaru. *J Ilmu Kedokt.* 2019;13(2):55.
18. Dogruman-Al F, Simsek Z, Boorum K, Ekici E, Sahin M, Tuncer C, et al. Comparison of methods for detection of blastocystis infection in routinely submitted stool samples, and also in IBS/IBD patients in Ankara, Turkey. *PLoS One.* 2010;5(11):1–7.
19. Al-Fellani MA, Khan AH, Al-Gazoui RM, Zaid MK, Al-Ferjani MA. Prevalence and clinical features of Blastocystis hominis infection among patients in Sebha, Libya. *Sultan Qaboos Univ Med J.* 2007;7(1):6.
20. Gong B, Liu X, Wu Y, Xu N, Xu M, Yang F, et al. Prevalence and subtype distribution of Blastocystis in ethnic minority groups on both sides of the China-Myanmar border, and assessment of risk factors. *Parasite.* 2019;26.
21. Cañete R, Díaz MM, Avalos García R, Laúd Martínez PM, Manuel Ponce F. Intestinal Parasites in Children from a Day Care Centre in Matanzas City, Cuba. *PLoS One.* 2012;7(12):1–4.
22. Kosik-Bogacka D, Lepczyńska M, Kot K, Szkup M, Łanocha-Arendarczyk N, Dzika E, et al. Prevalence, subtypes and risk factors of Blastocystis spp. infection among pre- and perimenopausal women. *BMC Infect Dis.* 2021;21(1):1–15.
23. Candela E, Goizueta C, Periago MV, Muñoz-Antoli C. Prevalence of intestinal parasites and molecular characterization of Giardia intestinalis, Blastocystis spp. and Entamoeba histolytica in the village of Fortín Mbororé (Puerto Iguazú, Misiones, Argentina). *Parasites and Vectors.* 2021;14(1):1–16.
24. Al-Shamiri AH, Alzubairy AH, Al-Mamari RF. The prevalence of cryptosporidium spp. in children, Taiz District, Yemen. *Iran J Parasitol.* 2010;5(2):26–32.
25. Chang T, Jung BK, Shin H, Hong S, Ryoo S, Lee J, et al. Genotypes of Blastocystis sp. among elderly health checkup people in South Korea with a questionnaire on risk factors. *Parasitol Res.* 2021;120(9):3297–306.
26. Onder Z, Yildirim A, Pekmezci D, Duzlu O, Pekmezci GZ, Ciloglu A, et al. Molecular identification and subtype distribution of Blastocystis sp. in farm and pet animals in Turkey. *Acta Trop [Internet].* 2021;220(March):105939. Available from: <https://doi.org/10.1016/j.actatropica.2021.105939>
27. Udonsom R, Prasertbun R, Mahittikorn A, Mori H, Changbunjong T, Komalamisra C, et al. Blastocystis infection and subtype distribution in humans, cattle, goats, and pigs in central and western Thailand. *Infect Genet Evol [Internet].* 2018;65:107–11. Available from: <https://doi.org/10.1016/j.meegid.2018.07.007>

JOURNAL OF BIOMEDICINE AND TRANSLATIONAL RESEARCH

Available online at JBTR website: <https://jbtr.fk.undip.ac.id>

Copyright©2023 by Faculty of Medicine Universitas Diponegoro, Indonesian Society of Human Genetics and Indonesian Society of Internal Medicine

Original Research Article

Effect of Probiotic Supplementation on FSH, LH Levels and Folliculogenesis

Nur Rahman*, Syarif Thaoufik Hidayat, Besari Adi Pramono, Raden Soerjo Hadijono, Agoes Oerip Poerwoko, Arufiadi Anityo Mochtar

Department of Obstetrics and Gynecology, Faculty of Medicine, Universitas Diponegoro / Kariadi Medical Hospital, Semarang, Indonesia

Article Info

History

Received: 22 Dec 2022

Accepted: 27 Apr 2023

Available: 30 Apr 2023

Abstract

Background: Polycystic ovary syndrome (PCOS) is an endocrine disorder that often occurs in women of reproductive age. The main therapy currently used to treat PCOS patients is insulin sensitizer. In PCOS, there is an imbalance in the intestinal flora which causes activation of the immune system and an inflammatory response that leads to insulin resistance. The effect of probiotic supplementation on insulin resistance can have an impact on changes in reproductive hormone levels in PCOS women.

Objective: Analyze the effect of probiotic supplementation on levels of FSH, LH, and folliculogenesis in a study of PCOS Wistar rats.

Methods: Experimental research with a post-test only controlled group design. The research sample was 35 Wistar rats which were divided into 5 groups, (K-) were healthy rats, (K+) were PCOS rats without treatment, (P1) were PCOS rats received Metformin, (P2) were PCOS rats received Probiotics, and (P3) were PCOS rats that received Metformin + Probiotics. The intervention was carried out for 14 days. The dependent variables were levels of FSH, LH and folliculogenesis. Research data were analyzed using one-way ANOVA test, Fisher Exact test. Differences between groups and controls were tested with Dunnett's post hoc test. Significant $p < 0.05$

Results: Metformin + probiotic supplementation resulted in increased FSH levels, decreased LH levels and increased folliculogenesis when compared to the PCOS rats without treatment (K+).

Conclusion: Metformin + probiotic supplementation causes levels of FSH, LH and folliculogenesis activity in PCOS rats to resemble healthy rats.

Keywords: PCOS; metformin; probiotic; LH; FSH; folliculogenesis

Permalink/ DOI: <https://doi.org/10.14710/jbtr.v9i1.16824>

INTRODUCTION

Polycystic ovary syndrome (PCOS) is an endocrine disorder that often occurs in women of reproductive age. PCOS is often associated with obesity and reproductive health disorders.¹ PCOS occurs in around 116 million women in the world, with a percentage of 3.4% of the global population. PCOS accounts for 70% of anovulatory infertility.² Hyperandrogenism can be detected by increasing serum testosterone, serum androstenedione, or dehydroepiandrosterone. As a result of hyperandrogenism, PCOS can also have clinical manifestations in the form of hirsutism, acne, and/or alopecia.³

Many therapeutic methods have been applied to treat PCOS patients, including insulin sensitizers, lifestyle changes, and dietary interventions. The main therapy given as a treatment for PCOS patients currently is insulin sensitizer.⁴

* Corresponding author:

E-mail: dr_nurrahman86@yahoo.com
(Nur Rahman)

Table 1. Differences in FSH levels according to the treatment group

Variable	Group					P
	K -	K +	P1	P2	P3	
FSH Levels, IU/L	133.16 ± 12.79; 132.22 (119.29 – 159.73)	53.33 ± 11.75; 52.07 (34.03 – 68.95)	200.08 ± 26.76; 189.41 (173.48 – 235.20)	185.96 ± 31.93; 192.85 (117.18 – 210.41)	130.49 ± 18.79; 131.49 (106.89 – 162.92)	<0.001

ANOVA; significant $p < 0.05$ **Table 2.** Post-Hoc test results for different FSH levels between groups

Group (I)	Group (J)	Mean Difference (I-J)	p
P3	K-	-2.67	1.000
	K+	77.16	0.000
	P1	-69.58	0.000
	P2	-55.47	0.000

Bonferroni Post-Hoc; significant $p < 0.05$ **Table 3.** Differences in LH levels according to the treatment group

Variable	Group					P
	K -	K +	P1	P2	P3	
LH Levels, IU/L	22.71 ± 9.71; 21.75 (11.55 – 41.75)	75.09 ± 7.66; 75.37 (61.53 – 85.42)	37.58 ± 12.60; 40.57 (11.55 – 51.79)	42.55 ± 4.89; 42.94 (36.07 – 51.79)	26.81 ± 3.62; 26.06 (20.95 – 31.75)	<0.001

ANOVA; significant $p < 0.05$ **Table 4.** Post-Hoc test results for different LH levels between groups

Group (I)	Group (J)	Mean Difference (I-J)	p
P3	K-	-9.43	1.000
	K+	-61.80	0.000
	P1	-24.29	0.223
	P2	-29.27	0.014

Bonferroni Post-Hoc; significant $p < 0.05$ **Table 5.** Folliculogenesis Rates Between Groups

K+ (I)	Group (J)			
	K-	P1	P2	P3
Primary Follicle	0.42 ± 1.13	1.57 ± 1.27	1.42 ± 1.39	1.28 ± 1.70
Secondary Follicle	0.57 ± 1.27	0.57 ± 0.78	0.85 ± 1.77	0.71 ± 1.49
Tertiary Follicle	1.57 ± 1.51	0.29 ± 2.13	-0.57 ± 0.97	0.86 ± 1.34
Graaf's Follicle	0.57 ± 1.98	-1.14 ± 1.46	1.00 ± 1.41	0.42 ± 1.27
Corpus Luteum	3.71 ± 2.81	0.71 ± 0.95	1.71 ± 1.79	3.57 ± 2.22

Table 6. Differences in Ovarian Histopathology between groups

K-	Group			
	K+	P1	P2	P3
Primary Follicle	0.474	0.608	0.371	0.608
Secondary Follicle	0.292	1.000	0.062	0.619
Tertiary Follicle	0.138	0.523	0.068	0.776
Graaf's Follicle	0.608	0.042	0.510	1.000
Corpus Luteum	0.295	0.211	0.538	0.899

Fischer Exact; significant $p < 0.05$

Dysbiosis of gut microbiota (DOGMA) proposes the hypothesis that after an imbalance in the intestinal flora, there is an increase in intestinal permeability which can cause lipopolysaccharide leakage into the systemic circulation, which causes activation immune system and inflammatory responses that lead to insulin resistance.⁵

The use of probiotics and microorganisms in the digestive tract as a therapeutic method can have an impact on metabolic, inflammatory, and oxidative markers. Recent studies have shown data on a decrease in insulin concentration and insulin resistance in subjects given probiotics. The possible mechanism by which probiotic supplementation provides a beneficial effect is from the balance of the host's energy metabolism.⁴

The effect of probiotic supplementation on insulin resistance can also have an impact on changes in reproductive hormone levels in PCOS women. Several studies have also identified changes in hormone levels related to reproductive function in subjects receiving probiotic supplementation.

The purpose of this study was to prove the effect of probiotic supplementation on levels of FSH, LH, and folliculogenesis in a study of PCOS Wistar rats.

MATERIALS AND METHODS

Experimental research with a post-test only controlled group design. The study was conducted on the PCOS rat model induced by testosterone propionate through subcutaneous injection at the Faculty of

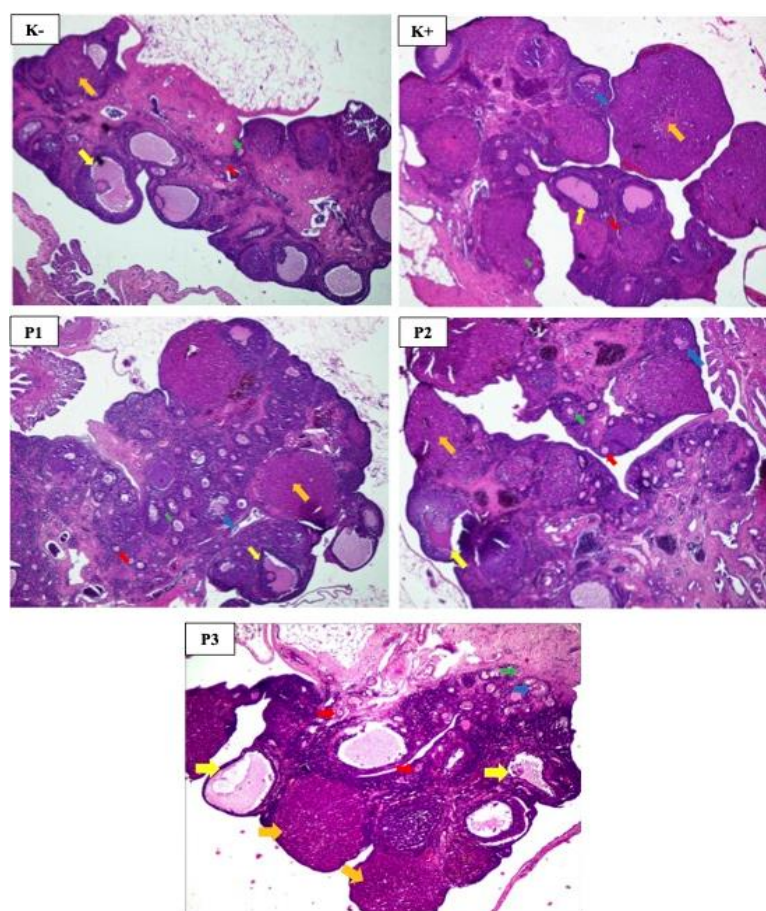


Figure 1. Features of folliculogenesis (K-, K+, P1, P2, P3). Red arrow = primary follicle; green arrow = secondary follicle; blue arrow = tertiary follicle; yellow arrow = Graaf follicle; orange arrow = corpus luteum. HE. 100x

Veterinary Medicine, Universitas Airlangga, Surabaya. The research sample was 35 wistar rats which were divided into 5 groups, (K-) were healthy rats, (K+) were PCOS rats without treatment, (P1) were PCOS rats received Metformin, (P2) were PCOS rats received Probiotics, and (P3) were PCOS rats that received Metformin + Probiotics. The intervention was carried out for 14 days. Probiotic supplementation was carried out using acidophilus liquid probiotics with a preparation of 45,000 bacteria per 1 mL, given at a dose of 6.15 mL/KgBB/rat/day, for 14 days, where rats are estimated to have experienced 3 cycles of ovarian hormone secretion. The dependent variables were levels of FSH, LH and folliculogenesis. The ELISA method was used to assess FSH and LH levels using blood samples obtained from the retroorbital vein as much as 3cc. Ovarian histopathological examination with hematoxylin eosin staining was used to assess folliculogenesis using ovarian samples obtained from laparotomy with left and right ovarian samples. Calculation of the number of ovarian follicles was carried out by Veterinary Pathology Laboratory, Faculty of Veterinary Medicine, Universitas Airlangga Research data were analyzed using one-way ANOVA test, and Fisher Exact test. Differences between groups and controls were tested with Dunnett's post hoc test. The data is said to be significant if the p value <0.05

Research by intervening in animal models had been carried out based on approval and ethical eligibility from

the Ethics Commission of the Faculty of Medicine, Universitas Diponegoro with no.130/EC/H/FK-UNDIP/XI/2022 All costs related to research became the responsibility of the researcher.

RESULTS

Based on the assessment conducted on 35 rats which were divided into 5 research groups namely K- (non-SOPK), K+ (SOPK), P1 (SOPK + Metformin), P2 (PCOS + Probiotics), and P3 (SOPK + Metformin + Probiotics), the following results were obtained. Table 1 explains the differences in FSH levels between study groups. In the PCOS (K+) group, low FSH levels were found. In the intervention group (P1, P2, and P3) there was an increase in FSH levels when compared to the PCOS group (K+). Based on table 2, FSH levels in the P3 group have the most similar values to FSH levels in the healthy group (K-).

Table 3 explains the differences in LH levels between study groups. In the PCOS (K+) group, high LH levels were found. In the intervention group (P1, P2, and P3) there was a decrease in LH levels when compared to the PCOS group (K+). Based on table 4, LH levels in the P3 group have the most similar values to LH levels in the healthy group (K-).

Figure 1 and table 5 explains the differences in folliculogenesis rates based on each follicular development between groups. When compared to the PCOS group (K+), there was an increase in the degree of

folliculogenesis in the intervention group (P1, P2 and P3) at almost all stages of follicular development. However, the increase in folliculogenesis in the P3 group resembled that of the healthy (K-) group. Based on table 6, it was found that, when compared with the healthy group (K-), there was no significant difference in the level of folliculogenesis between the P3 groups at all stages of follicular development.

DISCUSSION

PCOS rats without treatment (K+) had much lower FSH levels than healthy samples (K-). Intervention in all groups (P1, P2 and P3) resulted in an increase in FSH levels.

Khashchenko E, et al in his study on the assessment of hormone levels in PCOS patients and healthy patients found that PCOS patients had higher FSH levels than healthy patients, although there was no significant difference between the two groups ($p=0.285$).⁶ This result was also supported by the study of Jindal P, et al found that the average patients FSH levels before and after treatment were 10.55 ± 6.22 mIU/ml and 9.69 ± 4.07 mIU/ml, respectively ($p<0.137$).⁷ The results in this study were different from the results obtained by Khashchenko. E and Jindal P are suspected because both studies used human subjects, while this study used rat samples that received testosterone propionate injection. The results in this study were supported by Dardmeh F, et al who obtained similar results that probiotic supplementation increased testosterone, LH and FSH levels in research subjects.⁸

Karimi et al.⁹ and Heshmati et al.⁴ stated that PCOS patients generally have insulin resistance and increased serum insulin and abnormal lipoprotein metabolism. Rice S, et al in a study on the effect of using metformin on FSH levels in PCOS patients found that metformin significantly reduced FSH levels but not expression and aromatase activity stimulated by forskolin. This effect arises through inhibition of ligand- and basal-induced upregulation of FSH receptor expression. Metformin also reduces FSH-induced CREB phosphorylation and hence CRE activity, potentially interfering with the CRE-binding CREB-CREB2 protein coactivator complex at promoter II of the aromatase gene. This condition is mediated in a manner that is independent of AMP-activated protein kinases and does not involve changes in cAMP levels.¹⁰

PCOS is directly related to insulin disorders. Insulin resistance will cause hyperinsulinemia, which directly affects the role of ovarian receptors, inhibits insulin-binding protein and sex hormone-binding protein, while releasing testosterone and increasing ovarian androgens. Therefore, metformin is used to regulate insulin secretion and achieve the aim of effectively improving PCOS. Most approved weight management drugs are contraindicated in women of reproductive age, but metformin has fewer side effects, safer, and recommended for use in the treatment of PCOS.¹¹

PCOS can also cause systemic metabolic disorders (such as hyperinsulinemia and insulin resistance, obesity, increased risk of type II diabetes, cardiovascular disease) have played a fundamental role. The overwhelming evidence on the correlation between the gut microbiome and the occurrence of metabolic

disorders has led to the hypothesis that changes in the microbiome also involved in the pathogenesis of PCOS.¹² Dysbiosis of gut microbiota (DOGMA) demonstrated that, along with an imbalance in the gut flora, increased intestinal permeability can lead to leakage of lipopolysaccharide (LPS) into the systemic circulation. The net effect is activation of the immune system and an inflammatory response leading to insulin resistance.⁵

The condition that shows the role of the gut microbiome is the presence of lower concentrations of short chain fatty acids (SCFA) in stool samples of PCOS patients.¹³ The growth of *Faecalibacterium prausnitzii*, *Bifidobacterium* and *Akkermansia* was driven by probiotic supplementation, which are SCFA-producing bacteria, and led to an increase in intestinal SCFA. This SCFA binds to its receptor on the enteroendocrine cell membrane and directly stimulates the release of gut-brain mediators such as ghrelin and PYY, the increase of which can affect the secretion of sex hormones by the pituitary and hypothalamus through the gut-brain axis, thereby improving PCOS symptoms.¹⁴ Increased SCFA production also contribute to intestinal barrier function and reduce endotoxin translocation across the intestinal wall, thereby reducing inflammation and insulin resistance. Ultimately, there is a potential interaction between sex hormones and the gut microbiota, and this interaction may contribute to the pathogenesis of PCOS.¹⁵

Arab A, et al who conducted a study on the effect of probiotic supplementation on hormone levels and clinical outcomes of PCOS patients found that after 12 weeks of administration there was a decrease in FSH levels, but there was no significant difference ($p=0.188$).¹⁶ Consumption of probiotics balances intestinal pH and microbial flora, improves the absorption and digestion of nutrients, prevents the production of inflammatory cytokines, and improves lipid and carbohydrate metabolism in the gut.¹⁷ Probiotics also reduce blood glucose, insulin resistance, and de novo cholesterol formation, which in turn reduces the production of androgens including SHBG, DHEA, FAI, and testosterone.¹⁸

In this study, different results were obtained, namely a decrease in FSH levels in PCOS patients and an increase in FSH levels after the intervention of metformin and/or probiotics. Dardmeh F, et al found that after supplementation with *Lactobacillus rhamnosus* there was an increase in FSH, LH and testosterone levels between before and after administration ($p<0.05$).⁸ Szydłowska I, et al got similar results, namely an increase in FSH from the baseline value after administration of probiotics.¹⁹

PCOS samples that were not given treatment (K+) had much higher LH levels than healthy samples (K-). Giving interventions to all groups (P1, P2 and P3) caused a decrease in LH levels. There was a significant difference in LH levels between the K- and P1 and P2 groups.

Khashchenko E, et al also assessed LH levels, found that PCOS patients had higher LH levels than healthy patients, with a significant difference between the two groups ($p<0.001$).⁶ Jindal P, et al found similar results where the average LH level was before and after treatment respectively 22.34 ± 11.49 mIU/ml and 15.65 ± 6.09 mIU/ml ($p<0.0001$).⁷

Obese women with PCOS exhibit higher LH levels to stimulate androgen secretion, leading to excessive insulin and androgen resistance.²⁰ Based on existing guidelines, it is currently recommended that overweight women with PCOS use metformin for weight control and for endocrine and metabolic disorders. High levels of LH and androgens are considered to be the reason for the increasing number of oligomenorrheal patients. Metformin treatment reduces hyperinsulinemia. This is thought to be the cause of changes in pituitary sensitivity to gonadotropin-releasing hormone leading to excessive LH secretion. Administration of metformin causes a decrease in LH response to GnRH.¹⁶

The type of intervention that gave the most similar level of ovarian folliculogenesis to healthy samples (K-) was the P3 group, namely administration of metformin and probiotic supplementation.

Khashchenko E, et al found that the number of ovarian follicles in the PCOS group was higher than the control group with a significant difference between the two groups ($p < 0.001$).⁶

Primordial follicular growth is largely independent of gonadotropins and is primarily influenced by paracrine/endocrine factors, including several proteins of the TGF β superfamily (i.e., TGF β , anti-müllerian hormone [AMH], inhibin, activin, bone morphogenetic protein-15 [BMP15] and growth differentiation factor 9 [GDF9]).²¹ Several of these TGF- β -related proteins are dysregulated in PCOS follicles. Oocytes in PCOS patients experience a decrease in GDF9 mRNA levels, which interferes with growth from the primordial follicle to the development of small antral follicles, and is accompanied by impaired follicle growth.

Insulin sensitivity in PCOS patients is intrinsically impaired from abnormal post-receptor signal transduction, reducing insulin-mediated glucose uptake, but not ovarian steroidogenesis. Consequently, the hyperinsulinemia of insulin resistance in PCOS is independent of and related to obesity, with the combination of PCOS and obesity severely impairing glucose-insulin homeostasis, while enhancing ovarian steroidogenesis. Consequently, hyperinsulinemia due to insulin resistance in PCOS contributes to hyperandrogenism. This condition also promotes premature luteinization of granulosa cells in small antral PCOS follicles, as evidenced by LH receptor overexpression and P4 hypersecretion, leading to arrest of cell proliferation and follicular growth.

In this study, administration of metformin and probiotics to samples with PCOS resulted in a histopathological appearance of the ovaries resembling that of healthy samples (K-). It is suspected that the mechanism underlying this condition is through improvement in LH and FSH levels that resemble those of healthy samples (K-).

CONCLUSION

Metformin + probiotic supplementation causes levels of FSH, LH and folliculogenesis activity in PCOS rats to resemble healthy rats.

ACKNOWLEDGMENTS

The author would like to thank Prof Dr. drh. Widjiati, M.Sc., drh. Akhmad Afifudin Al-Anshori, M.Si., drh.

Mey Vanda Pusparina who had allowed me to carry out research at the Animal Laboratory of Universitas Airlangga.

REFERENCES

1. Osuka S, Nakanishi N, Murase T, Nakamura T, Goto M, Iwase A, et al. Animal models of polycystic ovary syndrome: A review of hormone-induced rodent models focused on hypothalamus-pituitary-ovary axis and neuropeptides. *Reprod Med Biol.* 2019 Apr 28;18(2):151–60. DOI: 10.1002/rmb2.12262
2. Brassard M, AinMelk Y, Baillargeon JP. Basic Infertility Including Polycystic Ovary Syndrome. *Medical Clinics of North America.* 2008 Sep;92(5):1163–92. DOI: 10.1016/j.mcna.2008.04.008
3. Fauser BCJM, Tarlatzis BC, Rebar RW, Legro RS, Balen AH, Lobo R, et al. Consensus on women's health aspects of polycystic ovary syndrome (PCOS): the Amsterdam ESHRE/ASRM-Sponsored 3rd PCOS Consensus Workshop Group. *Fertil Steril.* 2012 Jan;97(1):28–38.e25. DOI: 10.1016/j.fertnstert.2011.09.024
4. Heshmati J, Farsi F, Yosae S, Razavi M, Rezaeinejad M, Karimie E, et al. The Effects of Probiotics or Synbiotics Supplementation in Women with Polycystic Ovarian Syndrome: a Systematic Review and Meta-Analysis of Randomized Clinical Trials. *Probiotics Antimicrob Proteins.* 2019 Dec 13;11(4):1236–47. DOI: 10.1007/s12602-018-9493-9
5. Tremellen K, Pearce K. Dysbiosis of Gut Microbiota (DOGMA) – A novel theory for the development of Polycystic Ovarian Syndrome. *Med Hypotheses.* 2012 Jul;79(1):104–12. DOI: 10.1016/j.mehy.2012.04.016
6. Khashchenko E, Uvarova E, Vysokikh M, Ivanets T, Krechetova L, Tarasova N, et al. The Relevant Hormonal Levels and Diagnostic Features of Polycystic Ovary Syndrome in Adolescents. *J Clin Med.* 2020 Jun 11;9(6):1831. DOI: 10.3390/jcm9061831
7. Jindal P, Mehendiratta R, Sharma A, Takkar V, Kapila PT. Effect of Metformin on FSH, LH and Prolactin Levels in Patients with Polycystic Ovarian Syndrome. *International Journal of Medical Research Professionals.* 2016 Sep;2(5). DOI: 10.21276/ijmrp.2016.2.5.037
8. Dardmeh F, Alipour H, Gazerani P, van der Horst G, Brandsborg E, Nielsen HI. *Lactobacillus rhamnosus* PB01 (DSM 14870) supplementation affects markers of sperm kinematic parameters in a diet-induced obesity mice model. *PLoS One.* 2017 Oct 10;12(10):e0185964. DOI: 10.1371/journal.pone.0185964
9. Karimi E, Heshmati J, Shirzad N, Vesali S, Hosseinzadeh-Attar MJ, Moini A, et al. The effect of synbiotics supplementation on anthropometric indicators and lipid profiles in women with polycystic ovary syndrome: a randomized controlled trial. *Lipids Health Dis.* 2020 Dec 6;19(1):60. DOI: 10.1186/s12944-020-01244-4

10. Rice S, Elia A, Jawad Z, Pellatt L, Mason HD. Metformin Inhibits Follicle-Stimulating Hormone (FSH) Action in Human Granulosa Cells: Relevance to Polycystic Ovary Syndrome. *J Clin Endocrinol Metab.* 2013 Sep 1;98(9):E1491–500. DOI: 10.1210/jc.2013-1865
11. Thessaloniki ESHRE/ASRM-Sponsored PCOS Consensus Workshop Group. Consensus on infertility treatment related to polycystic ovary syndrome. *Human Reproduction.* 2008 Mar 1;23(3):462–77. DOI: 10.1093/humrep/dem426
12. Dabke K, Hendrick G, Devkota S. The gut microbiome and metabolic syndrome. *Journal of Clinical Investigation.* 2019 Oct 1;129(10):4050–7. DOI: 10.1172/JCI129194
13. Ratajczak W, Rył A, Mizerski A, Walczakiewicz K, Sipak O, Laszczyńska M. Immunomodulatory potential of gut microbiome-derived short-chain fatty acids (SCFAs). *Acta Biochim Pol.* 2019 Mar 4; DOI: 10.18388/abp.2018_2648
14. Zhang J, Sun Z, Jiang S, Bai X, Ma C, Peng Q, et al. Probiotic *Bifidobacterium lactis* V9 Regulates the Secretion of Sex Hormones in Polycystic Ovary Syndrome Patients through the Gut-Brain Axis. *mSystems.* 2019 Apr 30;4(2). DOI: 10.1128/mSystems.00017-19
15. Guo Y, Qi Y, Yang X, Zhao L, Wen S, Liu Y, et al. Association between Polycystic Ovary Syndrome and Gut Microbiota. *PLoS One.* 2016 Apr 19;11(4):e0153196. DOI: 10.1371/journal.pone.0153196
16. Arab A, Hossein-Boroujerdi M, Moini A, Sepidarkish M, Shirzad N, Karimi E. Effects of probiotic supplementation on hormonal and clinical outcomes of women diagnosed with polycystic ovary syndrome: A double-blind, randomized, placebo-controlled clinical trial. *J Funct Foods.* 2022 Sep;96:105203. DOI: 10.1016/j.jff.2022.105203
17. Shamasbi SG, Ghanbari-Homayi S, Mirghafourvand M. The effect of probiotics, prebiotics, and synbiotics on hormonal and inflammatory indices in women with polycystic ovary syndrome: a systematic review and meta-analysis. *Eur J Nutr.* 2020 Mar 29;59(2):433–50. DOI: 10.1007/s00394-019-02033-1
18. Hadi A, Ghaedi E, Khalesi S, Pourmasoumi M, Arab A. Effects of synbiotic consumption on lipid profile: a systematic review and meta-analysis of randomized controlled clinical trials. *Eur J Nutr.* 2020 Oct 22;59(7):2857–74. DOI: 10.1007/s00394-020-02248-7
19. Szydłowska I, Marciniak A, Brodowska A, Loj B, Ciećwież S, Skonieczna-Żydecka K, et al. Effects of probiotics supplementation on the hormone and body mass index in perimenopausal and postmenopausal women using the standardized diet. A 5-week double-blind, placebo-controlled, and randomized clinical study. *Eur Rev Med Pharmacol Sci.* 2021;25(10):3859–67. DOI: 10.26355/eurrev_202105_25953
20. Diamanti-Kandarakis E, Dunaif A. Insulin Resistance and the Polycystic Ovary Syndrome Revisited: An Update on Mechanisms and Implications. *Endocr Rev.* 2012 Dec 1;33(6):981–1030. DOI: 10.1210/er.2011-1034
21. Dumesic DA, Padmanabhan V, Abbott DH. Polycystic Ovary Syndrome and Oocyte Developmental Competence. *Obstet Gynecol Surv.* 2008 Jan;63(1):39–48. DOI: 10.1097/OGX.0b013e31815e85fc

JOURNAL OF BIOMEDICINE AND TRANSLATIONAL RESEARCH

Available online at JBTR website: <https://jbtr.fk.undip.ac.id>

Copyright©2023 by Faculty of Medicine Universitas Diponegoro, Indonesian Society of Human Genetics and Indonesian Society of Internal Medicine

Original Research Article

Renoprotective Effect of Sambiloto (*Andrographis paniculata*) Leaf Extract on Lipopolysaccharide – Induced Septic Rats

Adhika Bastian Bagas Prananta¹, Nyoman Suci Widyastiti^{2*}, Ariosta², Dwi Retnoningrum², Rezya Salsabela¹, Vega Karlowee³, Neni Susilaningsih⁴

¹Faculty of Medicine, Universitas Diponegoro. Semarang. Indonesia

²Department of Clinical Pathology. Faculty of Medicine. Universitas Diponegoro. Semarang. Indonesia

³Department of Pathology Anatomy. Faculty of Medicine. Universitas Diponegoro. Semarang. Indonesia

⁴Department of Anatomy-Histology. Faculty of Medicine. Universitas Diponegoro. Semarang. Indonesia

Article Info

History

Received: 27 Jan 2023

Accepted: 03 Mar 2023

Available: 30 Apr 2023

Abstract

Background: Acute kidney injury (AKI) is one of organ dysfunctions related to sepsis. AKI may be mediated by uric acid, and blood creatinine levels can be utilized to diagnose the condition to measure kidney function. Sambiloto (*Andrographis paniculata*) is a traditional medicine that has flavonoid compounds that can reduce creatinine levels and Xanthine Oxidase Inhibitors which can reduce uric acid levels.

Objective: Septic model rats generated by lipopolysaccharide were used to test the effects of sambiloto (*Andrographis paniculata*) leaf extract on serum creatinine and uric acid levels (LPS).

Methods: This study was experimental employing 25 rats split into 5 groups as the post-test alone control group: healthy control with standard feed (HC), negative control with LPS injection (NC), Treatment (T)1 (*A. paniculata* 200 mg/kgBW+LPS), T2 (*A. paniculata* 400 mg/kgBW+LPS), and T3 (*A. paniculata* 500mg/kgBW+ LPS). *A. paniculata* leaf extract was given via oral gavage on day 8-21. An intraperitoneal injection of LPS 5 mg/kgBW was given on day 22. On the 25th day, the blood serum was analyzed for creatinine levels using the Jaffe method, and uric acid was analyzed using the enzymatic photometric method. One-way analysis of variance (Kruskal-Wallis) and the Kruskal-Wallis test were used to evaluate the data.

Results: The mean creatinine levels of the HC, NC, T1, T2, and T3 groups were 0.7±0.01; 3.5±0.04; 2.9±0.03; 1.9±0.05; 1.3 ±0.04 mg/dl respectively. The mean uric acid levels of the HC, NC, T1, T2, and T3 groups were 1.7±0.05; 8.2±0.11; 4.5±0.03; 4.0±0.12; 3.0±0.19 mg/dl respectively. There were significant differences ($p<0.05$) in creatinine levels in groups T2 ($p=0.031$) and T3 ($p=0.001$) to NC group and serum uric acid levels in groups T1 ($p<0.001$), T2 ($p<0.001$), and T3 ($p<0.001$) to NC group which creatinine and uric acid levels were lower than NC group.

Conclusion: *Andrographis paniculata* leaf extract has a renoprotective effect against AKI in LPS-induced septic rats

Keywords: *Andrographis paniculata*; creatinine; uric acid; lipopolysaccharide; AKI; sepsis

Permalink/ DOI: <https://doi.org/10.14710/jbtr.v9i1.17286>

INTRODUCTION

Sambiloto (*Andrographis paniculata*) is one of medicinal plants that can thrive and has been cultivated in various parts of the world, including in Indonesia.¹ In Indonesia, sambiloto is marketed either in a single preparation or in combination with other natural ingredients in tablet dosage form.² It has been

recognized that Sambiloto has antipyretic, analgesic, nephroprotective, antibacterial, anti-inflammatory, and immunostimulating properties.

* Corresponding author:

E-mail: nyoman.suci@fk.undip.ac.id
(Nyoman Suci Widyastiti)

In addition, sambiloto contains bioactive compounds found in plants; including alkaloids, flavonoids, andrographolides, glycosides, saponins, steroids, tannins, diterpenes, and more.³

Flavonoids are among the compounds found in sambiloto. A broad class of polyphenolic chemicals, flavonoids have a benzo—pyron structure.⁴ Flavonoids have antimicrobial, antioxidant, anti-inflammatory, and anti-diabetic properties in the medical field.⁵ In addition, flavonoids are able to increase the glomerular filtration rate (GFR). An increment in the glomerular filtration rate might lead an increment of creatinine level which was excreted in the kidneys, in order to reduce creatine levels in the blood.⁶

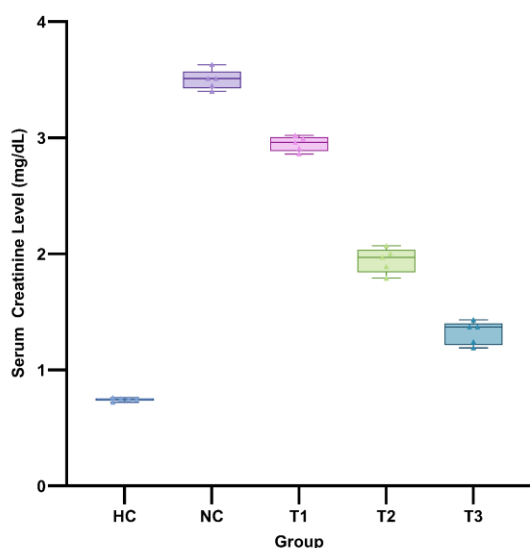


Figure 1. Box plot graph of serum creatinine levels

Sepsis is a life-threatening multi-organ dysfunction caused an abnormal immune response to infection.⁷ This condition, known as sepsis, by endotoxins such as lipopolysaccharides (LPS).^{8,9} The bacterial Gram-negative bacteria have a cell wall that is mostly made up of lipopolysaccharides (LPS). Toll-like receptor 4 (TLR4) transmembrane protein activity can be boosted by lipopolysaccharides. The TLR4 receptor makes use of the infrastructure of MD-2 protein to bind with receptors on lipopolysaccharides.

The process of presentation lipopolysaccharide to MD-2 may also be facilitated CD14 and LBP, among other proteins. Upon activation, TLR4 signals for the recruitment MyD88, Mal, Trif, and Tram are examples of intracellular adaptor molecules that indicate the activation of other molecules. The IRAK1, IRAK4, TBK1, and IKKi protein kinases may be activated as a result, allowing for a more robust signaling system and the activation or repression of genes that affect how the body reacts to inflammation.¹⁰

One way that kidney function is evaluated is by monitoring the creatinine level in the blood.¹¹ Renal function loss can occur for a variety of reasons, including An abrupt Injuries to the kidneys that happen suddenly can cause a drop in kidney function known as acute renal injury (AKI) various etiologies and pathophysiological processes.¹² Up to 50% of mortality in intensive care

unit patients are attributed to septic endotoxemia, which is often accompanied with AKI. The death rate for patients with AKI caused by sepsis was greater than that of those without sepsis. The main ingredient of the endotoxin produced from wall of Gram-negative bacteria is lipopolysaccharide (LPS), and it is primarily responsible for causing endotoxemia. Lipopolysaccharides activate the renal inflammatory cascade, which leads cause a cascade of inflammatory cytokines to be released, wreaking havoc on the kidneys an advanced state.¹³ Sepsis-related AKI is characterized by impaired glomerular filtration, elevated serum urea and creatinine levels, and acute tubular necrosis as a result of hypovolemia and poor tissue blood perfusion.¹⁴

Recently, it found out that uric acid is a potential mediator of AKI.¹⁵ Uric acid stimulate inflammatory pathways that can exacerbate the incidence of AKI through crystalline and non-crystalline mechanisms.^{16,17} Urine supersaturation, urate crystallization, and tubular lumina obstruction are just a few of the problems that might begin due to an increase in uric acid excretion, all of which can lead to localized granulomatous inflammation involving macrophages and T cell infiltration.¹⁸ In previous studies, it was found the existence of Xanthine Oxidase Inhibitors in flavonoids. The structure of benzopyran contributes to XO inhibition which can affect uric acid levels in the blood.¹⁹

Research shows that was an effect of giving a graded dose of sambiloto extract with kidney function, namely creatinine and uric acid in Wistar rats induced by lipopolysaccharide. The doses of sambiloto extract used in this study were 200, 400, and 500 mg/kgBW.

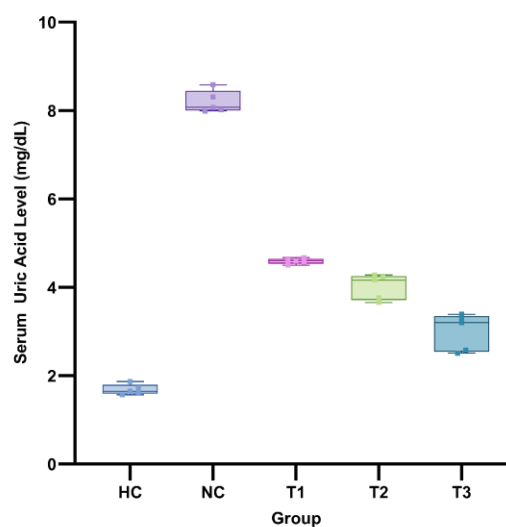


Figure 2. Box plot graph of serum uric acid levels

MATERIALS AND METHODS

We employed a true controlled experiment with a single post-test condition to conduct this analysis. From June through August of 2021, this study was conducted on male Wistar rats between the ages of two and three months. On May 24, 2021, The Medical Faculty at Diponegoro University's Research Ethics Commission issued protocol number 50/EC/H/FK-UNDIP/V/2021,

indicating that the study was given the green light from an ethical standpoint.

Twenty-five rats were split into five groups at the Experimental Animal Laboratory of PSPG Gadjah Mada University: the healthy control group (HC), which received only standard feed; the negative control group (NC), which received standard feed and an injection of lipopolysaccharide (5 mg/kgBW) on day 22; in addition to the First, Second, and Third Group Treatment (T1, T2, and T3), which received standard feed and sambiloto leaf extract (200, 400, or 500 mg/kgBW (on day 8th – 22th), and injected with lipopolysaccharide 5 mg/kgBW on day 22.

The inclusion criteria in this study were healthy male Wistar rats weighing 150-200 grams and 2-3 months of age while the exclusion criteria were rats with anatomical abnormalities, and the dropout criteria were weight loss of rats after the adaptation period, dead rats or illness rats during the experiment. On 25th days, each group was terminated using chloroform and blood samples were taken to measure creatinine levels using the jaffe method and uric acid using the enzymatic photometric method.

Data of creatinine and uric acid levels were analyzed using a computer program. After completing a descriptive analysis, the data normality was subjected to the Shapiro-Wilk test for validity. The Kruskal-Wallis test was used for the statistical analysis because the creatinine data did not have a normal distribution, while the uric acid data followed a normal distribution, and the ANOVA one-way test was utilized to complete the study. It can be said the results is significant if there is a difference with a p value ≤ 0.05 .

RESULTS

All rats were found to be alive and there is no rats with dropout criteria were found until the end research period. Data on creatinine and uric acid levels were tested for normality with the Shapiro-Wilk. Based on the normality test, data on serum creatinine levels were not normally distributed ($p < 0.05$) in one group serum uric acid levels exhibited normal distribution ($p > 0.05$), therefore the study proceeded with Other variables were examined using the Kruskal-Wallis and Mann-Whitney tests, parametric test of association (one-way ANOVA) and post-test non-parametric tests. The mean creatinine levels of the HC, NC, T1, T2, T3 were 0.7 ± 0.01 ; 3.5 ± 0.04 ; 2.9 ± 0.03 ; 1.9 ± 0.05 ; 1.3 ± 0.04 mg/dl respectively. The mean uric acid levels of the HC, NC, T1, T2, and T3 groups were 1.7 ± 0.05 ; 8.2 ± 0.11 ; 4.5 ± 0.03 ; 4.0 ± 0.12 ; 3.0 ± 0.19 mg/dl respectively.

Based on the Levene homogeneity test, the significance of data based on the median of the data on serum uric acid levels was 0.000 (< 0.05) so it can be concluded meaning that uric acid levels in the blood can fluctuate level data in five groups was not homogeneous.

Results from Using the Kruskal-Wallis test, a discernible variation in serum creatinine concentration was seen, with a significance level of 0.000 ($p < 0.05$). The Mann Whitney test results for HC-NC, HC-T1, HC-T2, HC-T3, NC-T1, NC-T2, NC-T3, T1-T2, T1-T3, and T2-T3 were 0.000, 0.001, 0.031, 0.282, 0.282, 0.031, 0.001, 0.282, 0.031, and 0.282 respectively. There is a statistically significant variation according to the analysis of variance finding of 0.000 in serum uric acid

levels ($p < 0.05$). The post hoc analysis results of serum uric acid levels for HC-NC, HC-T1, HC-T2, HC-T3, NC-T1, NC-T2, NC-T3, T1-T2, T1-T3, and T2-T3 were 0.000, 0.000, 0.000, 0.000, 0.000, 0.000, 0.002, 0.000, and 0.000 respectively.

DISCUSSION

The increment in serum creatinine levels in rats which had been administered with lipopolysaccharide injection against healthy controls indicates that the administration of lipopolysaccharide injection induced decline in renal function, manifested by an increase in blood creatinine levels. Endotoxin is an outer membrane protein produced through the involvement of When sepsis first sets in, gram-negative bacteria play a role. Research on sepsis has made extensive use of the LPS injection model. An increase in inflammation-inducing such cytokines as TNF-alpha and IL-1 other early clinical signs of sepsis, are triggered by LPS administration, although there is no bacteremia.²⁰

What we call "sepsis" is actually a variety of organ failure brought on by an abnormal immune response to infection.⁷ Gram-negative bacteria have an outer membrane is made of LPS. To do this, they bind to a lipid called lipid A. (the bioactive portion of LPS), LBP in the blood and extracellular fluid transports LPS to clusters of differentiation14 (CD14) on monocytes, macrophages, and neutrophils. To further increase the creation and release of inflammatory mediators, the LBP-LPS complex interacts with the CD14 receptor, generating LPS binding to TLR4. In addition, Proinflammatory cytokines stimulate endothelial cells by increasing the expression of adhesion receptors, allowing for the adherence of neutrophils, monocytes, macrophages, and platelets. When these cells are activated, they secrete endothelium-damaging mediators such as proteases, oxidants, prostaglandins, leukotrienes and contribute to increased permeability, vasodilation, and an imbalance between the procoagulant and anticoagulant systems. Nitric oxide (NO), a powerful vasodilator that can lead to sepsis, is produced in excess when iNOS activity is high.²¹ The rats model with systemic lipopolysaccharide induction was the most widely used in researches with sepsis rat model.⁷

The leading cause of Acute Kidney Injury is sepsis (AKI) through various mechanisms, some of which are inflammation, microvascular dysfunction, and metabolic reprogramming.²² A number of tubular transporters in the kidney, such as sodium/hydrogen exchanger 1, are directly inhibited by lipopolysaccharides (NHE1).²³ This mechanism promote serum creatinine levels which indicate impaired kidney function, especially in glomerular filtration function.²⁴

Results from this study demonstrate that serum creatinine T2 and T3 therapy groups had significantly lower levels than the control group when compared to serum creatinine levels in the NC group which was only given lipopolysaccharide injection. Based on previous research, the administration of sambiloto leaf extract has a renoprotective effect on Acute Kidney Injury.²⁵ It has been shown that the flavonoid compounds contained in *Andrographis paniculata* was able to increase the glomerular filtration rate (GFR).⁵ Over time, the kidneys were able to process the extra creatinine produced as a

result of an increase in GFR, lowering blood creatinine levels.⁶

T3 subjects fared worse than the healthy controls. showed no discernible deviations. This shows that the T3 group's creatinine levels dropped after being given sambiloto leaf extract at 500 milligrams per kilogram were almost similar with the healthy control group. Previous studies had shown that sambiloto leaf extract had an effect on oxidative stress at a dose of 500mg/kgBW and renoprotective effect on Wistar rats.^{25,26}

The rats that were administered with lipopolysaccharide injection show an increment in serum uric acid levels against healthy controls, this result indicates that the administration of lipopolysaccharide injection induce a severe condition of inflammatory on rats that could cause sepsis. It has recently been recognized that uric acid is hypothesized that this biological component may promote an inflammatory response that may exacerbate AKI and hence be considered a mediator of AKI.¹⁶ Evidence from prior research indicates that there are fundamental changes in the renal blood vessels due to the presence of hyperuricemia. Uric acid was found by Ryu et al. to inhibit E-cadherin epithelial cell expression, leading to a reduction in cell-to-cell contact in rat renal tubular cells. Cell-to-cell communication between epithelial cells is essential for the coordinated secretion of nitric oxide and other chemicals that improve renal blood flow. Moreover, prior research employing proximal tubular epithelial cells from normal adult male kidneys demonstrated that increased uric acid levels generate NADPH-dependent oxidative alterations that can promote apoptosis. The link between hyperuricemia and tubulointerstitial renal injury is clarified by these results.²⁷

Study from S´anchez-Lozada et al. determined that renal biopsy results of Afferent arterioles in rats with high serum uric acid levels were thickened. Arteriole thickness reduces blood flow to the kidneys, which leads to kidney disease. Endothelial function serum uric acid levels were reported to increase after xanthine treatment oxidase inhibitors.¹⁶

Results from previous study show that the administration of sambiloto leaf extract has a renoprotective effect in Acute Renal Failure.²⁵ Purine metabolism relies on xanthine oxidase, an enzyme that catalyzes the hydroxylation of hypoxanthine to xanthine as a further results in generating uric acid.²⁸

Compared to rats in the control group that received simply an injection of lipopolysaccharide, those in the treatment group that received *Andrographis paniculata* levels of uric acid in the blood were dramatically reduced in those who took the extract. The uric acid The treatment group's levels were dramatically lower than the control group's. Flavonoids' health benefits have been well-documented for some time contained in *Andrographis paniculata* has an ability to inhibit Xanthine Oxidase enzymes both competitively and non-competitively. Aliphatic chain substitution found in flavonoids increase hydrophobic interactions and bind tightly to binding sites.²⁸ Moreover, the sambiloto extract can inhibit xanthine oxidase activity so that it can reduce serum uric acid levels.²⁹

Histopathological and immunohistochemical analyses of Sambiloto (*Andrographis Paniculata*) leaf extract profile of sepsis-induced AKI is required to confirm to the advantage of Sambiloto (*Andrographis Paniculata*) leaf extract to prevent the sepsis-induced -AKI. Histopathological findings associated with Sambiloto (*Andrographis Paniculata*) leaf extract administration on sepsis-induced AKI may aid in gaining a deeper comprehension of disease pathways, increasing specificity of data, and improving the efficacy of treatment plans.

CONCLUSION

The present study suggests that Sambiloto (*Andrographis Paniculata*) leaf extract administration for fourteen days in dose 400 and 500 mg/kgBW as pretreatment before sepsis-induced -AKI exerts significant renoprotective effects in A Sepsis Model in Rats -induced -AKI.

ACKNOWLEDGEMENT

The authors are grateful to the Faculty of Medicine, Diponegoro University for the support provided under research grant no.1664/UN7.5.4.2/PP/2021

REFERENCES

1. Patin EW, Zaini MA, Sulastri Y. Pengaruh Variasi Suhu Pengeringan terhadap Sifat Fisikokimia Teh Daun Sambiloto (*Andrographis paniculata*). J Ilmu dan Teknol Pangan. 2018;4(1):251–8.
2. Sikumalay A, Suharti N, Masri M. Efek Antibakteri dari Rebusan Daun Sambiloto (*Andrographis paniculata* Nees) dan Produk Herbal Sambiloto Terhadap *Staphylococcus Aureus*. J Kesehatan Andalas. 2016;5(1):196–200. DOI:<https://doi.org/10.25077/jka.v5i1.468>
3. Soren P, Kumar P. Nephroprotective Efficacy of Methanolic Extract of Kalmegh (*Andrographis paniculata*) in Acute Renal Failure in Dogs. Int J Livest Res [Internet]. 2017;7(8):1. Available from: <http://www.ejmanager.com/fulltextpdf.php?mno=265587> DOI:10.5455/ijlr.20170610050222
4. Kumar S, Pandey AK. Chemistry and Biological Activities of Flavonoids: An Overview. Lu KP, Sastre J, editors. Sci World J [Internet]. 2013;2013:1–16. Available from: <https://doi.org/10.1155/2013/162750>
5. Panche AN, Diwan AD, Chandra SR. Flavonoids: an overview. J Nutr Sci [Internet]. 2016 Dec 29;5:e47. Available from: https://www.cambridge.org/core/product/identifier/S2048679016000410/type/journal_article DOI:10.1017/jns.2016.41
6. Jouad H, Lacaille-Dubois M., Lyoussi B, Eddouks M. Effects of the flavonoids extracted from *Spergularia purpurea* Pers. on arterial blood pressure and renal function in normal and hypertensive rats. J Ethnopharmacol [Internet]. 2001 Jul;76(2):159–63. Available from: <https://linkinghub.elsevier.com/retrieve/pii/S0378874101002094> DOI:10.1016/S0378-8741(01)00209-4

7. Korneev K V. Mouse Models of Sepsis and Septic Shock. *Mol Biol* [Internet]. 2019 Sep 18;53(5):704–17. Available from: <http://link.springer.com/10.1134/S0026893319050108> DOI:10.1134/S0026893319050108
8. Sampath V. Bacterial endotoxin-lipopolysaccharide; structure, function and its role in immunity in vertebrates and invertebrates. *Agric Nat Resour* [Internet]. 2018 Apr;52(2):115–20. Available from: <https://doi.org/10.1016/j.anres.2018.08.002> DOI:10.1016/j.anres.2018.08.002
9. Geng C, Guo Y, Wang C, Cui C, Han W, Liao D, et al. Comprehensive Evaluation of Lipopolysaccharide-Induced Changes in Rats Based on Metabolomics. *J Inflamm Res* [Internet]. 2020 Aug;Volume 13:477–86. Available from: <https://www.dovepress.com/comprehensive-evaluation-of-lipopolysaccharide-induced-changes-in-rats-peer-reviewed-article-JIR> DOI:10.2147/JIR.S266012
10. Wang X, Quinn PJ. Endotoxins: Structure, Function and Recognition [Internet]. Wang X, Quinn PJ, editors. Dordrecht: Springer Netherlands; 2010. 2–25 p. (Subcellular Biochemistry; vol. 53). Available from: <https://link.springer.com/10.1007/978-90-481-9078-2> DOI:10.1007/978-90-481-9078-2
11. Alfonso AA, Mongan AE, Memah MF. Gambaran kadar kreatinin serum pada pasien penyakit ginjal kronik stadium 5 non dialisis. *J e-Biomedik* [Internet]. 2016 Jan 27;4(1). Available from: <https://ejournal.unsrat.ac.id/index.php/ebiomedik/article/view/10862> DOI:10.35790/ebm.4.1.2016.10862
12. Liu X, Lu J, Liao Y, Liu S, Chen Y, He R, et al. Dihydroartemisinin attenuates lipopolysaccharide-induced acute kidney injury by inhibiting inflammation and oxidative stress. *Biomed Pharmacother* [Internet]. 2019;117(April):109070. Available from: <https://doi.org/10.1016/j.biopha.2019.109070> DOI:10.1016/j.biopha.2019.109070
13. Shi Y, Hua Q, Li N, Zhao M, Cui Y. Protective Effects of Evodiamine against LPS-Induced Acute Kidney Injury through Regulation of ROS-NF- κ B-Mediated Inflammation. *Evidence-Based Complement Altern Med* [Internet]. 2019 Mar 3;2019:1–9. Available from: <https://www.hindawi.com/journals/ecam/2019/2190847/> DOI:10.1155/2019/2190847
14. Húngaro TGR, Freitas-Lima LC, Gregnani MF, Perilhão MS, Alves-Silva T, Arruda AC, et al. Physical Exercise Exacerbates Acute Kidney Injury Induced by LPS via Toll-Like Receptor 4. *Front Physiol* [Internet]. 2020 Jul 17;11(July):1–13. Available from: <https://www.frontiersin.org/article/10.3389/fphys.2020.00768/full> DOI:10.3389/fphys.2020.00768
15. Ejaz AA, Johnson RJ, Shimada M, Mohandas R, Alquadan KF, Beaver TM, et al. The Role of Uric Acid in Acute Kidney Injury. *Nephron* [Internet]. 2019;142(4):275–83. Available from: <https://www.karger.com/Article/FullText/499939> DOI:10.1159/000499939
16. Hahn K, Kanbay M, Lanaspas MA, Johnson RJ, Ejaz AA. Serum uric acid and acute kidney injury: A mini review. *J Adv Res* [Internet]. 2017;8(5):529–36. Available from: <http://dx.doi.org/10.1016/j.jare.2016.09.006> DOI:10.1016/j.jare.2016.09.006
17. Kaushik M, Choo JCJ. Serum uric acid and AKI: is it time? *Clin Kidney J* [Internet]. 2016 Feb;9(1):48–50. Available from: <https://academic.oup.com/ckj/article-lookup/doi/10.1093/ckj/sfv127> DOI:10.1093/ckj/sfv127
18. Ejaz AA, Mu W, Kang DH, Roncal C, Sautin YY, Henderson G, et al. Could Uric Acid Have a Role in Acute Renal Failure? *Clin J Am Soc Nephrol* [Internet]. 2007 Jan;2(1):16–21. Available from: <https://journals.lww.com/01277230-200701000-00007> DOI:10.2215/CJN.00350106
19. Alnajjar B. Computational studies of natural flavonoids towards the discovery of a potential xanthine oxidase inhibitor. MSc Thesis, Universiti Sains, Malaysia; 2008.
20. Doi K, Leelahavanichkul A, Yuen PST, Star RA. Animal models of sepsis and sepsis-induced kidney injury. *J Clin Invest* [Internet]. 2009 Oct 1;119(10):2868–78. Available from: <http://www.jci.org/articles/view/39421> DOI:10.1172/JCI39421
21. Purwanto DS, Astrawinata DAW. Mekanisme Kompleks Sepsis dan Syok Septik. *J BIOMEDIK* [Internet]. 2018 Dec 18;10(3):143. Available from: <https://ejournal.unsrat.ac.id/index.php/biomedik/article/view/21979> DOI:10.35790/jbm.10.3.2018.21979
22. Peerapornratana S, Manrique-Caballero CL, Gómez H, Kellum JA. Acute kidney injury from sepsis: current concepts, epidemiology, pathophysiology, prevention and treatment. *Kidney Int* [Internet]. 2019/06/07. 2019 Nov;96(5):1083–99. Available from: <https://pubmed.ncbi.nlm.nih.gov/31443997> DOI:10.1016/j.kint.2019.05.026
23. Yoo JY, Cha DR, Kim B, An EJ, Lee SR, Cha JJ, et al. LPS-Induced Acute Kidney Injury Is Mediated by Nox4-SH3YL1. *Cell Rep* [Internet]. 2020 Oct;33(3):108245. Available from: <https://doi.org/10.1016/j.celrep.2020.108245> DOI:10.1016/j.celrep.2020.108245
24. Sacher RA, McPherson RA. Pengaturan Asam-basa dan Elektrolit. In: *Tinjauan Klinis Hasil Pemeriksaan Laboratorium*. 2004. p. 320–40.
25. Singh P, Srivastava MM, Khemani LD. Renoprotective effects of *Andrographis paniculata* (Burm. f.) Nees in rats. *Ups J Med Sci* [Internet]. 2009 Jan 15;114(3):136–9. Available from: <https://ujms.net/index.php/ujms/article/view/6209> DOI:10.1080/03009730903174321
26. Rajendrakumar T, Rao S, Satyanarayana ML, Narayanaswami HD. Ameliorative effect of *Andrographis paniculata* against oxidative damage caused by cisplatin in rat kidney. 2020;9(3):356–9.

-
27. Giordano C, Karasik O, King-Morris K, Asmar A. Uric Acid as a Marker of Kidney Disease: Review of the Current Literature. *Dis Markers* [Internet]. 2015;2015:1–6. Available from: <http://www.hindawi.com/journals/dm/2015/382918> / DOI:10.1155/2015/382918
 28. Omar B, Mohamed N, Rahim RA, Wahab HA. Natural Flavonoids for the treatment of Hyperuricemia, Molecular Docking studies BT - World Congress on Medical Physics and Biomedical Engineering 2006. In: Magjarevic R, Nagel JH, editors. Berlin, Heidelberg: Springer Berlin Heidelberg; 2007. p. 178–82.
 29. Septianingsih U, Susanti H, Widyaningsih W. PENGHAMBATAN AKTIVITAS XANTHINE OXIDASE OLEH EKSTRAK ETANOL AKAR SAMBILOTO (*Andrographis paniculata*, Ness) SECARA IN VITRO. *Pharmaciana* [Internet]. 2012 Nov 1;2(2). Available from: <http://journal.uad.ac.id/index.php/PHARMACIAN> A/article/view/665 DOI:10.12928/pharmaciana.v2i2.665
-

JOURNAL OF BIOMEDICINE AND TRANSLATIONAL RESEARCH

Available online at JBTR website: <https://jbtr.fk.undip.ac.id>

Copyright©2023 by Faculty of Medicine Universitas Diponegoro, Indonesian Society of Human Genetics and Indonesian Society of Internal Medicine

Original Research Article

Effects of Tempeh Fermentation with *Rhizopus oligosporus* and *Lactobacillus rhamnosus* GG on Body Weight, Lee Index, hs-CRP, and Lipid Profile of Obese Rats

Fatih Az Zahra¹, Faizah Fulyani^{2*}, Nani Maharani³, Gemala Anjani¹, Etika Ratna Noer¹

¹Department of Nutrition Science, Faculty of Medicine, Universitas Diponegoro, Indonesia

²Department of Medical Biology and Biochemistry, Faculty of Medicine, Universitas Diponegoro

³Department Pharmacology and Therapy, Faculty of Medicine, Universitas Diponegoro

Article Info

History

Received: 06 Feb 2023

Accepted: 11 Mar 2023

Available: 30 Apr 2023

Abstract

Background: Tempeh is a fermented soybean containing isoflavones that shows good benefits against obesity. Co-fermentation of tempeh using *Lactobacillus rhamnosus* GG could increase the bioavailability of isoflavones.

Objective: This study aimed to determine the effect of co-fermented tempeh using *Lactobacillus rhamnosus* GG (tLGG) on body weight (B.W.), Lee Index, high sensitivity C Reactive Protein (hs-CRP), and lipid profile of obese rats.

Methods: A total of 30 Male Sprague Dawley obese rats were divided into five groups and were given different diets for four weeks: the high-fat high sucrose (HFHS) diet (negative control group), HFHS diet + orlistat (positive control group), HFHS diet + standard tempeh fermented with *Rhizopus oligosporus* (tS group), HFHS diet + 60 mg/kg B.W./day tLGG (low tLGG group), and HFHS diet + 120 mg/kg B.W./day tLGG (high tLGG group). Body weight and Lee Index were measured before and after the intervention; meanwhile, hs-CRP, total cholesterol (TC), triglyceride (TG), HDL, and LDL were measured after the interventions. In addition, the total flavonoid and genistein of tempeh were also analyzed.

Results: Compared to the negative control, all diet interventions on obese rats prevented further increase in Lee index level and were able to deplete it significantly. Importantly tLGG group demonstrated a better Lee index decrease compare to tS group; yet, there was no significant weight gain differences. Additionally, the tLGG group also exhibited lower hs-CRP levels, TG, TC, and LDL and higher HDL ($p < 0.001$). Finally, we confirmed the total flavonoid and genistein levels were higher in co-fermented tempeh than in standard one.

Conclusion: co-fermented tempeh tLGG showed a beneficial effect on obese rats by preventing weight gain, Lee index reduction, lipid profile improvement and systemic inflammation due to its high flavonoid and genistein content

Keywords: Tempeh; Lactic acid bacteria; High fat high sucrose diet; Obesity

Permalink/ DOI: <https://doi.org/10.14710/jbtr.v9i1.17381>

INTRODUCTION

The prevalence of obesity has increased more than four times since 1975 along with increasing high-fat high-sucrose diet consumption.¹ Obesity is defined as excessive fat accumulation in the body (Body Mass Index, BMI ≥ 30), which can increase the risk of metabolic syndrome; among which the most common are dyslipidemia, cardiovascular disease, and insulin resistance.²⁻³ Excessive fat accumulation in the body

generate a high level of free fatty acid; thus, obese people have high triglyceride level. It is also associated with chronic inflammation of white adipose tissue. Adipocytes secrete pro-inflammatory cytokines and induce the production of C-reactive protein.

* Corresponding author:

E-mail: f.fulyani@fk.undip.ac.id
(Faizah Fulyani)

Together, these processes could lead to impaired immune systems.³ Several drugs for obesity have been developed. One of the most commonly used is orlistat, yet the existing drugs are costly and have side effects such as vitamin deficiency and gastrointestinal and kidney disorders.⁴ Improving an active lifestyle and a healthy diet can be an alternative strategy to overcome obesity.

Food containing bioactive compounds that are beneficial for obesity has been studied extensively. Tempeh is a traditional food made from the fermentation of soybean and *Rhizopus spp.* Soybean contains bioactive substances, such as peptides, phytosterols, soy saponin, and isoflavones.⁵ Isoflavones are the most abundant substances contained in soybean. Isoflavones, such as genistein and daidzein, could reduce lipid accumulation in the early stages of adipogenesis. They act upon the attenuation of the phosphatidylinositol 3-kinase (PI3K)/Akt pathway and increase brown adipose activity through the induction of uncoupling protein 1 (UCP-1); thus it could inhibit body weight gains in obesity.⁶ Isoflavones could improve the lipid profile and inflammatory status in obesity through several mechanisms. They can decrease the expression of stearoyl coenzyme A desaturase 1 (SCD1), peroxisome proliferator-activated receptors (PPAR) α and γ protein, adenosine 5'-monophosphate (AMP)-activated protein kinase (AMPK), tumor necrosis factor (TNF)- α , interleukin (IL)-1, and nuclear factor kappa-light-chain-enhancer of activated B cells (NF- κ B) in white adipose tissue and liver.⁶ Apart from their benefits, intestinal epithelium hardly absorbs Isoflavones. Yet, several studies have demonstrated that fermentation can increase the bioavailability of soy isoflavones.⁶

Recently, lactic acid bacteria (LAB) have been used to optimize soy isoflavones' bioavailability while inhibiting pathogens and mycotoxins.⁷ *Lactobacillus rhamnosus* G.G. shows the highest β -glucosidase activity compared to other *Lactobacillus* bacteria, which could increase the hydrolysis of isoflavone glucosides into more optimal aglycones.⁸ Several studies have shown the benefits of *Lactobacillus rhamnosus* G.G. against obesity. *L. rhamnosus* demonstrated the ability to suppress several lipogenic and pro-inflammatory genes, normalizing intestinal microbiota dysbiosis, and improving leptin response, triglyceride, and cholesterol levels in blood.⁹⁻¹¹ Research using *Lactobacillus rhamnosus* G.G. in whole soybean fermentation showed that it could grow stably up to 10 hrs of fermentation at 37°C. This bacterium continued to show its metabolic activity even during storage.¹² These bacteria are relatively stable and can survive up to a temperature of 54°C.¹³ Importantly, *Lactobacillus rhamnosus* G.G., in live or dead state, still shows the same benefits in reducing pro-inflammatory mediators and increasing anti-inflammatory mediators.¹⁴

Tempeh is a fermented soybean product using *Rhizopus oligosporus* as a starter that is widely consumed daily in Asia, especially in Indonesia. This fungus can grow fast at 30-42°C so tempeh can be made at room temperature.¹⁵ Tempeh is rich in nutrients, can decrease phytic acid (nutrient absorption inhibitor), metabolizing 5-hydroxy isoflavones (genistein, biochanin A) and 5-deoxyisoflavones (daidzein,

formononetin), and producing α -galactosidase.¹⁵ Despite the improved nutritional value of co-fermented tempeh, the effect of co-fermentation of tempeh using *Rhizopus oligosporus* and *Lactobacillus rhamnosus* G.G. on obese rats has not been demonstrated yet. Therefore, this study aimed to analyze the effect of co-fermentation tempeh using *Lactobacillus rhamnosus* G.G. on diet-induced obesity rats.

MATERIALS AND METHODS

Research design

The research design was a true experiment with a randomized pre-test post-test for body weight, body weight gains, and Lee Index data, while post-test-only control group design was used for lipid profile and systemic inflammation measurements. Sample preparation was conducted in the Universitas Diponegoro Integrated Laboratory. Experimental animal treatment and biomarker testing were conducted in the Experimental Animal Laboratory at Gadjah Mada University. Tests for total flavonoid and genistein were conducted at Satyawacana Christian University.

Sample preparation

Lactobacillus rhamnosus were obtained from the Center for Food and Nutrition Studies, Gadjah Mada University. The soybeans used were local organic yellow soybeans from Sleman, Yogyakarta, obtained through the Lingkar Organik. *Rhizopus oligosporus* used were Ragi Raprima. The procedure for making probiotic fermented tempeh was based on Nout and Kiers.¹⁵ Soybeans were washed and soaked for 90 min, and the outer membranes were removed. The beans were then cooked in water at 100°C for 30 min. The hot water was then removed and cooled at room temperature to 25°C. Afterward, 10⁵ CFU/g of *L. rhamnosus* G.G. and 10⁴ CFU/g of *R. oligosporus* were inoculated at 30°C and mixed with beans homogeneously into polythene bags, followed by incubation for 48 hrs at 25°C. Determination of total bacterial levels of *L. rhamnosus* G.G. based on research by Petruláková and Valík that showed 10⁵ CFU/g *L. rhamnosus* G.G. could grow well on soybeans.¹² Standard tempeh preparation is the same as the probiotic fermented tempeh preparation procedure without adding *Lactobacillus rhamnosus* G.G. The tempeh samples obtained were then cut into 0.5 cm and freeze-dried for 48 hrs. The samples were ground with a grinder and stored until reuse at -20°C.

Animal and diets

Male Sprague Dawley (n=36, 200 to 215-gram, age eight weeks) was obtained from the Experimental Animal Laboratory at Gadjah Mada University in a healthy condition. The selection of male rats was based on the sensitivity of the rats to a high-fat high-sucrose diet and metabolic syndrome and to eliminate the variation of metabolic outcomes. Rats were housed in an individual cage with a temperature of 25±2°C, a humidity of 55-60%, light/dark cycle of 12 hrs. All groups were adapted for one week and given a standard diet of 10 gr/day with free access to water. After acclimatization, rats were divided into six groups. One group was designated as normal control and was fed the standard diet. The rest of the groups were orally administered high fat and high

sucrose diet (HFHS diet) for two weeks to induce obesity. The composition of the HFHS diet was based on AIN-93M formulation with some modifications to provide a high-fat and high-sucrose diet (Table 1). A total of 30 g/day HFHS diet was administered orally to rats at three meal time points. After obesity was confirmed (Lee Index > 300), rats were divided into five groups and fed different diets for four weeks. The negative control: HFHS diet; Positive control: HFHS + 120 mg/kg B.W./day of Orlistat; tS group: HFHS + 60 mg/kg B.W./day standard tempeh; low dose tLGG: HFHS + 60 mg/kg B.W./day tLGG; high dose tLGG: HFHS + 120 mg/kg B.W./day tLGG. M Body weight was measured once every week using a digital analytical scale. Body length and lee index were measured before and after intervention (Figure 1). The body length of the rats was measured from nose to anus or vice versa using a standard measuring tape with an accuracy of 0.01 cm. Lee index was obtained from the following calculation by Lee formulation¹⁶:

$$\text{Lee index} = \frac{\sqrt[3]{\text{body weight in gram}}}{\text{body length in cm}} \times 1000.$$

Lee index > 300 indicates that the rats are obese.¹⁶ Before weighing and measuring the body length of the rats, the rats were anesthetized using ketamine 75–100 mg/kg + xylazine 5–10 mg/kg. On the last day of the experiment, the blood was collected through the rat's orbital eye and centrifuged at 3500 rpm for five min to obtain blood plasma. The blood was then stored at -20°C until used for further analysis.

Inflammatory marker

Hs-CRP was analyzed using the ELISA method (Enzyme-linked immunosorbent assay). ELISA kits were obtained from Elabscience Biotechnology Inc., and the assay was performed according to the protocols provided by the commercial kits.

Table 1. Experimental diet composition (g/kg)

Ingredient	AIN 93M (standard diet)	HFHS
Cornstarch	465.692	365.692
Casein	200	200
L-Cystine	2	2
Sucrose	100	300
Cellulose (CMC)	50	50
Soybean oil	50	50
Cholin Chloride	2	2
Tert-Butylhydroquinone (TBHQ)	0,014	0,056
Lard	100	200
Mineral mix AIN-93- MX	35	35
Vitamin mix AIN-93- VX	10	10

HFHS (High-fat High-Sucrose); AIN 93M (American Institute of Nutrition 93 Maintenance)

Lipid profile measurements

Total cholesterol, low-density lipoprotein (LDL), and high-density lipoprotein (HDL) were analyzed using CHOD/PAP calorimetry method (Cholesterol Oxidase Phenol Amino Phenazone). Triglycerides were analyzed using GPO-PAP (Glycerol-3-Phosphatase Oxidase-Phenol Amino Phenazone). Kits for determining lipid profile were obtained from Diagnostic System GmbH & Co Kit or DiaSys of 500 nm. The assay was performed according to the protocols provided, and absorbance was measured by spectrophotometer (Merck-Microlab) at a wavelength of 500 nm.

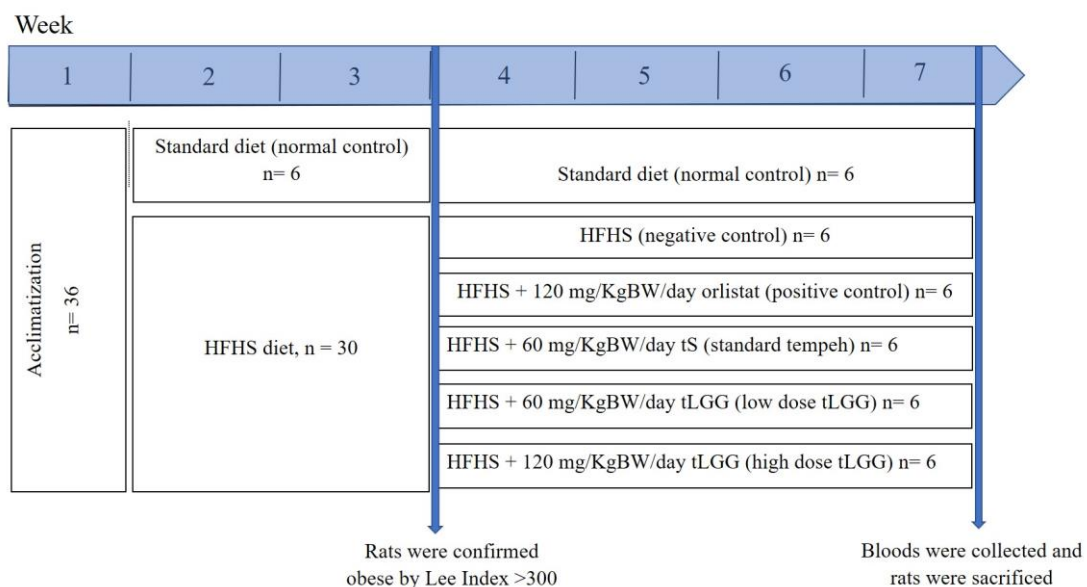


Figure 1. Schematic of the experimental timeline. HFHS (High fat high sucrose) diet, tS (standard tempeh), tLGG (co-fermented tempeh with *L. rhamnosus* GG).

Tempeh extraction

One gram of tempeh was mixed with 25 mL of 60% ethanol v/v in a glass container. Extraction was carried out using an ultrasonicator at 40°C for 15 min. The extract solution was filtered, and the residue was re-extracted with 25 mL 60% ethanol v/v. These stages were repeated three times. The obtained filtrate was combined into a 100 mL volumetric flask, and 60% v/v ethanol solvent was added until it met the measuring line, and 10 mg/mL tempeh extract was obtained.

standard was obtained from HWI pharma service GmbH Germany. One mL of tempeh extract was pipetted, added to four mL of distilled water, and homogenized with a vortex mixer. Afterward, 0.3 mL NaNO₃ of 0.5%, 0.3 mL of 10% AlCl₃, and 2 mL of 1 M NaOH were added consecutively and mixed for another five min. Distilled water was added to the mixture so that the end volume was 10 mL and left at room temperature for 15 min before measurement. The absorbance was determined using the UV-Vis spectrophotometry method at a maximum wavelength of 510 nm (the result of running the quercetin standard). Conversion of absorbance values into total

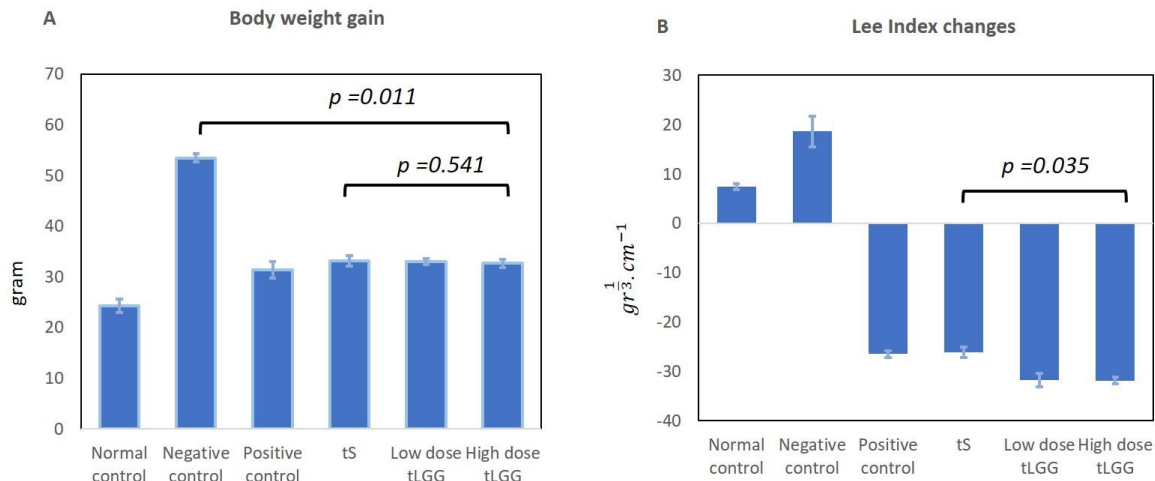


Figure 2. Effect of different diet interventions on body weight gain and Lee index changes in obese rat. Values were presented as mean \pm standard deviation (SD). Normal control (standard diet); Negative control (HFHS diet only); Positive control (HFHS diet+120 mg/kg BW/day orlistat); tS (HFHS diet + 60 mg/kg BW/day standard tempeh); Low dose tLGG (HFHS diet +60 mg/kg BW/day probiotic fermented tempeh); High dose tLGG (HFHS+120 mg/kg BW/day probiotic fermented tempeh).

Table 2. Changes in weight and Lee index of obese rats in different groups which were fed with various diets for four weeks.

Group	Initial BW (gram)	Week 1 (gram)	Week 2 (gram)	Week 3 (gram)	Week 4 / Final BW(gram)	Initial Lee index	Lee index at week 4
Normal control	226,00 \pm 3,16 ^a	232,00 \pm 3,58 ^a	238,50 \pm 3,83 ^a	244,17 \pm 3,49 ^a	250,33 \pm 3,44 ^a	281,73 \pm 2,70 ^a	289,20 \pm 2,79 ^a
Negative control	239,17 \pm 2,48 ^b	251,67 \pm 2,58 ^b	264,83 \pm 2,93 ^b	279,50 \pm 1,87 ^b	292,67 \pm 2,16 ^b	328,75 \pm 4,98 ^{bd}	347,38 \pm 2,22 ^b
Positive control	238,83 \pm 4,54 ^b	247,67 \pm 4,59 ^b	254,83 \pm 4,07 ^c	262,17 \pm 4,62 ^c	270,17 \pm 5,12 ^{ce}	332,99 \pm 5,00 ^{bc}	306,51 \pm 4,49 ^c
tS	244,00 \pm 3,16 ^b	253,33 \pm 3,08 ^b	260,67 \pm 2,74 ^{bc}	269,17 \pm 3,76 ^d	277,17 \pm 3,71 ^d	334,07 \pm 3,48 ^b	307,945 \pm 2,60 ^c
Low dose tLGG	244,67 \pm 3,56 ^b	253,83 \pm 4,26 ^b	261,67 \pm 3,50 ^{bd}	269,67 \pm 3,88 ^d	277,67 \pm 3,56 ^d	334,87 \pm 5,06 ^b	303,14 \pm 3,76 ^c
High dose tLGG	241,17 \pm 2,79 ^b	250,50 \pm 3,27 ^b	257,50 \pm 2,74 ^{cd}	264,83 \pm 3,19 ^{cd}	273,83 \pm 3,19 ^{de}	327,70 \pm 2,39 ^{acd}	295,89 \pm 1,81 ^d
	<0,001*	<0,001*	<0,001*	<0,001*	<0,001*	<0,001**	<0,001*

*One-way ANOVA **Kruskall wallis. All parametric data was measured using one-way ANOVA test and continued using post hoc Bonferroni test for homogen data or Games Howell test for non homogen data. Kruskall wallis was used for non-parametric data and continued using post hoc Dunn test. Means with different superscripts (a,b,c,d) are significantly different at p-value <0.05 between groups while those with similar letters are non-significant. Normal control (standard diet); Negative control (HFHS); Positive control (HFHS+120 mg/kg BW/day orlistat); tS (HFHS + 60 mg/kg BW/day standard tempeh); Low dose tLGG (HFHS+60 mg/kg BW/day probiotic fermented tempeh); High dose tLGG (HFHS+120 mg/kg BW/day probiotic fermented tempeh).

Total flavonoids assay

Total flavonoid content was determined using a PG T60 spectrophotometer. Standard reagents and markers were obtained from E-Merck Germany. The quercetin

flavonoid concentrations based on the quercetin calibration curve, i.e., $y = 0.00060x + 0.00070$. Calibration curves were made based on a series of quercetin concentrations of 20, 40, 60, 80, and 100 μ g/mL.

Total genistein assay

Total genistein was measured using isocratic elution reversed-phase HPLC (High-Performance Liquid Chromatography) method with HPLC instrument Knauer, GMBH Germany. All standard reagents and markers were obtained from E-Merck, Germany. Ten mg/mL of tempeh extract was filtered using a 0.45 µm Whatman micro membrane filter prior to HPLC analysis. Twenty µL of the tempeh filtrate was injected using a microinjector and separated in the column based on the difference in polarity at a temperature of 30°C. Components were detected at a wavelength of 254 nm and displayed as peaks that appeared based on the retention time. The column phase (stationary) was Eurosphere C-18 (250 × 4.6 mm, 5µm) GJ 95. The mobile phase used 0.1% v/v acetic acid: methanol in a ratio of 52:48 v/v, and the pH was adjusted to pH 3.

Statistical analysis

SPSS 27 were used for statistical analysis. All data are presented as means ± S.D. (Standard Deviation). Data were analyzed using repeated measures ANOVA for body weight variables. Weight changes were analyzed using a t-test. Other variables used one-way ANOVA. Next, Post Hoc Bonferroni and Games Howell were used to compare variables. Post Hoc Bonferroni was used for homogeneous data; otherwise, Games Howell was applied. Means with different superscripts (a,b,c,d) significantly differ at p -value <0.05.

Ethical consideration

This study was approved by the Health Research Ethics Committee, Faculty of Medicine, Universitas Diponegoro, Semarang, Indonesia No.125/EC/H/FK-UNDIP/XI/2022.

RESULTS

Body Weight and Lee Index

In this study, the obese rats (Lee index >300) were intervened with different diets for four weeks. Table 2

shows the body weight of all groups during the diet intervention. By the end of the intervention, obese rats receiving no diet intervention shows the highest body weight among other groups. On the other hand, rats receiving co-fermented tempeh (tLGG group) showed lower body weight gain against negative control ($p=0.011$). Furthermore, the weight gain in the high-dose tLGG group was comparable with the positive control group ($p>0.001$); yet no significant difference was observed between tLGG against the tS group ($p=0.054$) (Figure 2A). Importantly, the effect of diet intervention using co-fermented tempeh was demonstrated in Lee index reduction. Figure 2B showed that intervention of high dose tLGG significantly reduced the lee index compare to intervention with the standard tempeh (tS group) ($p=0.035$).

Inflammatory marker

After four weeks of intervention, rats administered tLGG showed lower hs-CRP compared to the negative control, positive control, and tS group ($p<0.001$) (Table 3). Rats in the negative control group demonstrated the highest level of hs-CRP, while rats in the normal control group showed the lowest level of hs-CRP among all groups ($p<0.001$) (Table 3). hs-CRP levels of rats in the positive control group, standard tempeh (tS), or tLGG tended to be lower than those of the negative control group ($p<0.001$) (Table 3). Rats administered a high-dose probiotic fermented tempeh (tLGG) group had the lowest Lee Index at week four among all the HFHS groups ($p<0.001$) (Table 3).

Lipid profile

Rats administered tLGG for four weeks showed lower triglyceride, total cholesterol, and LDL levels but a higher HDL level compared to the negative control, positive control, and tS group ($p>0.001$) (Table 3). The lipid profile of rats administered orlistat group (positive control), standard tempeh (tS), or probiotic fermented tempeh (tLGG) tended to be better than those of the

Table 3. Serum biochemical parameters in rats fed a high-fat diet for 4 weeks and administered standard tempeh and differe dose of *Lactobacillus rhamnosus* co-fermented tempeh orally during the last 4 weeks.

Group	hsCRP (pg/ml)	Triglyceride (mg/dl)	Total cholesterol (mg/dl)	LDL (mg/dl)	HDL (mg/dl)
Normal control	2,99±0,125 ^a	66,93±2,94 ^a	86,89±3,14 ^a	27,24±1,69 ^a	83,61±2,59 ^a
Negative control	17,45±0,84 ^b	129,12±7,05 ^b	196,81±3,28 ^b	87,93±1,34 ^b	21,00±2,02 ^b
Positive control	4,24±0,42 ^c	77,87±3,03 ^c	104,66±3,88 ^{cd}	36,44±2,92 ^c	69,24±2,32 ^c
tS	7,78±0,44 ^d	98,42±3,77 ^d	118,75±3,14 ^e	51,73±5,47 ^d	63,55±2,59 ^d
Low dose tLGG	5,07±0,24 ^e	81,29±4,89 ^c	100,49±3,56 ^{cd}	37,75±4,34 ^c	66,94±1,76 ^{cd}
High dose tLGG	3,98±0,31 ^c	74,57±2,38 ^{ac}	95,22±2,01 ^d	30,59±2,16 ^{ac}	74,79±2,12 ^e
	<0,001*	<0,001*	<0,001*	<0,001*	<0,001*

* One Way ANOVA test and continued using post hoc Bonferroni test for homogen data or Games Howell test for non homoge data.

Means with different superscripts (a,b,c,d) are significantly different at p -value <0.05 between groups while those with simil letters are non-significant. Normal control (standard diet); Negative control (HFHS); Positive control (HFHS+120 mg/kg BW/day orlistat); tS (HFHS + 60 mg/kg BW/day standard tempeh); Low dose tLGG (HFHS+60 mg/kg BW/day probiotic fermented tempeh); High dose tLGG (HFHS+120 mg/kg BW/day probiotic fermented tempeh).

negative control group ($p < 0.001$) (Table 3). Rats administered a high-dose probiotic fermented tempeh (tLGG) group showed the best improvement in all lipid profile parameters among all the HFHS groups ($p < 0.001$) (Table 3).

Table 4. Total Isoflavones and Genistein in standard and *Lactobacillus rhamnosus* co-fermented tempeh

Group	Total flavonoid	Total genistein
	%w/w	%w/w
tS	0,095	2,63
tLGG	0,137	3,88

tS: standard tempeh; tLGG: co-fermented tempeh with *L. rhamnosus* GG: w/w: weight/weight

Total flavonoid and genistein

The results of the analysis showed that probiotic fermented tempeh (tLGG) had higher levels of total flavonoid (0.137% w/w) and genistein (3.88% w/w) than standard tempeh (tS) (Table 4).

DISCUSSION

Obesity is characterized by disorder of the lipid profile due to fat accumulation, an increase in inflammatory status, higher body weight, and body mass index (BMI) ≥ 30 . In rats, the Lee index was used instead of BMI. Lee Index >300 shows that rats are obese. The goal of obesity therapy is to lose weight and improve lipid profile and inflammatory status, including high sensitivity C Reactive Protein as a sensitive inflammatory marker for obesity. The anti-obesity effect of soy isoflavones has been widely documented; hence soy isoflavones have low bioavailability.⁵⁻⁶ The bioavailability of soy isoflavones can be increased through the fermentation process. Through fermentation, isoflavone glycosides are hydrolyzed into aglycones, which more easily absorbed in the intestine. This study demonstrated for the first time that during four weeks of treatment, probiotics co-fermented Tempeh with *Lactobacillus rhamnosus* G.G. could improve the obesity parameters (body weight, Lee index, hs-CRP, and lipid profile) of HFHS-induced obesity rats. Probiotic fermented tempeh also increased total flavonoid and genistein compared to standard tempeh.

In this study, obesity is induced by the HFHS diet for two weeks. During this period, rats showed body weight gain and obesity was confirmed by Lee Index >300 . Increased body weight is related to increased fat accumulation in adipocytes due to chronic HFHS administration. Chronic administration of HFHS increases fat storage in adipocytes, leading to adipocyte proliferation and enlargement.¹⁷ In addition, HFHS diet increases insulin secretion, suppresses lipolysis, induces free fatty acids release from adipocytes, and directs fat to be stored.¹⁸ Administration of high dose tLGG resulted in better Lee Index reduction in rats compared to negative control and tS group. Improvement in Lee Index depletion of tLGG group most probably due to bioavailability increase of isoflavone in co-fermented tempeh (tLGG). Increasing the bioavailability of isoflavones enhances the benefits of isoflavones in reducing lipid accumulation in the early stages of

adipogenesis via inhibition and attenuation of the PI3K/Akt signaling pathway.⁶ This effect was also associated with *L. rhamnosus* administration to tempeh. Previous studies have shown that *L. rhamnosus* can reduce lipid accumulation and inhibit adipocyte differentiation by downregulating adipogenic transcription factors in white adipocytes 3T3-L1 and browning white adipose tissue through the expression of the PPAR gene.¹⁹⁻²⁰ *Lactobacillus rhamnosus* also improves leptin response by decreasing leptin resistance in obesity by reducing the ratio of bacterial phyla in the crypt, decreasing the proportion of proteobacteria and Firmicutes/Bacteroidetes ratio.²¹

All groups treated with HFHS diet has higher hs-CRP, triglyceride, total cholesterol, and LDL and decreased HDL compare to normal control group. This condition is related to increased lipotoxicity caused by chronic HFHS administration. Lipotoxicity triggers adipocytes to increase macrophage secretion, which stimulates an increase in the inhibitory enzyme nuclear factor kappa beta Kinase B (NF- κ B) and the release of pro-inflammatory cytokines from adipocytes such as adipocyte TNF α , IL1, and acute phase proteins.^{17,22} These pro-inflammatory cytokines cause high levels of CRP in the blood, which can cause cell damage.²³ Conversely, in obese conditions, cholesterol absorption is mediated by NPC1L1.²⁴ Lipotoxicity due to HFHS inhibiting lipoprotein lipase activity, which increases triglyceride levels in the blood.²² This HFHS-induced lipotoxicity is indicated by a decrease in HDL levels which is associated with an increase in HDL absorption by adipocytes and an increase in apolipoprotein A-I catabolism in HDL particles.²⁵ An increase in free fatty acids in adipocytes also increases the absorption and accumulation of fat in the liver, which increases VLDL and its release into the bloodstream.²¹ Nonetheless, treatment of high-dose tLGG showed significant benefits in improving the inflammatory status and lipid profile in rats given HFHS. Among all HFHS treatment groups, the high-dose tLGG group showed the lowest value of hs-CRP, triglycerides, total cholesterol, and LDL, while the highest value of HDL. These results are in accordance with Huang et al., which showed that combining *Rhizopus oligosporus* with *Lactobacillus* bacteria can achieve a synergistic effect in improving the lipid profile.²⁶ The low value of hs-CRP in the high dose tLGG was associated with the ability of aglycone isoflavones to reduce the expression of proteins PPAR α , PPAR γ , adenosine 5'-monophosphate (AMP)-activated protein kinase (AMPK), malonaldehyde (MDA), TNF- α , IL-1, NFIL3, and NF- κ B in white adipose tissue and liver.⁶ This benefit was also derived from the ability of *L. rhamnosus* to decrease LPS levels and the inflammatory parameters PPAR γ , TNF- α , and IL-1 in serum and mRNA, forming linoleic acid and improving several biomarkers of obesity through the acetyl Co-A and fatty acid synthase pathways.²⁷

CONCLUSION

co-fermented tempeh tLGG diet showed significantly higher Lee Index depletion compared to negative control and tS groups. Moreover, the high dose tLGG diet showed lower the hs-CRP, triglyceride, total cholesterol, LDL, and higher HDL compared to negative control and

tS group. Diet containing the co-fermentation tempeh with *L.rhamnonsus* GG has better effect on obese rats; most likely due to its higher flavonoid and genistein content.

Research Limitations

Random sampling analysis of rats' total genistein from time to time and fat mass needs to be done for more specific data. Optimization co-fermented tempeh to increase isoflavones needs to be done to get more optimal benefits from the product.

REFERENCES

- World Health Organization. Obesity and overweight fact sheet. 2021 (cited 2021 Oct 18)). *World Health Organization*. Available from: <https://www.who.int/news-room/fact-sheets/detail/obesity-and-overweight>.
- Hruby A, Manson JE, Qi L, Malik VS, Rimm EB, Sun Q, Willet WC, Hu FB. Determinants and Consequences of Obesity. *Am J Public Health*. 2016;106(9):1656-62. DOI: 10.2105/AJPH.2016.303326.
- Nimptsch K, Konigorski S, Pischon T. Diagnosis of obesity and use of obesity biomarkers in science and clinical medicine. *Metabolism*. 2019;92:61-70. DOI: 10.1016/j.metabol.2018.12.006.
- Tak YJ, Lee SY. Anti-Obesity Drugs: Long-Term Efficacy and Safety: An Updated Review. *World J Mens Health*. 2021;39(2):208. DOI: <https://doi.org/10.5534/wjmh.200010>.
- Xianli W, Jie K. Phytochemicals in soy and their health effects. INTECH Open Access Publisher. Rasooli (Ed.), *Phytochemicals – bioactivities and impact on health*. 2011: 43–76. DOI: 10.5772/26026.
- Hsiao Y, Ho C, Pan M. Bioavailability and health benefits of major isoflavone aglycones and their metabolites. *Journal of Functional Foods*. 2020;74:104164. DOI: <https://doi.org/10.1016/j.jff.2020.104164>.
- Licandro H, Ho PH, Nguyen TKC, Petchkongkaew A, Nguyen HV, Chu-Ky S, Nguyen TVA, Lorn D, Wache Y. How fermentation by lactic acid bacteria can address safety issues in legumes food products?. *Food Control*. 2020;110:106957. DOI: <https://doi.org/10.1016/j.foodcont.2019.106957>.
- Marazza JA, Nazareno MA, de Giori GS, Garro MS. Enhancement of the antioxidant capacity of soymilk by fermentation with *Lactobacillus rhamnosus*. *Journal of Functional Foods*. 2012;4(3):594-601. DOI: <https://doi.org/10.1016/j.jff.2012.03.005>.
- Kim B, Park K, Ji Y, Park S, Holzapfel W, Hyun C. Protective effects of *Lactobacillus rhamnosus* GG against dyslipidemia in high-fat diet-induced obese mice. *Biochemical and Biophysical Research Communications*. 2016;473(2):530-6. DOI: <https://doi.org/10.1016/j.bbrc.2016.03.107>.
- Xu H, Wang J, Cai J, Feng W, Wang Y, Liu Q, Cai L. Protective Effect of *Lactobacillus rhamnosus* GG and its Supernatant against Myocardial Dysfunction in Obese Mice Exposed to Intermittent Hypoxia is Associated with the Activation of Nrf2 Pathway. *Int J Biol Sci*. 2019;15(11):2471-83. DOI: <https://doi.org/10.7150/ijbs.36465>.
- Cheng Y, Liu J. Effect of *Lactobacillus rhamnosus* GG on Energy Metabolism, Leptin Resistance, and Gut Microbiota in Mice with Diet-Induced Obesity. *Nutrients*. 2020;12(9):2557. DOI: <https://doi.org/10.3390/nu12092557>.
- Petruláková M, Valík L. Legumes as Potential Plants for Probiotic Strain *Lactobacillus rhamnosus* GG. *Acta Univ Agric Silv Mendelianae Brun*. 2015;63(5):1505-11. DOI: 10.11118/actaun201563051505.
- Liu B, Fu N, Woo MW, Chen XD. Heat stability of *Lactobacillus rhamnosus* GG and its cellular membrane during droplet drying and heat treatment. *Food Research International*. 2018;112:56-65. DOI: <https://doi.org/10.1016/j.foodres.2018.06.006>.
- Li N, Russell WM, Douglas-Escobar M, Hauser N, Lopez M, Neu J. Live and Heat-Killed *Lactobacillus rhamnosus* GG: Effects on Proinflammatory and Anti-Inflammatory Cytokines/Chemokines in Gastrostomy-Fed Infant Rats. *Pediatr Res*. 2009;66(2):203-7. DOI: <https://doi.org/10.1203/PDR.0b013e3181aabd4f>.
- Nout M, Kiers J. Tempe fermentation, innovation and functionality: update into the third millenium. *J Appl Microbiol*. 2005;98(4):789-805. DOI: 10.1111/j.1365-2672.2004.02471.x.
- Lee S-I, Kim J-W, Lee Y-K, Yang S-H, Lee I-A, Suh J-W, et al. Anti-obesity Effect of *Monascus pilosus* Mycelial Extract in High Fat Diet-induced Obese Rats [Internet]. Vol. 54, *Journal of Applied Biological Chemistry*. Korean Society for Applied Biological Chemistry; 2011. p. 197–205. DOI: <http://dx.doi.org/10.3839/jabc.2011.033>
- Mingrone G, Castagneto M. The Pathophysiology of Obesity. In: Lucchese M., Scopinaro N. (eds) *Minimally Invasive Bariatric and Metabolic Surgery*. Springer, Cham; 2015: 17-23. DOI: https://doi.org/10.1007/978-3-319-15356-8_3.
- Heymsfield SB, Wadden TA. Mechanisms, Pathophysiology, and Management of Obesity. *N Engl J Med*. 2017;376(3):254-66. DOI: 10.1056/NEJMr1514009. PMID: 28099824.
- Sanchez M, Darimont C, Drapeau V, Emady-Azar S, Lepage M, Rezzonico E, Ngom-Bru C, Berger B, Philippe L, Ammon-Zuffrey C, Leone P, Chevrier G, St-Amand E, Marette A, Dore J, Tremblay A. Effect of *Lactobacillus rhamnosus* CGMCC1.3724 supplementation on weight loss and maintenance in obese men and women. *Br J Nutr*. 2014;111(8):1507-19. DOI: 10.1017/S0007114513003875.
- Cao S, Zhao C, Xu X, Tang G, Corke H, Gan R, Li H. Dietary plants, gut microbiota, and obesity: Effects and mechanisms. *Trends in Food Science & Technology*. 2019;92:194-204. DOI: <https://doi.org/10.1016/j.tifs.2019.08.004>.

21. Lee CS, Park MH, Kim BK, Kim SH. Antiobesity Effect of Novel Probiotic Strains in a Mouse Model of High-Fat Diet-Induced Obesity. *Probiotics & Antimicro Prot.* 2021;13(4):1054-67. DOI: <https://doi.org/10.1007/s12602-021-09752-0>.
22. Redinger RN. The pathophysiology of obesity and its clinical manifestations. *Gastroenterol Hepatol (N Y)*. 2007;3(11):856-63. PMID: 21960798.
23. Zhu Y, Xian X, Wang Z, Bi Y, Chen Q, Han X, Tang D, Chen R. Research Progress on the Relationship between Atherosclerosis and Inflammation. *Biomolecules*. 2018;8(3):E80. PMID: 30142970.
24. Kyriakopoulou K, Dekkers B, Van der Goot AJ. Plant-Based Meat Analogues. In: Galanakis CM, editor. *Sustainable Meat Production and Processing*. Academic Press; 2019:103–126. DOI: <https://doi.org/10.1016/B978-0-12-814874-7.00006-7>.
25. Chen Y, Hsieh S, Hu C. Effects of Red-Bean Tempeh with Various Strains of Rhizopus on GABA Content and Cortisol Level in Zebrafish. *Microorganisms*. 2020;8(9):1330. DOI: 10.3390/microorganisms8091330.
26. Huang Y, Wu B, Chu Y, Chang W, Wu M. Effects of Tempeh Fermentation with *Lactobacillus plantarum* and *Rhizopus oligosporus* on Streptozotocin-Induced Type II Diabetes Mellitus in Rats. *Nutrients*. 2018;10(9):1143. DOI: <https://doi.org/10.3390/nu10091143>.
27. Wang T, Yan H, Lu Y, Li X, Wang X, Shan Y, Yi Y, Liu B, Zhou Y, Lu X. Anti-obesity effect of *Lactobacillus rhamnosus* LS-8 and *Lactobacillus crustorum* MN047 on high-fat and high-fructose diet mice base on inflammatory response alleviation and gut microbiota regulation. *Eur J Nutr*. 2020;59(6):2709-28. DOI: <https://doi.org/10.1007/s00394-019-02117-y>.

JOURNAL OF BIOMEDICINE AND TRANSLATIONAL RESEARCH

Available online at JBTR website: <https://jbtr.fk.undip.ac.id>

Copyright©2023 by Faculty of Medicine Universitas Diponegoro, Indonesian Society of Human Genetics and Indonesian Society of Internal Medicine

Review Article

Understanding Platelet-Rich Plasma as Potential Therapy to Improve Cardiac Function after Myocardial Infarction: Based on the in-vitro and animal model evidence

Linda Chiuman¹, Dearn Anggita Krismayani Purba², Hendy Million Samin^{3*}

¹Department of Biomedical Science, Faculty of Medicine, Prima Indonesia University, Indonesia

²Faculty of Medicine, University of North Sumatra, Indonesia

³ Faculty of Medicine, Prima Indonesia University, Indonesia

Article Info

History

Received: 09 Feb 2023

Accepted: 14 Apr 2023

Available: 30 Apr 2023

Abstract

Myocardial infarction is the leading cause of death in the world's population. The cardiac remodeling and disproportion of the loss and the new formation of contractile cells will ultimately reduce the function of the heart muscles after infarction. Platelet-rich plasma (PRP) in the last decade has been attracted attention regarding its role in cell regeneration. The content of cytokines and growth factors contained in PRP such as platelet-derived growth factor (PDGF), transforming growth factor-beta 1 (TGF-B1), epidermal growth factor (EGF), vascular endothelial growth factor (VEGF), basic fibroblast growth factor (bFGF) and others are known to be involved in the migration, proliferation, and differentiation of various cell types and to induce post-ischemic angiogenesis. This review aims to analyze and investigate the benefits of PRP therapy in myocardial infarction. Recent literatures regarding the use of PRP in myocardial infarction was collected by searching PubMed and Google Scholar databases with the keywords of "platelet-rich plasma", "myocardial infarction", "reperfusion", and "angiogenesis". The researchers used was published between January 2011 and December 2022. Based on the in-vitro and animal model evidence, platelet-rich plasma (PRP) is considered capable of accelerating angiogenesis and mitogenesis, protecting cells from free radicals, reducing infarct area and scar tissue in myocardial infarction, and also increasing ejection fraction.

Keywords:

Platelet-rich plasma; Myocardial infarction; Angiogenesis; Cardiac function

Permalink/ DOI: <https://doi.org/10.14710/jbtr.v9i1.17379>

INTRODUCTION

Myocardial infarction is the leading cause of death and premature mortality in the world's population.¹ Myocardial infarction can destroy approximately 25% or one million cardiomyocytes in the left ventricle. The cardiac remodeling that happens after infarction and the disproportion of the loss and the new formation of contractile cells will ultimately reduce the function of the heart muscles.² Cardiac remodeling is defined as the volume increase of the left ventricular cavity with a reduced LV ejection fraction following myocardial infarction. The hemodynamic overload activates maladaptive remodeling cascade, resulting in compensatory left ventricle hypertrophy. On the other hand, cytokine release and inflammation lead to

fibroblast proliferation and metalloproteinase activation cause fibrosis.³ Cardiomyocyte cell regeneration can be achieved by implantation or by stimulation the capacity of endogenous cells to proliferate.^{2,3}

Platelets are one source of growth factors involved in essential processes, such as blood clots, immune response, angiogenesis, and cell proliferation in the body.⁴

* Corresponding author:

E-mail: hendy.samin1988@gmail.com

(Hendy Million Samin)

Table 1. Summary of MeSH terms, inclusion and exclusion criteria to filter the literature for this study

MeSH terms	Inclusion	Exclusion
“Platelet-rich plasma” “Myocardial infarction” “Reperfusion” “Angiogenesis”	(1) Prospective clinical trials	Review
	(2) Animal studies	Case report and case series
	(3) Studies assessing PRP in patients with myocardial infarction	Commentaries
	(4) Effects of PRP on cardiac function after myocardial infarction	Letters to the Editor
	(5) Research in English	Short communications

After myocardial infarction occurs, platelets will release granules and microparticles that regulate: 1) the extravasation and accumulation of inflammatory cells in the myocardium after infarction; 2) the immunoreactive response of leukocytes, especially neutrophils and monocytes/macrophages (M1) and activated M2 to regenerate tissue; 3) the activation and transformation of fibroblasts into myofibroblasts to synthesize extracellular matrix (ECM); 4) the proliferation, migration and differentiation of cardiac progenitor cells; 5) the differentiation of progenitor cells into cardiomyocytes; 6) the increased inotropic activity of cardiomyocytes and the release of antiapoptotic signals.⁵

Platelet-rich plasma (PRP) is an autologous plasma taken from a blood sample and centrifuged to obtain a platelet-rich supernatant. PRP contains concentrates and platelets which can be activated by additional products such as calcium chloride, thrombin, or fibrinogen.^{6,7} Several studies regarding the role of PRP in cell regeneration in myocardial infarction have been conducted in the last decade. In addition, the use of PRP also attracts attention because of its economic reason, does not require complex tools and materials, and does not require trained experts. PRP is also a relatively non-invasive technique with low risk of infection and immunological reactions.^{8,9}

MATERIAL AND METHODS

Focused question

This study aims to review the beneficial effect of PRP in myocardial infarction systematically. The research question developed through the Preferred Reporting Items for Systematic Reviews and Meta Analyses (PRISMA) protocol: “What is the benefit of PRP in myocardial infarction?” and “What is the benefit of PRP to improve cardiac function after myocardial infarction?”

Selection criteria

The studies included in this systematic review are: (1) prospective clinical trials; (2) animal studies; (3) studies assessing PRP in patients with myocardial infarction; (4) the effect of PRP on cardiac function after myocardial infarction; (5) research in English. Articles in the form of reviews, case reports and case series, commentaries, letters to the editor, short communications were excluded.

Search methodology

In this article, we summarize the latest literatures regarding the use of PRP in myocardial infarction searched through PubMed and Google Scholar databases

with the “platelet-rich plasma”, “myocardial infarction”, “reperfusion”, and “angiogenesis” keywords. The research used is research published between January 2011 to December 2022. A summary of the search criteria and the use of MeSH terms is shown in Table 1.

RESULTS

The benefits of PRP have been reported in various organs, but its specific efficacy in cases of myocardial infarction is still limited. After eliminating the same research, in our primary search we found 41 articles. Based on the abstract, title and exclusion criteria, 7 relevant articles were obtained which are described in Table 2.

DISCUSSION

PRP is a platelet-rich product resulting from blood centrifugation which can be activated if combined with calcium chloride, thrombin, or fibrinogen.¹⁷ The number of platelets that occurred in PRP was $4,410 \pm 34 \times 10^3$, higher than platelet-poor plasma (PPP) ($p < 0.005$) and found to be 250% more in numbers than platelets in whole blood preparations.^{18,19} PRP containing 15 ml/kg (equivalent to 2.0×10^{10} platelets/kg) can increase circulating platelets by about 40% ($p = 0.03$).²⁰

Although the molecular mechanism is unclear, PRP is known to be involved in the migration, proliferation, and differentiation of various cell types.^{21,22} PRP can accelerate the differentiation of Human-Induced Pluripotent Stem Cells (iPSCs) into cardiomyocytes.¹⁶ Suryawan, 2020 reported that GATA-4 expression in PRP-administered AMSCs was found to be higher compared to negative and positive controls (67.04 ± 4.49 vs 58.15 ± 1.23 $p < 0.05$; 67.04 ± 4.49 vs 52.96 ± 2.02 $p < 0.05$). GATA-4 is a specific transcription factor indicating cardiomyocyte development in the cardiac progenitor formation phase. The finding was supported by immunocytochemical results on troponin expression, which showed a marked increase in the PRP group compared to negative and positive controls (38.13 ± 5.2 vs 10.73 ± 2.39 $p < 0.05$; 38.13 ± 5.2 vs 26.00 ± 0.4 $p < 0.05$).¹⁵ This study supports previous flow cytometry analysis confirming that cardiac progenitor cells (CPC) and AMSCs express the same markers CD90 and CD105.²³ Several previous attempts have been made to facilitate AMSCs, such as the administration of 5-azacytidine, and the result was that 5-azacytidine was insufficient in supporting AMSCs to differentiate into cardiomyocytes fully.²⁴ However, since this is the first study of PRP on AMSCs, it still needs further investigation.

Table 2. Summary of the effect of Platelet-Rich Plasma (PRP) on myocardial infarction

No	Author, year	Sample	Study Group	Duration	PRP Concentration	Route of Administration	Effect	Ref
1.	Mishra <i>et al</i> , 2011	Twenty-eight mice	Four groups consisting of two treatments: 1. Permanent Ligation: Revaten PRP (n=5) and control group with 50 µl phosphate buffered saline (n=4) 2. Ischemia and Reperfusion: PRP (n=10) and control group with 50 µl of phosphate buffered saline (n = 9)	Seven days for group with Permanent Ligation and twenty-one days for group with ischemia and reperfusion	50 µl PRP	Intramyocardial injection	Improved cardiac function (ejection fraction) after myocardial infarction.	10
2.	Cheng <i>et al</i> , 2012	Seventy-eight wistar-kyoto female rats	Two groups: Control (n=39) and PRP group (n=39)	Six weeks (observations were made on day 0, week 3 and week 6)	150µl platelet gel: 75µl host plasma were mixed with 75µl pre-warmed DMEM	Intramyocardial injection	PRP caused de novo angiogenesis, producing more cardiomyocytes and endothelial cells and improve heart function.	11
3.	Hargrave <i>et al</i> , 2012	Eight white rabbits	Two groups: Control (n=3) and PRP group (n=5)	Two weeks	200µl (0,21 mg) PRP per heart	Intramyocardial injection	PRP significantly reduced the size of the myocardial infarction area, improved post-infarction ventricular function, decreased production Reactive Oxygen Species (ROS), and decreased mitochondrial depolarization	12
4.	Vu <i>et al</i> , 2015	Thirty Yorkshire female pigs (65-70 kg)	Five groups: 1) Hyaluronic acid-based hydrogel (n=6); 2) autologous platelet-rich plasma (PRP) (n=6); 3) ascorbic acid-enriched hydrogel (50 mg/L), combined with IV ibuprofen (25 mg/kg) and allopurinol (25 mg/kg) (cocktail group) (n=6); 4) PRP and cocktail (full-compound) (n=6); or 5) saline (control) (n=6).	Eight weeks	8 ml PRP	Intramyocardial injection	PRP can reduce scar tissue in the left ventricle after infarction, inhibit the expansion of infarct size and promote the formation of new blood vessels.	13
5.	Hehanusa <i>et al</i> , 2019	Mononuclear cell	Three groups: 1) PRP group; 2) PPP group (0.5 mL); 3) Control.	Two weeks	0,5 mL PRP	In vitro	Significantly increased myocardial endothelial progenitor cell growth	14

Several PRP cytokines and growth factors that have been proposed as the underlying mechanism, such as platelet-derived growth factor (PDGF) which stimulates the formation of type I collagen and triggers the process of angiogenesis; transforming growth factor-beta 1 (TGF-β1) which stimulates the proliferation and differentiation of stem mesenchymal cells, synthesis the type I collagen, and triggers the angiogenesis; epidermal

growth factor (EGF) which stimulates tissue granulation; vascular endothelial growth factor (VEGF) which induces endothelial cell chemotaxis and proliferation, triggers angiogenesis, prompts vascular hyperpermeability, and precipitate renal stem cell differentiation; basic fibroblast growth factor (b-FGF) that induces post-ischemic angiogenesis; insulin-like growth factor (IGF) which promotes angiogenesis and

Table 2. Continuous..

No	Author, year	Sample	Study Group	Duration	PRP Concentration	Route of Administration	Effect	Ref
6.	Suryawan <i>et al</i> , 2020	Adipose derived Mesenchymal Stem Cell	Three groups: 1) negative control group (α -mem medium-no fluorescence); 2) Positive control group (Cardiomyogenic kit medium-with fluorescence); 3) The PRP group	Two weeks	5×10^9 /L PRP	In vitro	PRP-administered group had a higher adipose derived mesenchymal stem cells (AMSCs) differentiation rate into cardiomyocytes than the positive and negative control groups.	15
7.	Torabi <i>et al</i> , 2020	Human-Induced Pluripotent Stem Cells (iPSCs)	Two groups: the control group with 5mL phosphate buffered saline and the PRP group.	Four weeks	5 ml PRP	In vitro	PRP can accelerate the differentiation of Human-Induced Pluripotent Stem Cells (iPSCs) into cardiomyocytes.	16

myogenesis; platelet factor 4 (PF4); adenosine triphosphate (ATP); adenosine diphosphate (ADP); angioprotein-2; fibronectin; osteocalcin; serotonin; and thrombospondin-1 (TSP-1), and others.^{17,25} Furthermore, the presence of leukocytes and interleukins in PRP play essential role in its antimicrobial effect.²⁶

The most common growth factor in PRP due to its concentrations was TGF- β 1 ($30,500 \pm 20,500$ pg/ml), followed by PDGF-BB (9440 ± 1620 pg/ml), VEGF (2040 ± 971 pg/ml), EGF (906 ± 206 pg/ml) and bFGF (32.6 ± 8.7 pg/ml).²⁷ The mean value of VEGF in PRP was higher than expected plasma/serum; compared to the control group receiving saline solution, the value was 1.42 times higher ($p = 0.017$).^{28,29} The study of protocol preparation of PRP reported that the release of VEGF, EGF, bFGF, IL-17, and IL-8 were significantly higher when PRP was incubated at 4°C before coagulated. This cold temperature also increases the activation of p38, which is involved in the process of angiogenesis.³⁰

Research on PRP in organs has been widely carried out. PRP with saline solution can increase 25-50% angiogenesis and regeneration in wound healing process.³¹ In 56 patients with chronic diabetic ulcers, a significant healing process occurred in PRP-treated group compared to the control group (86% vs 68%).³² Based on color, surface appearance, hair growth and wound drying, better healing was found in the combination of PRP and stromal vascular fraction (SVF).³³ Patients with thromboangiitis obliterans also experienced a decrease in their VAS Score around 50% within 24 hours after PRP was given (mean VAS score 4.35).³⁴

Post-infarction platelets injection increases the number of cardiomyocytes and endothelial cells, thereby promoting mitogenesis and angiogenesis. Within seven days of observation, mature blood vessels were found in the PRP group.¹¹ This new blood vessel formation was

found not only in the infarcted area but also significantly in the peri-infarction area.¹³

The infarction area in the PRP-treated rabbit model was found to be smaller than in the control group ($p < 0.05$).¹² Confirmed by histopathological analysis, scar tissue was also found to be more abundant in the control group with phosphate-buffered saline than in the PRP group.¹⁰ Through the examination of flow cytometry, PRP was able to significantly reduce ROS production in H9c2 cells at concentrations of 44 mM ($p < 0.05$) and 8.8 mM ($p < 0.05$). Decreased ROS production causes a decrease in mitochondrial depolarization, which is often used as a marker of apoptosis in nucleated and non-nucleated cells. Thus, PRP was said to protect the heart muscle from expanding ischemic areas.^{12,35} The combination of PRP with antioxidants and anti-inflammatories also resulted in a lighter left ventricular mass post-infarction than the control group (196 ± 15 g vs 269 ± 20 g; $p < 0.05$).¹³

Cardiomyocyte cells will die and undergo necrosis after myocardial infarction. Then, these necrotic cardiomyocytes will be gradually replaced by noncontractile fibroblasts, thus interfering with cardiac function.^{36, 37} PRP was found to increase the left ventricular ejection fraction (LVEF) and to decrease the exacerbation of inflammation after myocardial infarction.¹¹ Administration of PRP for 7 days in rats whose anterior descending artery was ligated could increase LVEF by 38% ($p = 0.27$). In contrast, the administration of PRP for 21 days in groups of rats undergoing post-ischemic reperfusion therapy could increase LVEF by 28% ($p = 0.038$).¹⁰ Administration of PRP therapy in mice with myocardial infarction also showed tissue protection, endogenous regeneration, greater capillary density, and lower myocyte hypertrophy than the control group.¹¹

The risk of bleeding can occur in patients after myocardial infarction due to anti-platelet consumption.³⁸

Studies in animals receiving the anti-platelet vorapaxar, aspirin, and clopidogrel have shown that PRP reduces bleeding risk by reducing bleeding times by 150 seconds after treatment.³⁹ Another advantage of PRP can be judged by its safety. A retrospective study involving 611 patients post cardiac stenting (post myocardial infarction), diabetes mellitus, stroke, osteoarthritis, anti-aging, hypertension, etc., found no side effects such as allergies, infections, and coagulation problems in patients receiving PRP therapy.^{40,41}

PRP also shows its existence as a protective factor against free radicals. The levels of reactive oxygen species (ROS) and pro-inflammatory cytokines in cases of skin trauma can be reduced by PRP by decreasing the expression of pASK-1 and pNF-KB.⁴² Decreased total oxidant status, oxidative stress index, and ischemic score on histopathological results of ovarian torsion in rats were found after PRP administration.⁴³ In addition, this cytoprotective effect was also reported in cases of testicular torsion in rats in which there is a decrease of nitric oxide (NO), IL1B, TNF- α , caspase 3; and increased CAT, GST, GSH, and BCL2 as evidenced by histological improvement.²⁶

The use of PRP has so far been limited due to its short half-life. After PRP was purified and injected, its effect disappeared within 5-7 days because PRP is easily broken down in the blood vessels and excreted. Therefore, several studies have found that the single use of PRP is less effective in promoting angiogenesis and recommends its combination with other preparations such as gelatin hydrogel to prolong the duration of action. This combination is reported to be much more potent and effective for restoring blood perfusion in ischemic conditions.^{18,44}

Although many studies support the benefits of using PRP, one study reported that administration of PRP could increase the ischemic area of renal tissue. Histopathological examination, ultrasound renal flow parameters, serum creatinine levels, urea levels, renal mass and volume confirmed this condition. Several hypotheses have been proposed to support this situation, namely: (1) the possibility of thrombus in intrarenal vessels; (2) the damage occurred due to the higher osmolarity of PRP compared to saline solution in the control group; (3) the injected PRP also releases cytokines and leukocytes (Mean $5300 \pm 3600/\mu\text{L}$) along with growth factors, thereby worsening the work of the kidneys; (4) the PRP used induces an immune reaction because it is taken from another mouse sample; (5) PRP injection when the kidney is still ischemic has the potential to cause compartment syndrome; (6) this study is the first study on the kidney, so it is suspected that PRP is not effectively applied to solid organs.⁴⁵

CONCLUSION

Platelet-rich plasma (PRP) is considered capable of accelerating angiogenesis and mitogenesis, protecting cells from free radicals, reducing infarct area and scar tissue in myocardial infarction, and also increasing ejection fraction. However, this review is based on in-vitro and animal model evidence; it remains unknown in humans. The potential use of PRP as a modality to improve cardiac function after myocardial infarction should be further investigated.

ACKNOWLEDGEMENTS

Thank you to all parties who have facilitated and assisted in this review, especially to Dr. dr. Linda Chiuman, MKM for her guidance on this manuscript.

REFERENCES

1. Khan MA, Hashim MJ, Mustafa H, Baniyas MY, Al Suwaidi SK, AlKatheeri R, Alblooshi FM, Almatrooshi ME, Alzaabi ME, Al Darmaki RS, Lootah SN. Global epidemiology of ischemic heart disease: Results from the global burden of disease study. *Cureus*. 2020 Jul;12(7). DOI: <https://doi.org/10.7759/cureus.9349>
2. Giacca M. Cardiac regeneration after myocardial infarction: an approachable goal. *Current Cardiology Reports*. 2020 Oct;22(10):1-8. DOI: <https://doi.org/10.1007/s11886-020-01361-7> PMID:32778947 PMCID: PMC7417409
3. Schirone L, Forte M, Palmerio S, Yee D, Nocella C, Angelini F, Pagano F, Schiavon S, Bordin A, Carrizzo A, Vecchione C. A review of the molecular mechanisms underlying the development and progression of cardiac remodeling. *Oxidative medicine and cellular longevity*. 2017 Oct;2017. <https://doi.org/10.1155/2017/3920195> PMID:28751931 PMCID: PMC5511646
4. Le AD, Enweze L, DeBaun MR, Dragoo JL. Current clinical recommendations for use of platelet-rich plasma. *Current reviews in musculoskeletal medicine*. 2018 Dec; 11:624-34. DOI: <https://doi.org/10.1007/s12178-018-9527-7> PMID:30353479 PMCID: PMC6220007
5. Walsh TG, Poole AW. Do platelets promote cardiac recovery after myocardial infarction: roles beyond occlusive ischemic damage. *American Journal of Physiology-Heart and Circulatory Physiology*. 2018 May 1;314(5):H1043-8. DOI: <https://doi.org/10.1152/ajpheart.00134.2018> PMID:29547023 PMCID: PMC6008147
6. Lee JW, Kwon OH, Kim TK, Cho YK, Choi KY, Chung HY, et al. Platelet-rich plasma: quantitative assessment of growth factor levels and comparative analysis of activated and inactivated groups. *Archives of plastic surgery*. 2013; 40(5):530-5. DOI: <https://doi.org/10.5999/aps.2013.40.5.530> PMID:24086805 PMCID: PMC3785585
7. Andia I, Abate M. Platelet-rich plasma: underlying biology and clinical correlates. *Regenerative medicine*. 2013 Sep;8(5): 645-58. DOI: <https://doi.org/10.2217/rme.13.59> PMID: 23998756
8. De Pascale MR, Sommese L, Casamassimi A, Napoli C. Platelet derivatives in regenerative medicine: an update. *Transfusion medicine reviews*. 2015 Jan 1;29(1): 52-61. DOI: <https://doi.org/10.1016/j.tmr.2014.11.001> PMID:25544600
9. Burnouf T, Strunk D, Koh MB, Schallmoser K. Human platelet lysate: replacing fetal bovine serum as a gold standard for human cell propagation? *Biomaterials*. 2016 Jan 1; 76:371-87. DOI: <https://doi.org/10.1016/j.biomaterials.2015.10.065> PMID:26561934

10. Mishra A, Velotta J, Brinton TJ, Wang X, Chang S, Palmer O, Sheikh A, Chung J, Yang PC, Robbins R, Fischbein M. RevaTen platelet-rich plasma improves cardiac function after myocardial injury. *Cardiovascular Revascularization Medicine*. 2011 May 1;12(3):158-63. DOI: <https://doi.org/10.1016/j.carrev.2010.08.005> PMID:21122486
11. Cheng K, Malliaras K, Shen D, Tseliou E, Ionta V, Smith J, Galang G, Sun B, Houde C, Marbán E. Intramyocardial injection of platelet gel promotes endogenous repair and augments cardiac function in rats with myocardial infarction. *J Am Coll Cardiol*. 2012 Jan 17;59(3):256-64. DOI: <https://doi.org/10.1016/j.jacc.2011.10.858> PMID: 22240131 PMCID: PMC3581074
12. Matsui M, Tabata Y. Enhanced angiogenesis by multiple release of platelet-rich plasma contents and basic fibroblast growth factor from gelatin hydrogels. *Acta biomaterialia*. 2012 May 1;8(5):1792-801. DOI: <https://doi.org/10.1016/j.actbio.2012.01.016> PMID: 22293581
13. Vu TD, Pal SN, Ti LK, Martinez EC, Rufaihah AJ, Ling LH, Lee CN, Richards AM, Kofidis T. An autologous platelet-rich plasma hydrogel compound restores left ventricular structure, function and ameliorates adverse remodeling in a minimally invasive large animal myocardial restoration model: a translational approach: Vu and Pal "Myocardial Repair: PRP, Hydrogel and Supplements". *Biomaterials*. 2015 Mar 1; 45:27-35. DOI: <https://doi.org/10.1016/j.biomaterials.2014.12.013> PMID: 25662492
14. Hehanusa RR, Andrianto A, Pikir BS. Effect of Platelet Rich Plasma on Proliferation of Endothelial Progenitor Cell (EPC) of Stable Coronary Artery Disease Patient. *Indonesian Journal of Cardiology*. 2019 Sep 11;40(2). DOI: <https://doi.org/10.30701/ijc.v40i2.851>
15. Suryawan IG, Andrianto A, Anggaraeni AD, Agita A, Nugraha RA. The Role of Human Platelet-Rich Plasma to Enhance the Differentiation from Adipose derived Mesenchymal Stem Cells into Cardiomyocyte: An Experimental Study. *bioRxiv*. 2021 Jan 1:2020-12. DOI: <https://doi.org/10.1101/2020.12.10.420679>
16. Torabi M, Abazari MF, Zare Karizi S, Kohandani M, Hajati-Birgani N, Norouzi S, Nejati F, Mohajerani A, Rahmati T, Mokhames Z. Efficient cardiomyocyte differentiation of induced pluripotent stem cells on PLGA nanofibers enriched by platelet-rich plasma. *Polymers for Advanced Technologies*. 2021 Mar;32(3):1168-75. DOI: <https://doi.org/10.1002/pat.5164>
17. Ozcelik U, Ekici Y, Bircan HY, Aydogan C, Turkoglu S, Ozen O. Effect of topical platelet-rich plasma on burn healing after partial-thickness burn injury. *Med Sci Monit*. 2016;22:1903-9. DOI: <https://doi.org/10.12659/MSM.895395> PMID: 27262706 PMCID: PMC4913826
18. Everts P, Onishi K, Jayaram P, Lana JF, Mautner K. Platelet-rich plasma: new performance understandings and therapeutic considerations in 2020. *International journal of molecular sciences*. 2020 Oct 21;21(20):7794. DOI: <https://doi.org/10.3390/ijms21207794> PMID:33096812 PMCID: PMC7589810
19. Karina KA, Sobariah S, Rosliana I, Rosadi I, Widyastuti T, Afini I, Wanandi SI, Soewondo P, Wibowo H, Pawitan JA. Evaluation of platelet-rich plasma from diabetic donors shows increased platelet vascular endothelial growth factor release. *Stem cell investigation*. 2019;6. DOI: <https://doi.org/10.21037/sci.2019.10.02> PMID: 32039265 PMCID: PMC6987324
20. Cai TQ, Wickham LA, Sitko G, Michener MS, Raubertas R, Handt L, Chintala M, Seiffert D, Forrest M. Platelet transfusion reverses bleeding evoked by triple anti-platelet therapy including vorapaxar, a novel platelet thrombin receptor antagonist. *European journal of pharmacology*. 2015 Jul 5; 758:107-14. DOI: <https://doi.org/10.1016/j.ejphar.2015.03.073> PMID:25857224
21. Alsousou J, Ali A, Willett K, Harrison P. The role of platelet-rich plasma in tissue regeneration. *Platelets*. 2013 May 1;24(3):173-82. DOI: <https://doi.org/10.3109/09537104.2012.684730> PMID:22647081
22. Rosadi I, Karina K, Rosliana I, Sobariah S, Afini I, Widyastuti T, Barlian A. In vitro study of cartilage tissue engineering using human adipose-derived stem cells induced by platelet-rich plasma and cultured on silk fibroin scaffold. *Stem cell research & therapy*. 2019 Dec;10(1):1- 5. DOI: <https://doi.org/10.1186/s13287-019-1443-2> PMID: 31801639 PMCID: PMC6894137
23. Yee-Goh AS, Yamauchi A, van Hout I, Bellae Papannarao J, Sugunesegran R, Parry D, Davis P, Katare R. Cardiac Progenitor Cells and Adipocyte Stem Cells from Same Patients Exhibit In Vitro Functional Differences. *International Journal of Molecular Sciences*. 2022 May 17;23(10):5588. DOI: <https://doi.org/10.3390/ijms23105588> PMID:35628402 PMCID: PMC9141982
24. Malandraki-Miller S, Lopez CA, Al-Siddiqi H, Carr CA. Changing metabolism in differentiating cardiac progenitor cells-can stem cells become metabolically flexible cardiomyocytes? *Frontiers in cardiovascular medicine*. 2018 Sep 19; 5:119. DOI: <https://doi.org/10.3389/fcvm.2018.00119> PMID:30283788 PMCID: PMC6157401
25. Oh JH, Kim WO, Park KU, Roh YH. Comparison of the cellular composition and cytokine-release kinetics of various platelet-rich plasma preparations. *The American journal of sports medicine*. 2015 Dec;43(12):3062-70. DOI: <https://doi.org/10.1177/0363546515608481> PMID:26473014
26. Samy A, El-Adl M, Rezk S, Marghani B, Eldomany W, Eldesoky A, Elmetwally MA. The potential protective and therapeutic effects of platelet-rich plasma on ischemia/reperfusion injury following experimental torsion/detorsion of testis in the

- Albino rat model. *Life sciences*. 2020 Sep 1; 256:117982. DOI: <https://doi.org/10.1016/j.lfs.2020.117982> PMID: 32562693
27. Matsui M, Tabata Y. Enhanced angiogenesis by multiple release of platelet-rich plasma contents and basic fibroblast growth factor from gelatin hydrogels. *Acta biomaterialia*. 2013 May 1;8(5):1792-801. DOI: <https://doi.org/10.1016/j.actbio.2012.01.016> PMID: 22293581
 28. Karina K, Biben JA, Ekaputri K, Rosadi I, Rosliana I, Afini I, Widyastuti T, Sobariah S, Subroto WR. In vivo study of wound healing processes in Sprague-Dawley model using human mesenchymal stem cells and platelet-rich plasma. *Biomedical Research and Therapy*. 2021 Apr 30;8(4):4316-24. DOI: <https://doi.org/10.15419/bmrat.v8i4.670>
 29. Moog P, Kirchhoff K, Bekeran S, Bauer AT, von Isenburg S, Dornseifer U, Machens HG, Schilling AF, Hadjipanayi E. Comparative evaluation of the angiogenic potential of hypoxia preconditioned blood-derived secretomes and platelet-rich plasma: An in vitro analysis. *Biomedicine*. 2020 Jan;8(1):16. DOI: <https://doi.org/10.3390/biomedicine8010016> PMID: 31963131 PMCID: PMC7168246
 30. Etulain J, Mena HA, Meiss RP, Frechtel G, Gutt S, Negrotto S, Schattner M. An optimised protocol for platelet-rich plasma preparation to improve its angiogenic and regenerative properties. *Scientific reports*. 2018 Jan 24;8(1):1-5. DOI: <https://doi.org/10.1038/s41598-018-19419-6> PMID: 29367608 PMCID: PMC5784112
 31. Oneto P, Zubiry PR, Schattner M, Etulain J. Anticoagulants interfere with the angiogenic and regenerative responses mediated by platelets. *Frontiers in bioengineering and biotechnology*. 2020 Mar 20; 8:223. DOI: <https://doi.org/10.3389/fbioe.2020.00223> PMID: 32266247 PMCID: PMC7098916
 32. Ahmed M, Reffat SA, Hassan A, Eskander F. Platelet-rich plasma for the treatment of clean diabetic foot ulcers. *Annals of vascular surgery*. 2017 Jan 1; 38:206-11. DOI: <https://doi.org/10.1016/j.avsg.2016.04.023> PMID: 27522981
 33. Karina MF, Rosadi I, Afini I, Widyastuti T, Sobariah S, Remelia M, Puspitasari RL, Rosliana I, Tunggadewi TI. Combination of the stromal vascular fraction and platelet-rich plasma accelerates the wound healing process: pre-clinical study in a Sprague-Dawley rat model. *Stem cell investigation*. 2019;6. DOI: <https://doi.org/10.21037/sci.2019.06.08> PMID: 31463311 PMCID: PMC6691081
 34. Sharma D, Agarwal P, Jain S, Kothari R. Autologous platelet-rich plasma for treatment of ischemic ulcers in buerger's disease: A pilot study with short-term results. *Indian Journal of Vascular and Endovascular Surgery*. 2018 Jan 1;5(1):14. DOI: https://doi.org/10.4103/ijves.ijves_47_17
 35. Gyulkhandanyan AV, Allen DJ, Mykhaylov S, Lyubimov E, Ni H, Freedman J, Leytin V. Mitochondrial Inner Membrane Depolarization as a Marker of Platelet Apoptosis: Disclosure of Nonapoptotic Membrane Depolarization. *Clin Appl Thromb Hemost*. 2017 Mar;23(2):139-147. DOI: <https://doi.org/10.1177/1076029616665924> PMID: 27637909
 36. Hirt MN, Hansen A, Eschenhagen T. Cardiac tissue engineering: state of the art. *Circulation research*. 2014 Jan 17;114(2):354-67. DOI: <https://doi.org/10.1161/CIRCRESAHA.114.300522> PMID: 24436431
 37. Goradel NH, Hour FG, Negahdari B, Malekshahi ZV, Hashemzahi M, Masoudifar A, Mirzaei H. Stem cell therapy: a new therapeutic option for cardiovascular diseases. *Journal of cellular biochemistry*. 2018 Jan;119(1):95-104. DOI: <https://doi.org/10.1002/jcb.26169> PMID: 28543595
 38. Mullen L, Meah MN, Elamin A, Aggarwal S, Shahzad A, Shaw M, Hasara J, Rashid M, Fisher M, Ali T, Patel B. Risk of Major Bleeding with Potent Antiplatelet Agents After an Acute Coronary Event: A Comparison of Ticagrelor and Clopidogrel in 5116 Consecutive Patients in Clinical Practice. *Journal of the American Heart Association*. 2021 Apr 20;10(8): e019467. DOI: <https://doi.org/10.1161/JAHA.120.019467> PMID: 33834845 PMCID: PMC8174168
 39. Cai TQ, Wickham LA, Sitko G, Michener MS, Raubertas R, Handt L, Chintala M, Seiffert D, Forrest M. Platelet transfusion reverses bleeding evoked by triple anti-platelet therapy including vorapaxar, a novel platelet thrombin receptor antagonist. *European journal of pharmacology*. 2015 Jul 5; 758:107-14. DOI: <https://doi.org/10.1016/j.ejphar.2015.03.073> PMID: 25857224
 40. Karina K, Ekaputri K, Biben JA, Purwoko RH, Sibuea TP, Astuti SL, Loho AM, Limengka Y, Agustini S, Krisandi G, Maryam A. Evaluating the Safety of Intravenous Delivery of Autologous Activated Platelet-rich Plasma. *Journal of Health Sciences*. 2020. DOI: <https://doi.org/10.17532/jhsci.2021.1276>
 41. Patel AN, Selzman CH, Kumpati GS, McKellar SH, Bull DA. Evaluation of autologous platelet rich plasma for cardiac surgery: outcome analysis of 2000 patients. *Journal of cardiothoracic surgery*. 2016 Dec;11(1):1-6. DOI: <https://doi.org/10.1186/s13019-016-0452-9> PMID: 27068030 PMCID: PMC4828785
 42. Rah DK, Min HJ, Kim YW, Cheon YW. Effect of platelet-rich plasma on ischemiareperfusion injury in a skin flap mouse model. *International journal of medical sciences*. 2017;14(9):829 DOI: <https://doi.org/10.7150/ijms.19573> PMID: 28824320 PMCID: PMC5562190
 43. Bakacak M, Bostanci MS, İnanc F, Yaylali A, Serin S, Attar R, Yildirim G, Yildirim OK. Protective effect of platelet rich plasma on experimental ischemia/reperfusion injury in rat ovary.

-
- Gynecologic and obstetric investigation. 2016;81(3):225-31.
DOI: <https://doi.org/10.1159/000440617> PMid: 26496072
44. Kim YH, Furuya H, Tabata Y. Enhancement of bone regeneration by dual release of a macrophage recruitment agent and platelet-rich plasma from gelatin hydrogels. *Biomaterials*. 2014 Jan 1;35(1):214-24.
DOI: <https://doi.org/10.1016/j.biomaterials.2013.09.103>
PMid:24125774
45. Martin-Sole O, Rodo J, Garcia-Aparicio L, Blanch J, Cusi V, Albert A. Effects of platelet-rich plasma (PRP) on a model of renal ischemia-reperfusion in rats. *PLoS One*. 2016 Aug 23;11(8): e0160703.
DOI: <https://doi.org/10.1371/journal.pone.0160703>
PMid: 27551718 PMCID: PMC4994962
-